Immediate and Delayed Suppression of Type I Interferon Induction in Porcine Immune Cells by Nipah Virus Malaysia V Protein

By Graham Owen Casey

A Thesis submitted to the Faculty of Graduate Studies of

The University of Manitoba

in partial fulfilment of the requirements of the degree of

Master of Science

Department of Medical Microbiology and Infectious Diseases

University of Manitoba

Winnipeg, Manitoba, Canada

Abstract

Nipah virus Malaysia genotype (NiV-M) is an emerging zoonotic paramyxovirus. The non-structural P gene products of NiV-M (the V and W proteins) have been implicated in the block of type I interferon signaling, but live virus investigations of their roles in the porcine host are lacking. In this investigation, recombinant NiV-M that do not express either the V or W proteins were used to examine the relevance of these proteins to the induction of type I IFN in porcine immune cells. The V protein was found to be important to the production of infectious virus in porcine immune cells by limiting the production of type I IFNs both immediately after entry and later in the infectious cycle. Immunogold electron microscopy (IEM) imaging indicated that the NiV-M V and W proteins are incorporated into the NiV-M virion by attachments to the nucleocapsid. These findings show that the V protein of NiV-M suppresses type I IFN production throughout infection of porcine immune cells and demonstrate a mechanism by which NiV-M modulates the immune response in swine.

Acknowledgements

I would like to thank Dr. Hana Weingartl for her guidance, advice, support, and the opportunity to do such interesting work. I am especially grateful for her contagious passion for virology, her significant expertise, and for believing in me when I found it hard to. Thanks also to my committee members, Dr. Blake Ball, Dr. Charles Nfon, and Dr. Thomas Murooka, for their advice and support. Thank you to Dr. Chieko Kai and Dr. Misako Yoneda for the use of their recombinant NiV-M plasmid system, without which this work would not have been possible. I am also thankful for the National Sciences and Engineering Research Council of Canada (NSERC) for providing the funding for me to pursue this research (NSERC Grant #327187-2012).

For the tons of technical support, advice, and BSL4 buddying, I would like to thank Greg Smith and Peter Marszal. Thank you for answering all my questions and for sticking with me even when “about 15 minutes” turned into an hour. A big thanks to Nikesh Tailor for going through the graduate journey with me. I would also like to thank the other members of the Special Pathogens Unit, notably Dr. Samantha Kasloff, Dr. Andrea Kroeker, Dr. Bradley Pickering, and Dr. Chandrika Senthilkumaran, for scientific discussions that developed insights into my project and into scientific work in general.

I would like to thank André Dufresne for his expertise in IEM staining, for searching for gold with me, and ultimately for providing the IEM images of the NiV-M nucleocapsids. I would also like to thank Kathy Handel for providing plenty of guidance for my sequencing adventures.

Thanks also to Brad Collignon for never rejecting a radio, and to Kate Hole for her technical advice and skillful troubleshooting. It takes a village to raise a graduate student, and although I cannot here list everyone at the Canadian Food Inspection Agency NCFAD who played an important part in my graduate school journey, I am forever grateful for everyone’s support (scientific, technical, and moral) and enthusiasm.

Finally, thanks to my family. Without your love, support, encouragement, and motivating examples you all set for me, I would never have been able to accomplish this work. Thank you all for being people to look up and forward to.

Table of Contents

List of Abbreviations

293T	human embryonic kidney 293 cells, with Simian virus 40 T antigen
5'ppp	5' triphosphates
6-FAM	6-carboxyfluorescein
aa	amino acids residues
ATP	adenosine triphosphate
AU-rich	adenine/uracil-rich
AUD	animal use document
BEI	binary ethylenimine
BLAST	basic local alignment search tool
(k)bp	(kilo)base pairs
BSL4	biosafety level 4
CARD	caspase activation and recruitment domain
Cardif	CARD adaptor inducing IFNβ (same as MAVS, IPS-1, VISA)
CD	cluster of differentiation
cDC	conventional dendritic cell
CFIA	Canadian Food Inspection Agency
CL	containment level
CMC	carboxymethylcellulose
CNS	central nervous system
CPE	cytopathic effect
CPT	cell preparation tube
CSCHAH	Canadian Science Centre for Human and Animal Health
C_T	cycling threshold

CTD	C-terminal domain
DC	dendritic cell
DI	defective interfering
DMEM	Dulbecco's modified Eagle medium
DNA	deoxyribonucleic acid
Dock2	dedicator of cytokinesis 2
dpi	days post-infection
ds	double-stranded
ECL	enhance chemiluminescent
EDTA	ethylenediaminetetraacetic acid
eIF2α	eukaryotic translation initiation factor 2 subunit alpha
ELISA	enzyme-linked immunosorbent assay
EMEM	Eagle's minimum essential medium
F protein	fusion protein
FBS	fetal bovine serum
G protein	glycoprotein
gs	gene start sequence
ge	gene end sequence
HEp-2	human epithelial type 2 cell line
HeV	Hendra virus
HMVEC-L	human microvascular lung endothelial cells
HMW	high molecular weight
hpi	hours post-infection
HRP	Horse radish peroxidase
HUVEC	human umbilical vein cord endothelial cells

IBRS-2	porcine kidney epithelial cell line
IDR	intrinsically disordered region
IEM	immunoelectron microscopy
IFNAR	interferon-α/β receptor
IFNα/β	interferon alpha/beta
IgG	immunoglobulin G
IKKα	IκB kinase alpha
IKKε	inhibitor of NF-κB kinase subunit epsilon
IL	interleukin
IPAM	immortalized porcine alveolar macrophage cell line
IPS-1	interferon-β promoter stimulator 1(same as MAVS, VISA, Cardif)
IRAK	interleukin-1 receptor-associated kinase
IRF	interferon regulatory factor
ISG	interferon-stimulated gene
ISRE	interferon-sensitive response element
IκB	inhibitor of NF-κB
JAK	Janus kinase
kDa	kilodaltons
L protein	large protein, viral RNA-dependent RNA polymerase
LGP2	laboratory of genetics and physiology 2
MAVS	mitochondrial antiviral-signaling protein (same as IPS-1, VISA, Cardif)
MDA5	melanoma differentiation-associated protein 5
MDBK	Madin-Darby bovine kidney epithelial cell line
MeV	Measles virus

MGB NFQ	minor Groove Binding Non-Fluorescent Quencher
miRNA	microRNA
moDC	monocyte-derived dendritic cell
MOI	multiplicity of infection
MOPS	3-(N-morpholino)propanesulfonic acid
MRC5	human lung fibroblast cell line
mRNA	messenger RNA
MuV	Mumps virus
MWCO	molecular weight cut-off
MX1	myxovirus-resistance protein 1 (Interferon-induced GTP-binding protein Mx1)
MyD88	myeloid differentiation primary response 88
N protein	nucleoprotein
N^0	soluble, monomeric N protein
NCBI	National Center for Biotechnology Information
NCFAD	National Centre for Foreign Animal Disease
NDV	Newcastle disease virus
NEMO	NF-κB essential modulator
NES	nuclear export signal
NF-κB	nuclear factor kappa-light-chain-enhancer of activated B cells
NK cells	natural killer cells
NLS	nuclear localization sequence
N^{NUC}	nucleocapsid- and RNA-associated N protein
nt	nucleotides
NTC	no-template control

NTD	N-terminal domain
OAS1	2’-5’-oligoadenylate synthetase 1
OPNi	intracellular osteopontin
ORF	open reading frame
P protein	phosphoprotein
P_4	P protein tetramer
PAGE	polyacrylamide gel electrophoresis
PAMP	pathogen-associated molecular pattern
PBMC	peripheral blood mononuclear cells
PBS	Phosphate-buffered saline
PCT	P protein C-terminal region
pDC	plasmacytoid dendritic cell
PEG	polyethylene glycol
PFU	plaque-forming unit
PIV5	parainfluenza virus 5
PKR	protein kinase R
PMD	P protein multimerization domain
PNT	P protein N-terminal region
PolyI:C	polyinosinic:polycytidylic acid
poly-U	poly-uracil
PP1 α/γ	protein phosphatase 1 alpha or gamma
PRR	pattern recognition receptor
P_{XD}	P protein X domain
rcf	relative centrifugal force
RdRp	RNA-dependent RNA polymerase

RIG-I	retinoic acid-inducible gene I
RING	really interesting new gene
Riplet	RING finger protein leading to RIG-I activation
RLR	RIG-I-like receptor
RNA	ribonucleic acid
RNase L	ribonuclease L
rNiV	recombinant NiV (M)
rp	recombinant porcine
rRT-PCR	real-time semi-quantitative reverse transcriptase polymerase chain reaction
SDS	sodium dodecyl sulfate
SeV	Sendai virus
ss	single-stranded
ST	swine testes fibroblast cell line
STAT	signal transducer and activator of transcription
SV5	Simian virus 5
TAMRA	6-carboxy-tetramethyl-rhodamine
TANK	TRAF family member-associated NK-κB activator
TBE	tris/Borate/EDTA
TBK	TANK binding kinase
TBS-T	tris-buffered saline-Tween 20
TET	6-carboxy-1,4-dichloro-2',7'-dichlorofluorescein
T_H1	type I helper T cells
TIR	Toll/interleukin-1 receptor
TLR	Toll-like receptor

TMB	3,3’,5,5’-tetramethylbenzidine
TNF	tumour necrosis factor
tP	truncated P protein
TRAF	TNF Receptor-associated factor
TRIF	TIR-domain-containing adaptor-inducing interferon-β
TRIM25	tripartite motif containing 25
TYK2	non-receptor tyrosine-protein kinase 2
UBX	ubiquitin regulatory X
UBXN1	UBX domain protein 1
v/v	volume by volume
Vero	African green monkey kidney epithelial cell line
VISA	virus-induced signaling adaptor (same as IPS-1, MAVS, Cardif)
VLP	virus-like particle
VSV	vesicular stomatitis virus

List of Tables

List of Figures

Introduction

1.1 Nipah Virus (NiV) Overview

Nipah virus (NiV) is an emerging zoonotic paramyxovirus of the genus *Henipavirus*, discovered in an outbreak in Malaysia in 1998-1999 [Chua *et al* 1999]. There are two distinct genotypes of NiV: the Malaysia genotype (NiV-M), which caused the initial outbreak in Malaysia; and the Bangladesh genotype (NiV-B), which has caused and continues to cause multiple smaller outbreaks in India and Bangladesh. The reservoir hosts for both strains of NiV are fruit bats of the genus *Pteropus* [Lo and Rota 2008].

1.1.1 NiV-M Transmission and Epidemiology

The first outbreak of NiV in humans and the only outbreak of NiV-M to date occurred in Malaysia and Singapore in 1998 to 1999. This outbreak resulted from the transmission of the virus from pteropid bats to pigs and then from infected pigs to humans [Chua 2003]. NiV-M does not cause clinical disease in pteropid bats but is shed occasionally in their urine. Transmission of NiV among pteropid bats likely occurs by direct contact, aided by their use of urine for grooming [Middleton *et al* 2007]. The virus may have been transmitted to pigs by consumption of fruit that had been partially eaten or contaminated by bats [Luby *et al* 2009]. The outbreak was spread throughout Malaysia and to Singapore by movement of pigs between pig farms and was eventually controlled by the culling of almost a million pigs [Mohd Nor *et al* 2000]. NiV-M infection of pigs can have considerable economic and public health consequences for the affected regions.

During the Malaysia/Singapore outbreak, swine served as the amplifying host for NiV-M due to the rapid spread of NiV-M among pigs. In addition, NiV-M infection of pigs is difficult to

detect because pigs often show no or mild clinical signs and mortality rates among pigs are relatively low (about 5% for adult pigs). The presentation of the infection was similar to that of other respiratory diseases of pigs: the most specific clinical sign was a harsh, non-productive, barking cough. Despite the limited clinical signs, NiV-M is highly infectious in pigs and the infection rate among pigs in a NiV-M-infected herd is essentially 100%. The high infection rate is likely due to substantial NiV-M shedding by infected pigs, which can occur even in the absence of clinical signs, and by the swine industry practice of keeping pigs in close quarters [Mohd Nor *et al* 2000, Epstein *et al* 2006].

Almost all human cases in the 1998/1999 outbreak were due to exposure to infected pigs. In humans, NiV-M caused severe and rapidly progressive encephalitis with an approximately 40% mortality rate. The predominating clinical features were neurological, although respiratory signs and symptoms were also present. Cases of relapse encephalitis occurred in some patients who had recovered from the infection; late-onset encephalitis was also observed [Chua 2003, Tan *et al* 2002].

Since the initial 1998/1999 outbreak of NiV-M, all subsequent outbreaks of NiV have been caused by NiV-B and have occurred in Bangladesh or India; there is evidence that a closely related, NiV-like henipavirus caused an outbreak in the Philippines, but the genotype of this virus is unknown [Clayton 2017]. Although NiV-B shares substantial similarity with NiV-M [Harcourt *et al* 2005], the two genotypes are epidemiologically and clinically distinct. Transmission of NiV-B from bats to humans has been frequently associated with human consumption of raw date palm sap contaminated by bat secretions rather than via infected domestic animals. Outbreaks of NiV-B have also involved human-to-human spread, which was not common in the NiV-M outbreak [Luby *et al* 2009]. Clinically, human disease caused by

NiV-B has a greater respiratory component than disease caused by NiV-M, while NiV-M appears to cause a more severe encephalitic disease than NiV-B. NiV-B also has a higher case-fatality ratio (~70%) than NiV-M (~40%) [Chong *et al* 2008, Lo and Rota 2008].

NiV-M infection has been seen in many species other than bats, humans, and pigs. The range of susceptible hosts is broad: henipaviruses are the only zoonotic paramyxoviruses and can establish infection in the greatest number of different mammalian orders of all known paramyxoviruses to date [Middleton and Weingartl 2012, Geisbert *et al* 2012, Eaton *et al* 2006]. Table 1 summarizes the different mammalian orders and species found to be naturally and experimentally susceptible to NiV infection. The broad host range of NiV is thought to be attributable to the evolutionary conservation of the cellular receptors it uses for attachment and entry, ephrin B2 and ephrin B3 [Pernet *et al* 2012]. NiV-M infection in swine is the focus of this investigation because of its epidemiological relationship with spillover into human populations from bats via pigs as an amplifying host.

1.2 NiV-M Pathogenesis in Swine

Tissue tropism of NiV-M appears to follow ephrin B2/B3 expression. Ephrin B2 is expressed on arterial endothelial cells, smooth muscles cells, neurons, bronchial epithelial cells, and cells involved in immune activation and bone formation; while ephrin B3 is expressed predominantly in the central nervous system [Pernet *et al* 2012, Maisner *et al* 2009].

In pigs infected intranasally, NiV-M replicates in the upper respiratory tract initially before spreading to the lungs, the lymphoid system, and the central nervous system (CNS) [Weingartl *et al* 2005, Middleton and Weingartl 2012]. NiV-M likely establishes infection in the olfactory and respiratory epithelial cells, cranial nerves (olfactory and trigeminal), and immune cells sampling

Table 1: Host range of Nipah virus.

Order	**Animal Infected**
Chiroptera	Pteropid bats [Yob *et al* 2001, Chua *et al* 2002]
Artiodactyla	Pigs [Mohd Nor *et al* 2000, Chua *et al* 2000] Goats [Mohd Nor *et al* 2000, Luby *et al* 2009[NB]] Cows[NB] [Hsu *et al* 2004]
Primate	Humans [Chua *et al* 1999] African Green Monkeys* [Geisbert *et al* 2010] Squirrel monkeys* [Marianneau *et al* 2010]
Carnivora	Dogs [Mills *et al* 2009] Cats [Hooper *et al* 2001] Ferrets* [Bossart *et al* 2009]
Perissodactyla	Horses [Mohd Nor *et al* 2000, Hooper *et al* 2001]
Rodentia	Golden hamsters* [Wong *et al* 2003] Guinea pig* [Wong *et al* 2003]

*=experimentally; [NB]=natural infection observed with NiV-B but not NiV-M

the airway [Weingartl *et al* 2005, Lamp *et al* 2013]. Invasion of the CNS by NiV-M in pigs can occur by infection of cranial nerves, allowing retrograde transport of the virus into the brain [Weingartl *et al* 2005]. CNS invasion may also occur through viremia, possibly involving passage through the choroid plexus, infection of blood-brain barrier endothelial cells, or cell-associated transmigration in NiV-M-infected immune cells [Weingartl *et al* 2005, Middleton *et al* 2002].

NiV-M likely does not cross the epithelial cell barrier by direct infection of epithelial cells at early time points post-inoculation because progeny NiV-M is only released from the apical side of such cells, even though it can infect polarized epithelial cells at either the apical or basolateral pole. This is thought to be a result of the localization of the M protein specifically to the apical side of polarized epithelial cells. As a result, at early time points, NiV-M only accumulates in the luminal compartment after infection of polarized epithelial cells [Lamp *et al* 2013]. NiV-M may instead cross the epithelial cell barrier by infecting immune cells in the mucosa such as dendritic cells (DCs) that extend processes across the epithelial cell barrier to sample the airway for antigen. These DCs could then bring NiV-M to the lymph nodes in the normal process of presenting encountered antigen and thus spread the virus to susceptible cells of the lymphoreticular system [Weingartl *et al* 2005, Lamp *et al* 2013, Steinman and Banchereau 2007]. Detection of NiV-M in the lymph nodes draining the mouth and nasal cavity at early time points post-inoculation as well as the apparent targeting of lymphoid organs in NiV-M infection [Middleton and Weingartl 2012] would be consistent with infection of antigen-presenting cells in the oronasal mucosa early post-infection.

NiV-M-infected immune cells or, at later time points, infected respiratory epithelial cell syncytia facilitate spread of NiV-M into the endothelial cells of small blood and lymph vessels

[Weingartl *et al* 2005, Lamp *et al* 2013, Middleton and Weingartl 2012]. Endothelial cell infection together with the infection of circulating infected immune cells contributes to viremia [Middleton and Weingartl 2012, Stachowiak and Weingartl 2012]. Viremia allows dissemination of NiV-M to organs throughout the body influenced by its specific tropism: NiV-M will infect the small blood vessels of the body, particularly in the blood-air and blood-brain barriers, as well as lymphoid organs [Maisner *et al* 2009, Middleton and Weingartl 2012].

1.2.1 Effects on Immunity and Immune Cells

In NiV-M infections of pigs, lymphoid organs stain positively for NiV-M antigen and later in infection suffer depletion, reduction of germinal centres, and occasionally lymphoid necrosis. Infiltrating immune cells (e.g. DCs or lymphocytes) in the brain and lungs also stain positive for NiV-M antigen [Middleton and Weingartl 2012].

Destruction of lymphoid tissues and infection of immune cells by NiV-M has consequences for the immune response of swine. NiV-M-infected pigs show signs of transient immunosuppression, especially after the acute phase of infection [Berhane *et al* 2008]. The development of neutralizing antibodies towards NiV-M in pigs is delayed compared to the neutralizing antibody response against HeV or influenza virus [Berhane *et al* 2008, Li *et al* 2010, Pomorska-Mól *et al* 2012]. The anti-NiV-M neutralizing antibody response peaks by 16 dpi but does not adequately control infection: NiV-M could still be isolated from serum at 24 dpi, and viral RNA was still detectable at 29 dpi. NiV-M-infected pigs also developed secondary bacterial infections after 7 dpi, indicative of immunosuppression [Berhane *et al* 2008].

Despite the delayed neutralizing antibody response, NiV-M does not productively infect the immune cells that direct the humoral immune response, porcine B lymphocytes or CD4+CD8-

helper T cells [Stachowiak and Weingartl 2012]. Among porcine peripheral blood mononuclear cells (PBMCs), NiV-M productively infects monocytes, CD6+CD8+ T lymphocytes, and natural killer (NK) cells. However, CD8+ and CD4+CD8- T cell populations in porcine PBMCs both were observed to decline in *in vitro* and *in vivo* NiV-M-infection. The decline of CD4+CD8- populations *in vitro* was thought to be a bystander effect mediated by soluble factors released by other dying PBMCs [Stachowiak and Weingartl 2012]. In contrast to the variety of porcine PBMCs productively infected with NiV-M, only DCs are permissive among human PBMCs [Mathieu *et al* 2011].

1.2.2 Cytokine Dysregulation

The dysregulation of the immune response likely involves NiV-M mediated effects on the innate immune system. NiV-M infection was observed to downregulate IFNα mRNA expression in infected porcine CD6+ T cells, indicating that the inhibition of antiviral mediator secretion by NiV-M in infected porcine immune cells may contribute to the dysregulation of the porcine immune response to NiV-M [Stachowiak and Weingartl 2012].

NiV-M infection of human monocyte-derived DCs (moDCs) stimulated the release of a variety of pro-inflammatory cytokines but not IFNα or IFNβ [Gupta *et al* 2013]. However, because NiV-M infection of human PBMCs differs substantially from its infection of porcine PBMCs, the effects of NiV-M on immune cells in pigs and humans should not be expected to parallel each other.

1.3 NiV-M Molecular Biology

As all other Paramyxoviridae, NiV is an enveloped virus with a negative sense (-), non-

segmented, single-stranded (ss)RNA genome. Members of the genus *Henipavirus* have larger genomes than most other Paramyxoviridae, and NiV-M has a genome of 18,246 nucleotides (nt) [Eaton *et al* 2006]. The NiV-M genome also adheres to the rule of six, which prescribes that paramyxovirus genomes must be evenly divisible by six as a consequence of the requirement for each nucleoprotein subunit to associate with six nucleotides of RNA [Halpin *et al* 2004].

The NiV-M genome contains 6 genes and encodes 9 different proteins as depicted in Figure 1A. The N gene produces the nucleoprotein (N protein) which associates with genomic and antigenomic RNA to form the nucleocapsid. The P gene encodes four proteins: the phosphoprotein (P protein), a structural protein required for proper nucleocapsid assembly and polymerase activity [Longhi *et al* 2017, Jamin and Yabukarski 2017]; and the V, W, and C proteins, three proteins with auxiliary functions relevant to pathogenesis but not essential for the virus life cycle. These co-amino-terminal P, V, and W proteins are visualized in Figure 1B and their origin is described in depth in section 1.4.5 of this thesis. The M gene encodes the matrix (M) protein, which is important for virion assembly and is the primary viral protein responsible for budding and release; there is also some evidence that the M protein can block the induction of the antiviral response [Bharaj *et al* 2016]. The F and G genes encode the two surface glycoproteins of NiV: the fusion (F) glycoprotein and the attachment (G) glycoprotein, respectively. The G protein is responsible for attachment to ephrin B2 and ephrin B3 on cells, which function as receptors for the virus. The F protein mediates fusion between the viral and host cell membranes during entry. Finally, the L gene produces the large (L) protein, which contains all the enzymatic activities of an RNA-dependent RNA polymerase (RdRp) for transcription and replication of viral RNA [Eaton *et al* 2006, Lamb and Parks 2013].

Figure 1. (A) NiV-M gene order and protein products of the P gene. (B) Location of known, important domains of co-amino-terminal P gene products. Domain locations found in [Habchi and Longhi 2015, Chan *et al* 2004, Yabukarski *et al* 2014, Shaw *et al* 2004, 2005, Rodriguez *et al* 2004, Ciancanelli *et al* 2009, Rodriguez *et al* 2002, Bruhn *et al* 2014, Chan *et al* 2004]. The unique regions of the P protein are shown in blue; of the V protein in yellow; and of the W protein in green. STAT1 = signal transducer and activator of transcription protein 1; PMD = P protein multimerization domain; N^0 = non-nucleocapsid bound nucleoprotein monomer; N^{NUC} = nucleoprotein in nucleocapsid; P_{XD} = N^{NUC} binding domain on P protein; NES = nuclear export sequence; NLS = nuclear localization sequence.

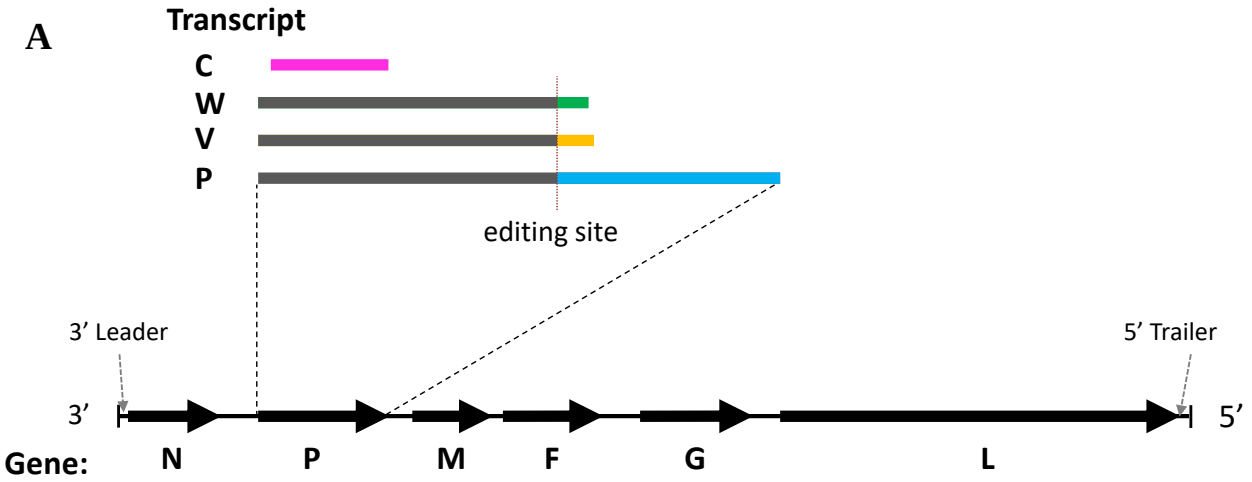
A
Transcript
C
W
V
P
editing site
3' Leader
5' Trailer
3'
5'
Gene:
N
P
M
F
G
L

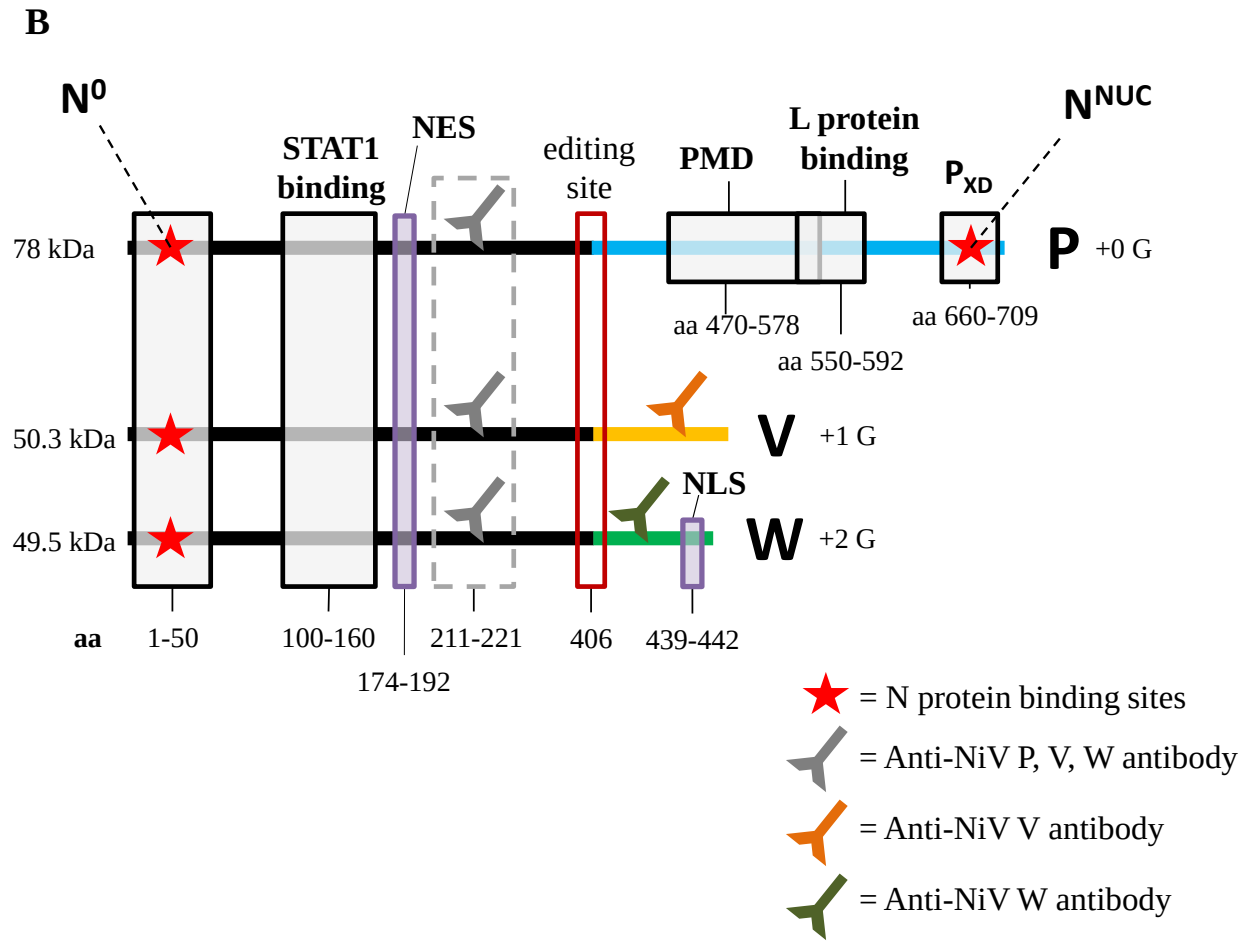
B
N0
STAT1 binding
NES
editing site
PMD
L protein binding
NNUC
PXD
78 kDa
P +0 G
aa 470-578
aa 550-592
aa 660-709
50.3 kDa
V +1 G
NLS
49.5 kDa
W +2 G
aa
1-50
100-160
174-192
211-221
406
439-442
= N protein binding sites
= Anti-NiV P, V, W antibody
= Anti-NiV V antibody
= Anti-NiV W antibody

Infectious wild-type NiV-M virions are pleomorphic in shape and have the F and G proteins on the surface. Within the virion, the NiV-M RNA genome is encapsidated by the N protein, and the P and L proteins are present in association with the N protein. The N protein-encapsidated RNA within the virion takes on a herringbone structure typical of paramyxoviruses. The M protein forms a shell inside the envelope of the virion that is thought to have multiple contacts with the nucleocapsid [Lamb and Parks 2013]; in some paramyxoviruses, notably Measles virus (MeV), the nucleocapsid may sometimes be coated with a layer of M protein [Cox and Plemper 2017].

The protein content of the nucleocapsid is predominantly N protein, with fewer copies of P protein and even fewer copies of L protein: the ratio of these proteins for paramyxoviruses in the subfamily *Paramyxovirinae* has been estimated to be approximately 2600 N : 300 P : 40 L based on analysis of Sendai virus (SeV) virions, with the amount of N proteins proportional to the length of the genome as dictated by the rule of six [Lamb *et al* 1976]. Based on these numbers, a NiV-M virion would be expected to contain approximately 3041 N proteins, 351 P proteins, and 47 L proteins. This approximation was made under the assumption that one genome is packaged per virion, which is not true for all paramyxoviruses [Lamb *et al* 1976, Loney *et al* 2009]. Based on the range of possible NiV-M virion sizes, NiV-M itself may package multiple genomes per virion [Goldsmith *et al* 2003].

Incorporation of the non-structural V, W, and C proteins has been detected in purified NiV-M virions although at fewer copies (as a ratio to the P protein content) than they are found in infected cell lysates [Lo *et al* 2009]. Incorporation of non-structural proteins into virions occurs in some but not all paramyxoviruses: the V protein is found in virions of simian virus 5 (SV5), mumps virus (MuV), and Hendra virus (HeV); but not in MeV or SeV [Lo *et al* 2009, Gombart

et al 1992]. No rigorous quantitation of the amount of non-structural proteins in NiV virions has been performed to date, and the location of these non-structural proteins in the NiV virion is also unknown. In SV5, the V protein was found to be closely associated to the nucleocapsid, although it is uncertain whether this interaction is direct between the V and the nucleocapsid proper or through the M protein of SV5 [Paterson *et al* 1995].

1.3.1 The Nucleoprotein (N Protein)

The primary function of the N protein is to homopolymerize on NiV genomic and antigenomic RNA to form the herringbone nucleocapsid structure and protect the RNA; for this, the NiV-M N protein requires multiple specific sequences between aa 30 to 404 which are highly conserved among paramyxoviruses [Ong *et al* 2009]. Intracellularly, the N protein exists in one of two principal conformations: the monomeric, soluble form called N^0; and the homopolymerized, nucleocapsid form called N^{NUC}. Expressed alone, the N protein will spontaneously encapsidate cellular RNA and also form small, abortive nucleocapsid fragments. Proper encapsidation of the RNA genome requires co-expression of the P protein [Habchi and Longhi 2015]. Only one region of the N protein, aa 473-493, participates in interactions with the polymerase complex, which it does by interacting with certain domains of the P protein [Blocquel *et al* 2012]. This region is found on the long, disordered, C-terminal tail of the NiV-M N protein [Habchi and Longhi 2015].

1.3.2 The Phosphoprotein (P Protein)

The NiV-M phosphoprotein (P protein) is a 709 aa protein required as a cofactor for virus replication. It forms a crucial component of the NiV-M polymerase machinery by linking the N

protein, the viral RdRp (the L protein), and the nucleoprotein-associated viral RNA. Structurally, the P protein can be divided into two regions by the editing site where the P, V, and W proteins diverge in their amino acid sequences: the P protein N-terminal region (PNT), consisting of aa 1-406; and the P protein C-terminal region (PCT), consisting of aa 407-709 [Habchi and Longhi 2015]. The domains of the P protein and their functions, where known, are represented in Figure 1B and summarized Table 2.

The well-ordered aa 1-50 of the PNT correspond to an N binding site for interacting with monomeric N^0 [Chan *et al* 2004, Yabukarski *et al* 2014]. By the P-N^0 interaction, the paramyxovirus P protein chaperones monomeric N protein to ensure proper assembly of the ribonucleocapsids [Yabukarski *et al* 2014, Errington and Emmerson 1997]. The previously-mentioned free N protein that controls the switch for viral transcription to replication refers to the N^0 that is kept in an accessible form by the P protein PNT.

The remainder of the PNT lacks a well-structured fold and is considered an intrinsically disordered region (IDR) [Habchi *et al* 2010]. The flexible, disordered portion of the PNT contains an amino acid sequence, aa 88-113, reported to be necessary for NiV polymerase core complex function in a minireplicon assay and leading to the hypothesis that the NiV-M PNT has a non-enzymatic polymerase cofactor function [Ciancanelli *et al* 2009]. This is unusual: in most paramyxoviruses, the P protein cofactor function can be mediated entirely by the PCT [Lamb and Parks 2013]. Other domains in the PNT are involved in auxiliary functions of the P protein that are not directly involved in replication. The binding domain for STAT1 (aa 114-140) is found in the PNT, as is a nuclear export signal (NES) at amino acids (aa) 174-192 that allows cytoplasmic accumulation of the protein [Rodriguez *et al* 2004, Ciancanelli *et al* 2009].

Table 2: P protein domain names, functions, and locations.

P protein N-terminal Region (PNT)			
Domain	**Function(s)**	**Location (amino acids)**	**Reference**
N^0-binding domain	Chaperones soluble N protein (N^0)	1-50	[Chan *et al* 2004; Yabukarski *et al* 2014]
STAT1 binding domain	IFN signalling inhibition	114-140	[Shaw *et al* 2004; Rodriguez *et al* 2004; Ciancanelli *et al* 2009]
Necessary polymerase cofactor region	Needed for polymerase complex function in minireplicon assay	88-113	[Ciancanelli *et al* 2009]
NES	Nuclear export signal	174-192	[Rodriguez *et al* 2002; Rodriguez *et al* 2004]
P protein C-terminal Region (PCT)			
Domain	**Function(s)**	**Location (amino acids)**	**Reference**
PMD	P multimerization domain	470-578	[Bruhn *et al* 2014]
L-protein binding domain	Binds L protein, required for replication	550-592	[Lamb and Parks 2013]
P_{XD}	Binds nucleocapsid-bound N protein (N^{NUC})	660-709	[Chan *et al* 2004]

In contrast to the disordered PNT, the PCT has more domains that are well-ordered. The P protein multimerization domain (PMD) at aa 470-578 mediates tetramerization of the P protein into P_4 [Bruhn *et al* 2014]; P protein multimerization is essential for replication of paramyxoviruses [Lamb and Parks 2013]. The P protein L-binding domain is predicted to be at aa 550-592 based on its location in other paramyxoviruses [Bruhn *et al* 2014]. The C-terminal residues aa 660-709 comprise the P protein X domain (P_{XD}), which is responsible for binding to nucleocapsid-assembled N^{NUC} [Chan *et al* 2004].

The P protein is important to many steps in NiV-M transcription and replication. P-N binding interactions induce conformational changes in the N protein that allow control over the assembly of N^0 into N^{NUC} and over access to the RNA by the P-L polymerase core complex. Binding of the PNT to the N^0 protein keeps the N protein in an open conformation, allowing it to close only on RNA in the presence of N^{NUC} proteins to build the nucleocapsid. The PCT interaction with L and N^{NUC} brings the L protein in contact with viral RNA for transcription and replication [Yabukarski *et al* 2014, Habchi and Longhi 2015].

1.4 NiV-M Life Cycle

1.4.1 Overview

The life cycle of NiV-M is summarized in Figure 2. NiV-M attaches to susceptible cells via its G protein and then the activated F protein mediates fusion of the viral envelope with the cell membrane. Upon fusion, the contents of the virion are released into the cell cytoplasm. Transcription of the genome begins soon after its release into the cytoplasm because all necessary polymerase components (namely the L and P proteins) are present with the genome in the virion and are available to begin RNA polymerization after the ribonucleocapsid enters the

Figure 2. The basic infectious cycle of NiV-M. (A) The infectious, wild-type NiV-M virion and its content. The ribonucleocapsid is represented as a stretch of N proteins, which occlude the actual genomic RNA: the repeating pattern of the N protein around the RNA genome creates the characteristic herringbone pattern that is visible under electron microscopy. (B) NiV-M attaches to ephrin B2/B3 receptors on susceptible cells via its G protein; then, the viral envelope fuses with the cell membrane via the F protein. Fusion with the membrane releases the virion's contents into the cell cytoplasm. (C) In the cytoplasm, the NiV-M genome is transcribed into mRNA; in the presence of adequate N protein, replication also occurs using the antigenome as an intermediate. Genes closer to the 3' end of the genome are transcribed to the greatest copy numbers. Capped and polyadenylated viral mRNAs are translated by host ribosomes. (D) With the viral glycoproteins on the cell surface and the genome and associated proteins brought to the membrane, the M protein drives the budding of new progeny NiV-M virion from the surface of the cell.

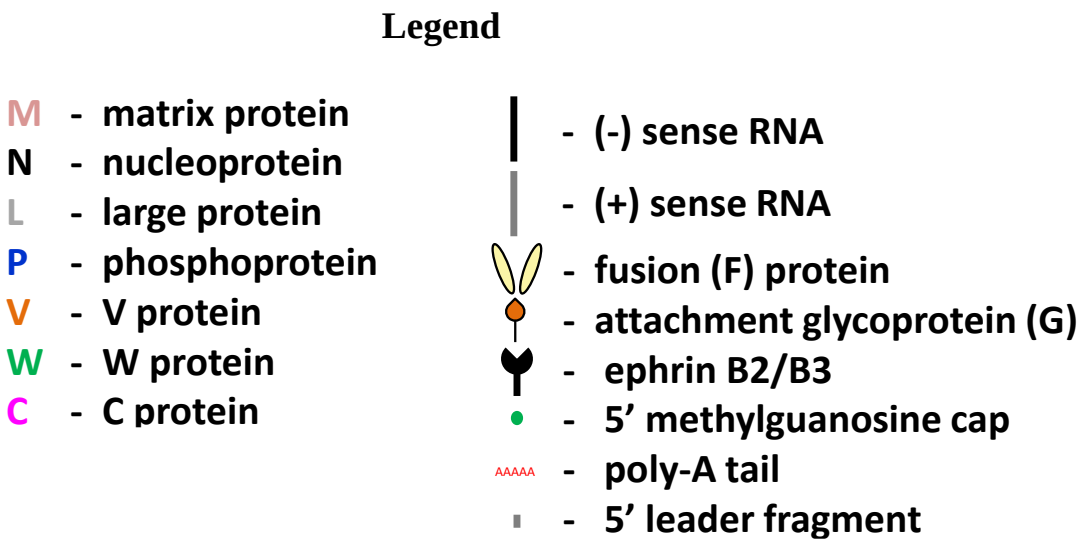

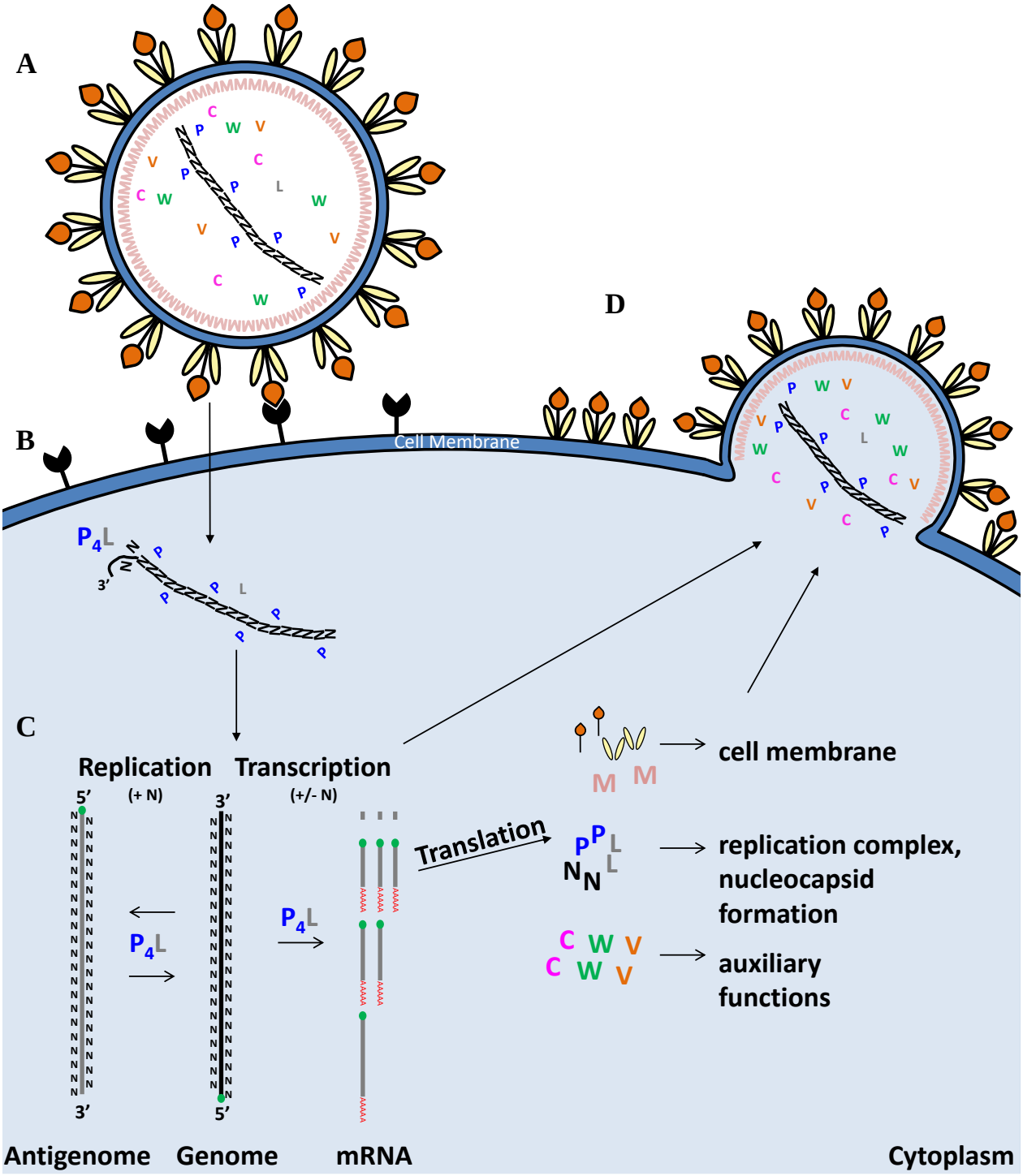
A
B
C
D
Cell Membrane
P4L
3'
Replication
Transcription
5'
(+ N)
3'
(+/- N)
P4L
P4L
Translation
M M
cell membrane
P P L
N N L
replication complex, nucleocapsid formation
C W V
C W V
auxiliary functions
Antigenome
Genome
mRNA
Cytoplasm

cytoplasm. Primary transcription occurs until enough N proteins are present to encapsidate nascent genomes. Replication leads to the production of full-length, positive-sense RNA antigenomes (directed by the leader promoter), and then full-length, negative-sense RNA genomes are produced from the antigenomes (under the direction of the trailer promoter). Secondary transcription begins when the newly produced progeny genomes are used along with the original incoming genomes to supplement viral transcription [Noton and Fearns 2015, Rima and Duprex 2009, Rota and Lo 2012].

Viral mRNA transcripts can be translated immediately after their production because the viral polymerase provides them with methylated 5' caps and poly-adenosine tails typical of cellular mRNA [Noton and Fearns 2015]. Some viral proteins are post-translationally modified in the infected cell after they are produced by acetylation, phosphorylation, or, in the case of the F protein, proteolytic activation [Rota and Lo 2012, Shiell *et al* 2003]. After they are produced, the F and G proteins, the surface glycoproteins of NiV-M, are trafficked to and expressed on the cell surface. Because they exist on the cell surface in an activated form, the F and G proteins can mediate fusion of the infected cell's membrane with adjacent ephrin B2/3-expressing cells, resulting in the formation of multinucleated cells (syncytia).

NiV-M exits infected cells by budding from the cell surface membrane [Hyatt *et al* 2001]. Budding is directed primarily by the M protein, and F and G proteins on the surface of the cell end up on the surface of the virions. It is not well understood how the ribonucleocapsids are included into the budding particles of paramyxoviruses, but the process does allow for the packaging of multiple genomes per virion [El Najjar *et al* 2014]. NiV-M virions are considered mature immediately after budding because the proteolytic activation of the F protein occurs in the infected cell prior to virion release.

1.4.2 Attachment and Entry

After NiV-M attaches to the ephrin B2 or ephrin B3 of a susceptible cell by its G protein, the F protein mediates fusion of the NiV membrane with the host cell membrane [Aguilar *et al* 2009]. The NiV F protein is activated by proteolytic cleavage in the endosomal compartment prior to virion release from infected cells [Diederich *et al* 2005]. Pre-release activation of the F protein obviates the requirement of endocytosis for NiV entry [Earp *et al* 2005, White and Whittaker 2016]. Concordantly, NiV-M entry into cells is pH-independent. Activated F protein on the surfaces of infected cells can mediate fusion with adjacent cells, causing the formation of syncytia [Lamb and Parks 2013].

Most paramyxoviruses are thought to enter cells by fusion at the plasma membrane, and this has been observed for NiV-M [Lamb and Parks 2013, Diederich *et al* 2008]. It has also been suggested that macropinocytosis is required for NiV-M entry into cells and that this is induced when the attachment of the G protein to ephrin B2/B3 initiates reverse signalling in the target cells [Pernet *et al* 2009]. This theory links the mechanism of entry of NiV-M with the known biological roles of the ephrin B2 and B3 in initiating cytoskeletal rearrangements involved in cell attraction/repulsion events [Pitulescu and Adams 2010]. However, cell-cell fusion by F and G protein expression alone did not require macropinocytosis, making it difficult to determine whether ephrin-induced macropinocytosis is necessary, enhancing, or simply incidental to NiV entry [Pernet *et al* 2009].

Discrepancies in observed entry mechanisms may also relate to differences in cell types. NiV-M appears to enter human DCs by macropinocytosis, which might be a common entry mechanism for cells that undergo large volumes of macropinocytosis constitutively such as DCs and macrophages [Mathieu *et al* 2011, Lim and Gleeson 2011]. The overall entry mechanism of

NiV-M into a particular cell may simply be the difference between the rate of membrane fusion [Aguilar *et al* 2010] and the rate of uptake by macropinocytosis [Kerr *et al* 2006], induced or constitutive, in the particular cell type. The mode of entry of NiV-M in particular cell types is important for understanding detection of the virus by host cells, as different entry modes expose a virus to different host proteins and systems involved in viral detection.

1.4.3 Transcription and Replication

In order to understand what NiV-M replication products are present either to allow detection of the virus by the host cell or to prevent such detection systems from functioning properly, it is important to understand the timing of replication of paramyxoviruses. There are several proposed mechanisms for how paramyxovirus transcription and replication are regulated. These are described by Noton and Fearns [2015] and summarized here:

Transcription and replication of the genome of paramyxoviruses requires the formation of a complex between the L protein, which provides the enzymatic functions; the phosphoprotein (P protein), which performs essential cofactor functions; and the nucleoprotein (N protein), which encapsidates the RNA genome and directs the P-L polymerase complex to the genome for transcription and replication. Both transcription and replication of viral RNA a start at the 3’ end of the genome where the viral polymerase complex binds to the 3’ leader promoter (or the trailer promoter, when the antigenome is the template for replication).

At the initiation of transcription, a short transcript of the 3’ leader sequence is produced as the viral polymerase scans the template for the first gene start (*gs*) sequence. In the absence of N protein, this leader transcript is released from the polymerase complex and the polymerase transcribes the viral genes in 3’ to 5’ order, initiating transcription at each gene’s *gs* sequence

and ending at the gene's gene end (*ge*) sequence. Stuttering of the viral polymerase on a tract of template uridine residues in the *ge* sequence results in polyadenylation of the viral mRNAs [Hausmann *et al* 1999, Rota and Lo 2012]; the L protein also provides all mRNA gene transcripts with a methylated 5' cap [Noton and Fearns 2015]. The leader transcript, however, is neither polyadenylated nor given a 5' cap [Plumet *et al* 2007].

The viral polymerase stuttering mechanism that polyadenylates the viral mRNA transcripts also mediates the co-transcriptional editing process that produces the P, V, and W proteins from overlapping reading frames in the P gene. At an editing site in the P gene, the viral polymerase can stutter to insert non-templated guanine (G) residues, pushing the subsequent sequence of the mRNA transcript out of frame. These transcripts are then translated into the P protein (reading frame is unchanged), the V protein (reading frame is +1), or the W protein (reading frame is +2) [Hausmann *et al* 1999, Lamb and Parks 2013], as shown in Figure 1.

Between each gene (after the *ge* sequence but before the next gene's *gs* sequence), there are intergenic regions that the viral polymerase does not transcribe. At the end of each *ge* sequence, the viral polymerase has a finite chance of becoming detached from the genome instead of continuing to the subsequent (5') gene. Because transcription always begins at the 3' leader sequence, this creates a transcription gradient: the genes closer to the 3' end of the genome are transcribed to the greatest number of mRNA copies, and the genes at the 5' end are transcribed to the least [Rota and Lo 2012]. The magnitude of the gradient has not been determined for NiV-M, but the N gene of HeV is transcribed to just over ten times as many copies as the L gene in infected Vero cells [Wright *et al* 2005]. The empirically determined N/L ratios of HeV and other paramyxoviruses are shown in Table 3.

Table 3: Published ratios of N to L mRNA copy numbers in *Paramyxovirus* family members.

Virus	Genus	N/L ratio	Literature Source	ΔC_T N-L
Hendra virus	*Henipavirus*	11.1	[Wright *et al* 2005]	-3.47
Sendai virus	*Respirovirus*	33.3	[Homann *et al* 1990]	-5.06
Measles virus	*Morbillivirus*	66.7; or 58.8	[Cattaneo *et al* 1987]; [Plumet *et al* 2005]	-6.06 -5.88

During replication, the leader transcript is encapsidated and not released from the polymerase complex. This allows the polymerase complex to ignore *gs* and *ge* sequence signals to generate complete, encapsidated, antigenomic copies of the viral RNA. Antigenomes are not transcribed but contain a trailer promoter to direct the viral polymerase to use them as a template for genome production. Both genomes and antigenomes are synthesized concomitantly with their N protein encapsidation so that no genome or antigenome exists without a nucleocapsid. Neither genomes nor antigenomes have a 5' cap [Noton and Fearns 2015, Plumet *et al* 2007].

Replication of the NiV-M genome occurs only if there is a sufficient local concentration of free N protein to encapsidate full-length viral genomes and antigenomes and so only occurs after a certain period of transcription and translation alone: viral transcription predominates early in infection. After enough N protein has been produced to initiate replication, enough N protein is produced by primary and secondary genome transcript that transcription and replication can be considered to occur more or less simultaneously [Noton and Fearns 2015, Plumet *et al* 2005].

1.4.4 Timeline of Transcription and Replication

Models for the timing of paramyxovirus transcription and replication are well-defined for MeV and are summarized in Figure 3. As previously stated, genome transcription can theoretically be initiated immediately after entry because infectious paramyxovirus virions contain P proteins, L proteins, and encapsidated genomic RNA. From 0 to 6 hours post-inoculation (hpi), viral mRNAs accumulate at a linear rate by the action of the pre-made L protein; from 6 to 12 hpi, viral mRNAs exponentially increase as more L proteins are produced to participate in transcription; at 12 hpi, replication begins and production of viral mRNAs, genomes, and antigenomes increases; and after 24 hrs, viral mRNA synthesis begins to slow and

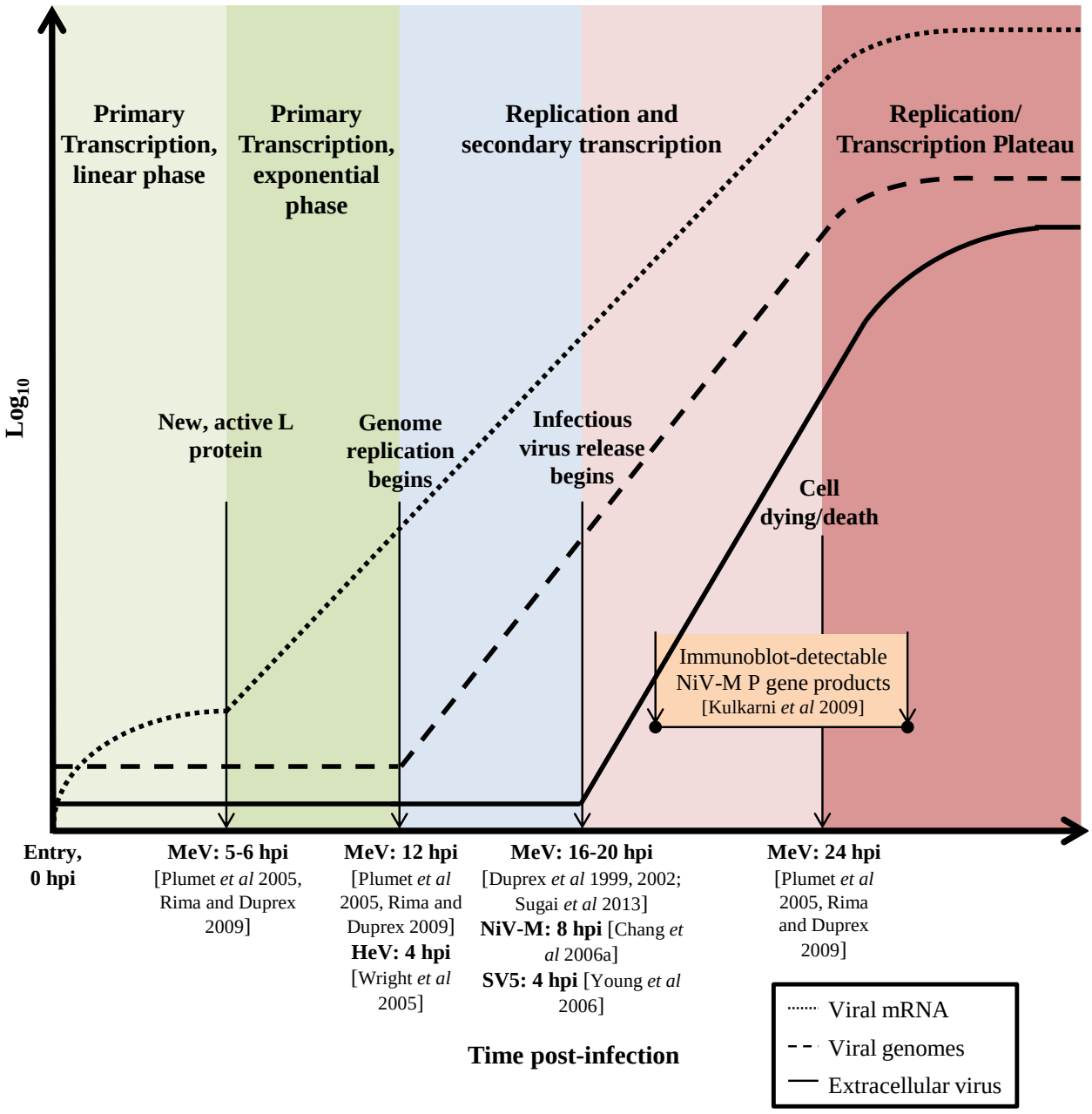

Figure 3. Timing of transcription and replication in paramyxoviruses. The time scale is relative to the particular virus; known times at which the important events indicated take place for particular viruses are listed below the x-axis. Lines represent trends and values are not to scale.

eventually plateau [Plumet *et al* 2005, Rima and Duprex 2009].

To the extent that the constraints of BSL4 work have allowed this type of investigation, this general trend seems to be similar for HeV and NiV-M although it occurs at a greater rate [Wright *et al* 2005, Chang *et al* 2006a]: while release of infectious, wild-type MeV may occur 16-20 hpi or even later, NiV-M release was detected as early as 8 hpi with the greatest increases in extracellular virus detection after 8 hpi [Sugai *et al* 2013, Chang *et al* 2006a]. The comparatively more rapid kinetics of release of NiV-M are similar to those of the related HeV, for which intracellular production of genomic RNA has been investigated. Intracellular production of HeV genomic RNA occurs at earlier time points than for MeV, with a significant increase in HeV genomic RNA occurring between 4 and 6 hpi compared to after 12 hpi for MeV [Wright *et al* 2005, Plumet *et al* 2005]. Some of the differences between these viruses may be attributable to the cell types used in these studies: replication of NiV-M has been found to be markedly slower in some susceptible cell types [Chang *et al* 2006b]; however, in the cell types in which they can be compared, the infectious cycles of NiV-M and HeV are faster than that of MeV [Plumet *et al* 2005, Sugai *et al* 2013, Chang *et al* 2006a, Wright *et al* 2005].

1.4.5 Viral Protein Synthesis

It is difficult to determine exactly when paramyxovirus proteins reach active concentrations in cells because it is likely that viral proteins have functional effects before they reach an amount that is detectable by immunoblot or other methods of detecting protein expression. For example, it can be inferred in MeV infections *in vitro* that newly synthesized L protein is active as early as 5 hpi based on the time point at which a change in the rate of genome/antigenome production occurs [Plumet *et al* 2005].

It is feasible that other viral proteins might be at active concentrations at 5 hpi because the transcription gradient produces transcripts for all of these proteins at higher copy numbers than the L protein [Rima and Duprex 2009, Lamb and Parks 2013]. The time point may be even earlier in faster-replicating paramyxoviruses: in SV5 infection of A549 cells, immunoblots could detect N protein at 4 hpi and P and V protein at 8 hpi (earlier time points not examined for P/V), whereas the MeV N protein was not detectable by immunoblot until 8 hpi [Young *et al* 2006, Sugai *et al* 2013]. Limited information is available on the protein production timelines of NiV-M. In 293T cells infected at MOI of 0.4 with NiV-M, the P gene products became detectable by immunoblot somewhere between 9.5 and 24 hpi [Kulkarni *et al* 2009], but no further resolution on the timing is available.

The P gene of NiV produces four distinct protein products. Transcription using only one reading frame and starting with the start codon at the beginning of the gene results in the production of the P protein, and the V and W proteins are made separately by a co-transcriptional editing mechanism whereby the viral polymerase adds non-templated guanine (G) residues to a growing P gene transcript at a certain frequency at a conserved editing site in the P gene (starting at nt 3618 in the NiV-Malaysia genome, NC_002728.1) [Lamb and Parks 2013]. By this mechanism, the P, V, and W proteins all share the same primary sequence up to aa 406 (corresponding to the PNT region of the P protein) and differ only by their unique C termini downstream of the editing site (aa 407-709 for the P protein; aa 407-456 for the V protein; and aa 407-449 for the W protein). The NiV-M V and W proteins are similar in size (50.3 kDa and 49.5 kDa, respectively; see Figure 1B) and as such are indistinguishable by size alone on immunoblots. The C protein is 19 kDa, 166 aa long, and is made by translation initiation at an alternate start site upstream of the P gene editing site (located at nt 2428 in NC_002728.1) but in

an alternate (+1) reading frame. As a result, the C protein primary sequence has no homology with the other P gene products.

The V, W, and C proteins are the primary proteins of NiV-M involved in the evasion of cellular detection. They are considered to be non-structural and accessory proteins, so they are not expected to mediate any biological effects until replication proceeds to the point where adequate amounts are newly synthesized. Production of the NiV V and W proteins is more delayed than that of the P protein because the editing frequency of the P gene initially favours P protein transcripts: at 2.5 hpi, 64-100% of P gene transcripts code for the P protein. The percent of V and/or W transcripts exceeds that of P transcripts somewhere between 6 and 9.5 hpi [Kulkarni *et al* 2009]. Likely, newly synthesized V/W proteins would not be expected to be at biologically relevant concentrations before 4 hpi; this approximately coincides with the time point where significant genome replication is thought to occur (discussed above). However, as previously discussed, the accessory proteins of NiV-M have been found in purified, concentrated virion preparations by immunoblot: potentially, the accessory P gene products proteins are present intracellularly immediately after the release of the viral envelope contents**.** To date, the significance of this has not been investigated.

1.4.6 Virus Maturation and Egress

NiV-M virions exit infected cells by budding from the surface plasma membrane. The NiV-M surface glycoproteins (G and F proteins) and the M protein are trafficked to the surface after their production: the F and G proteins are integral membrane proteins, while the M protein remains associates on the inside of the membrane with their cytoplasmic tails. The F protein is initially present in its inactive (F_0) form: to be activated, F_0 is endocytosed and cleaved by acid-

dependent proteases in the mature endosome into its heterodimeric active form (F_1/F_2), whereupon it is re-trafficked back to the cell surface. The F_1/F_2 form of the fusion protein is competent to mediate fusion with other plasma membranes, in conjunction with G protein binding. The M protein is the primary driver of virion budding and interacts with both the cytoplasmic tails of the F and G proteins and the ribonucleocapsid to bring these components together for budding of the virus [El Najjar *et al* 2014, Patch *et al* 2007]. After budding from the cell, virions containing complete NiV-M genomes are theoretically capable of initiating another cycle of infection in a susceptible cell.

1.5 The Antiviral Response: Type I Interferon (IFN)

1.5.1 Overview of the Type I IFN Response

Type I interferons (IFN) are soluble factors important for innate and adaptive antiviral immune responses. Consequently, most viruses (including NiV-M) have evolved mechanisms to combat or evade them. The most well-characterized of this family are IFNα and IFNβ. The porcine type I IFN family has 7 distinct type I IFNs (IFNα, β, δ, ω, ε, κ, and αω) and 17 subtypes of IFNα, while IFNβ is produced from a single gene [Sang *et al* 2014].

Most cells can produce IFNα and IFNβ [McNab *et al* 2015]. Cells are induced to produce IFNα/β after detection of intracellular pathogen-associated molecular patterns (PAMPs) using pattern recognition receptors (PRRs) such as endosomal Toll-like receptors (TLRs) and cytosolic RIG-I-like helicase Receptors (RLRs). Signalling by these PRRs induces IFNα/β production by the infected cells.

1.5.2 Constitutive Expression of Type I IFN

In addition to their role in viral infections, type I IFNs are constitutively expressed in humans and in swine [Gough *et al* 2012, Amadori *et al* 2010]. Constitutively expressed subtypes of type I IFN are different from the subtypes induced by virus infection and constitutive expression of type I IFN is greatly reduced compared to virus-induced expression [Razzuoli *et al* 2011, Tovey *et al* 1987]. Virus-independent type I IFN primes cells for an efficient antiviral response, enhances responsiveness to other cytokines, and is involved in normal cell functions and homeostasis [Hata *et al* 2001, Amadori 2007, Gough *et al* 2012]. Expression of type I IFN in pigs also increases in the absence of pathogen at predictable times, particularly post-wean; this increase is mediated by PBMCs [Amadori 2007]. In porcine PBMCs, monocytes and pDCs are the primary populations responsible for constitutive IFNα production [Amadori *et al* 2010]. Experimental infections of pigs with NiV were performed post-wean at 5 to 6 weeks of age due to space constraints in BSL4 animal holding facilities [Middleton and Weingartl 2012].

1.5.3 IFNα/β Signalling

Cells respond to produced IFNα/β via specific receptors expressed on all somatic cells [de Weerd and Nguyen 2012]. Binding of type I IFN to the transmembrane cell surface IFNα/β receptor (IFNAR), composed of IFNAR1 and IFNAR2 subunits, initiates a JAK/STAT signal transduction cascade involving the receptor-associated protein tyrosine kinases JAK1 and TYK2 and the cytoplasmic transcription factors STAT1 and STAT2. The cascade culminates in the phosphorylation and nuclear translocation of STAT1-STAT2 heterodimers in complex with IRF9 which bind to interferon-sensitive response elements (ISREs) to upregulate interferon-stimulated genes (ISGs) [Ivashkiv and Donlin 2014]. This signalling pathway is summarized in Figure 4.

Figure 4. Type I IFN signalling pathway for initiating antiviral state in responsive cells. Known points of inhibition of these pathways by NiV-M P gene products are also indicated.

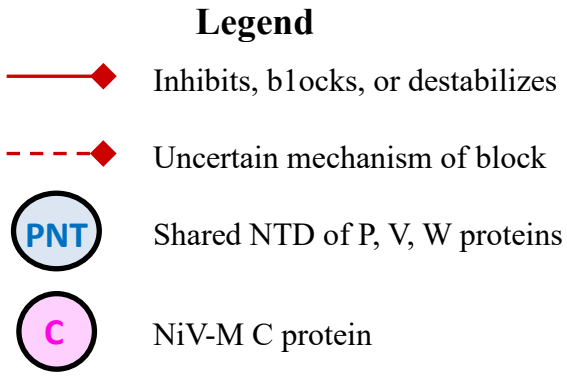

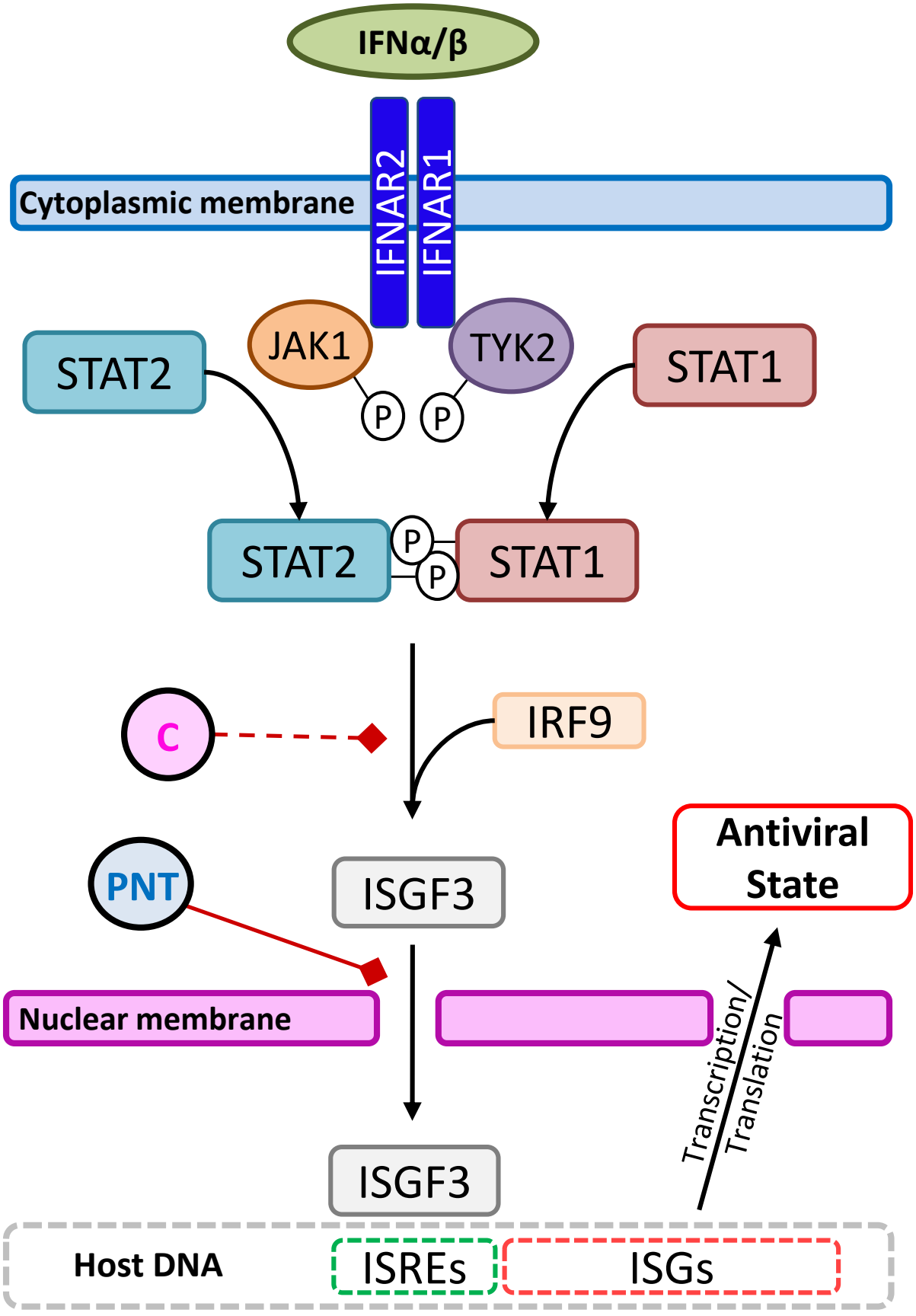
IFNα/β
IFNAR2
IFNAR1
Cytoplasmic membrane
JAK1
TYK2
P
P
STAT2
STAT1
STAT2
P
P
STAT1
C
IRF9
PNT
ISGF3
Antiviral State
Nuclear membrane
Transcription/ Translation
ISGF3
Host DNA
ISREs
ISGs

JAK/STAT signalling is important for both immune cell signalling and the activation of the antiviral state, which can be induced in any IFNAR-expressing cell (e.g. all somatic cells). Among the ISGs are proteins that directly interfere with the virus replication cycle by physical interaction (e.g. MX1); proteins that enhance the PAMP recognition and PRR signalling capabilities (e.g. IRF7, MAVS, PKR, and OAS1); proteins that degrade intracellular RNAs (e.g. OAS1 and RNase L); and proteins that globally shut down translation (e.g. PKR and eIF2α) [de Veer *et al* 2001]. The antiviral effects of type I IFN are important to early control of viral replication and limiting viral dissemination. Their effects on immune cells are also important to the development of a robust adaptive immune response.

1.5.4 Roles of Type I IFN in the Immune Response

IFNα/β enhances the link between innate and adaptive immune responses through their actions on DCs: type I IFNs promote the generation of DCs from precursor cells and maturation of DCs, increasing their T cell priming capacity. Type I IFNs will also indirectly drive proliferation and maturation of NK cells by inducing IL-15 production by monocytes, macrophages, and DCs, and will directly enhance NK cell cytotoxicity [Crouse *et al* 2015].

Type I IFN can also directly and indirectly influence cells of the adaptive immune response. Overall, IFNα/β can enable and potentiate an effective T cell response by skewing a T_H1 type response, which is appropriate to handling intracellular pathogens [Edelman and Heissmeyer 2014, Crouse *et al* 2015]. Directly, IFNα/β enhances the proliferation, survival, and/or differentiation into effector cells of many different cell types. This includes promoting survival of activated T cells; promoting development of memory T cells from antigen-specific T cells; encouraging the proliferation, survival, and differentiation of T_H1 CD4+ T cells [Crouse *et al*

2015]; inducing the generation of plasma cells that secrete virus-specific antibodies [Jego *et al* 2003]; and enhancing the survival and proliferation of antibody-producing B cells [Braun *et al* 2002]. IFNα/β will also confine lymphocytes to lymphoid tissues to prolong their exposure to antigen-presenting cells, strengthening the link between innate immune system detection of a pathogen and the adaptive response [Gommerman *et al* 2014]. Immune cells will respond to IFNα/β by producing cytokines of their own, which then mediate the indirect effects of type I IFN. For example, CD4+ T cells produce IL-10 and IFNγ in response to IFNAR stimulation; produced IL-10 will then activate cytotoxic T cells and stimulate plasma cell differentiation, thereby potentiating both the humoral and cell-mediated immune responses [Jego *et al* 2003]. Considering the broad effects of type I IFN, the ability to produce it in response to viral infection is important for the control and clearance of viral infections by both the innate and adaptive immune system.

1.5.5 Type I IFN Induction

This investigation was focused on the interaction between NiV-M and the system for inducing type I IFN in major type I IFN-producing cells. Considering the possible modes of entry of NiV-M, the major PRRs of interest for induction of type I IFN in response to NiV-M infection are the endosomal TLRs (TLR3 and TLR7) and the RLRs (RIG-I, MDA5, and LGP2).

1.5.6 Pattern Recognition Receptors: Endosomal Toll-like Receptors (TLRs)

The Toll-like receptors TLR3 and TLR7 are endosomal PRRs that recognize dsRNA (TLR3) and ssRNA (TLR7) found in the endosomal compartment. Endosomal TLRs require endosomal acidification in order to recognize and signal in response to their cognate ligands [Kawasaki and

Kawai 2014]. Endosomal acidification occurs concomitantly with endosomal maturation, so viruses such as paramyxoviruses that avoid mature endosomes at entry typically do not activate TLRs during the entry process. Viruses that are exposed to active TLR receptors during entry processes can induce TLR activation without viral replication [Kawai and Akira 2008].

Theoretically, pH-independent viruses could still be exposed to endosomal compartments during entry if they fail to fuse before the endosome matures. Alternatively, the replication products of any virus replicating in the cytoplasm can be exposed to activated TLR receptors by autophagy, the cellular process of degrading and recycling cellular components when autophagosomes containing viral replication products acidify and fuse with endosomes and then lysosomes [Kawai and Akira 2008].

TLR-dependent recognition of PAMPs by cells varies between cell types based on their expression of these TLRs. TLR3 is expressed by a variety of immune and non-immune cells types, including conventional DCs (cDCs), macrophages, fibroblasts, and epithelial cells; TLR7 expression is mainly restricted to immune cells and particularly to plasmacytoid DCs (pDCs), but it is also found in B cells and in induced myeloid cells [Kawai and Akira 2008, Petes *et al* 2017]. Recognition of virus by endosomal PRRs can also vary between cells with similar TLR expression profiles based on the entry mechanism of the virus into the cells (i.e. involving endosomal maturation or not) or on differences in autophagy: in some cell types, notably pDCs, high levels of autophagy occur constitutively, potentially enhancing the access of TLR3/7 to their cognate ligands [Lee *et al* 2007].

1.5.7 Endosomal TLR Detection of Paramyxoviruses

Recognition of NiV-M by endosomal TLRs likely does not occur during entry because, as previously described, NiV-M entry is pH-independent and can avoid the acidified endosomes in which the endosomal TLRs become activated.

However, TLR7 is involved in the detection of paramyxoviruses, particularly in infections of pDCs and myeloid cells (consistent with its expression pattern). TLR7 recognition of paramyxoviruses requires viral replication and likely occurs when some ssRNA replication or degradation product enters the endosomal compartment of the cell by autophagy [Hornung *et al* 2004, Melchjorsen *et al* 2005, Lee *et al* 2007].

Direct evidence for TLR3-dependent detection of most paramyxoviruses is largely absent [Schröder and Bowie 2005]. It is likely that TLR3 detection of paramyxoviruses is limited because the concomitant encapsidation of paramyxovirus genomes and antigenomes with their synthesis prevents the formation of dsRNA structures [Noton and Fearns 2015]. Experimentally, dsRNA was not detected during the replication of paramyxoviruses SeV and Newcastle disease virus (NDV), indicating they produce either no or very few dsRNA replication intermediates [Weber *et al* 2006]. TLR3 has been found to be involved in detection of the paramyxoviruses respiratory syncytial virus (RSV), but not of the paramyxoviruses SV5 and SeV [Liu *et al* 2007, Manuse and Parks 2010, López *et al* 2004].

1.5.8 TLR Signalling for Type I IFN Induction

TLR3 and TLR7 signalling start with the recruitment of an adaptor protein: TRIF for TLR3, and MyD88 for TLR7. Signal transduction pathways for these two endosomal PRRs are summarized in Figure 5. Signal transduction after ligand binding to TLR3 follows, in sequence,

Figure 5. Endosomal PRR (TLR3, 7) signalling pathways for induction of type I IFN. Known points of inhibition by NiV-M P gene products are indicated. Associated signalling pathways not directly involved in type I IFN induction are also shown (grey box).

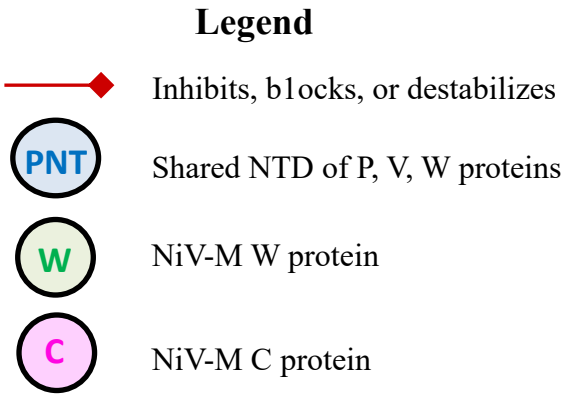

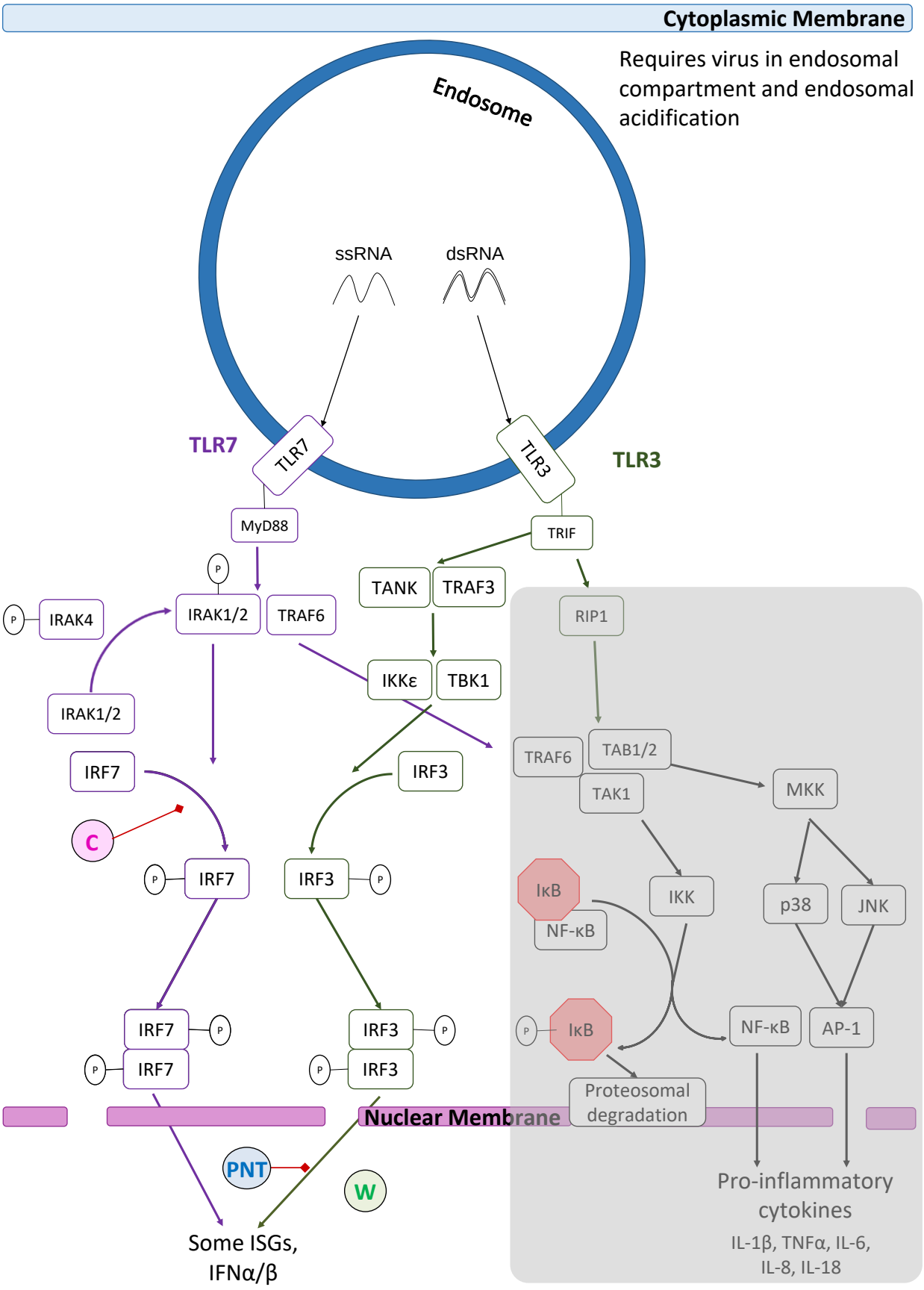
Cytoplasmic Membrane
Requires virus in endosomal compartment and endosomal acidification
Endosome
ssRNA
dsRNA
TLR7
TLR7
TLR3
TLR3
MyD88
TRIF
P
IRAK4
IRAK1/2
TRAF6
TANK
TRAF3
IKKε
TBK1
IRAK1/2
IRF7
IRF3
C
P
IRF7
IRF3
P
IRF7
P
IRF7
IRF3
P
IRF3
Nuclear Membrane
PNT
W
Some ISGs, IFNα/β
RIP1
TRAF6
TAB1/2
TAK1
MKK
IκB
NF-κB
IKK
p38
JNK
P
IκB
NF-κB
AP-1
Proteosomal degradation
Pro-inflammatory cytokines
IL-1β, TNFα, IL-6, IL-8, IL-18

the molecules TRIF, TRAF3, TBK1/IKKε/NEMO, and finally the transcription factors Interferon-Regulatory Factor (IRF)3/7 for the induction of type I IFN [Kawai and Akira 2007, Kawasaki and Kawai 2014].

Signal transduction for TLR7 generally does not involve IRF3 [Honda *et al* 2005]. Instead, IRF7 binds to MyD88 associated with TLR7 and forms a complex with several molecules (TRAF3, TRAF6, IRAK4, IRAK1, IKKα, OPNi, and Dock2); in this complex, IRAK1 and/or IKKα phosphorylates IRF7, which then dimerizes and translocates to the nucleus to upregulate type I IFN [Kawai and Akira 2007, Kawasaki and Kawai 2014].

1.5.9 Pattern Recognition Receptors: RIG-I-like Receptors (RLRs)

RIG-I-like receptors (RLRs) are expressed in a wide variety of tissues and cell types and are the primary source of RNA virus-induced type I IFN induction in non-immune cells. In contrast to TLRs, RLRs are found and recognize viral PAMPs in the cytoplasm [Loo and Gale 2011].

The main RLRs are RIG-I and MDA5, both of which have DExD/H box domains typical of RNA helicases and tandem caspase activation and recruitment domain (CARD) signalling modules that enable them to initiate innate immune signalling [Loo and Gale 2011]. Both MDA5 and RIG-I recognize dsRNA: RIG-I recognizes short dsRNAs (<300 bp) while MDA5 recognizes long dsRNAs (>1000 bp). RIG-I also recognizes 5’ triphosphates (5’ppp) of uncapped RNA, while MDA5 binds internally to long dsRNA with no end specificity [Reikine *et al* 2014]. Some evidence indicates RIG-I and MDA5 also have an affinity for AU-rich RNA sequences [Runge *et al* 2014]. In order for viral RNA to be recognized by either RIG-I or MDA5, some sort of RNA secondary or higher-order structure appears to be necessary, such as

stem/loop structures for RIG-I or RNA "webs" for MDA5 [Schmidt *et al* 2011, Pichlmair *et al* 2009].

A third RLR, LGP2, can also recognize dsRNA but lacks a CARD signalling module and thus cannot activate downstream signalling pathways. Instead, LGP2 regulates the activities of RIG-I and MDA5. Broadly, LGP2 enhances viral RNA recognition by MDA5 while downregulating RIG-I activity [Chan and Gack 2016].

1.5.10 RLR Detection of Paramyxoviruses

Initially, sensing of paramyxovirus infection was thought to be performed by RIG-I and not MDA5 [Kato *et al* 2006], but more recently MDA5 has been shown to be involved [Yount *et al* 2008, Ikegame *et al* 2010]. *In vivo*, MDA5 appears to be more important to sustained production of interferons later in acute paramyxovirus infection whereas RIG-I is important for the early response [Gitlin *et al* 2010].

Studies have found that some paramyxoviruses can be essentially undetectable to cytosolic PRRs during normal replication and infection, but detection can still occur when defective interfering (DI) particles produced stochastically during replication or found in the inoculum are detectable by PRRs [Killip *et al* 2012]. Even in virus preparations specifically reduced for DI particles, the build-up of DI paramyxovirus particles over time during an infection can contribute to the activation of MDA5 and RIG-I [Yount *et al* 2008].

The genomes and antigenomes of paramyxoviruses have 5'-ppp ends and purified NiV genomic RNA can in principle activate PRRs, but the ends of genomes/antigenomes are concealed by the encapsidating nucleoprotein [Habjan *et al* 2008, Plumet *et al* 2007]. This limits detection of incoming virus RNA by the RLRs. Encapsidation also prevents the formation of

dsRNA replication intermediates because it occurs concurrently with replication, preventing base-pairing between genomes and antigenomes and limiting the formation of RNA secondary structures [Plumet *et al* 2007].

Production of 5'ppp RNA is limited during the paramyxovirus life cycle as the L protein caps the 5' ends of viral mRNA transcripts. However, as mentioned previously, the 3' leader transcript is not capped and thus can be recognized by RIG-I [Plumet *et al* 2007]: the uncapped leader transcript could be the major PAMP allowing cellular detection of NiV. It is possible that this is not the only RLR-activating NiV product: the L gene mRNA of MeV and PIV5 have also been observed to bind MDA5 and RIG-I based on its nucleotide sequence, independently of any 5'-ppp [Runge *et al* 2014]. It is currently unknown whether the NiV L gene has a similar effect based on its sequence alone.

1.5.11 RLR Signalling for Type I IFN Induction

Signal transduction for the cytosolic PRRs RIG-I and MDA5 is summarized in Figure 6. Upon activation by a ligand, RIG-I or MDA5 are dephosphorylated by protein phosphatase 1 (PP1, α or γ). RIG-I (but not MDA5) then requires polyubiquitinylation by E3 ubiquitin ligases TRIM25 and Riplet. Subsequently, RIG-I and MDA5 multimerize and then activate the mitochondrial membrane protein MAVS (also known as IPS-1, VISA, or Cardif) through direct interaction. Activated MAVS results in downstream activation of TRAF3, which activates the kinases TBK1 and IKKε; these kinases subsequently phosphorylate IRF3 and/or IRF7, which translocate to the nucleus to upregulate type I IFN production [Chan and Gack 2016].

Figure 6. Cytosolic PRR (RIG-I, MDA5, and LGP2) signalling pathways for induction of type I IFN. Known points of inhibition by NiV-M P gene products are indicated. Associated signalling pathways not directly involved in type I IFN induction are also shown (grey box).

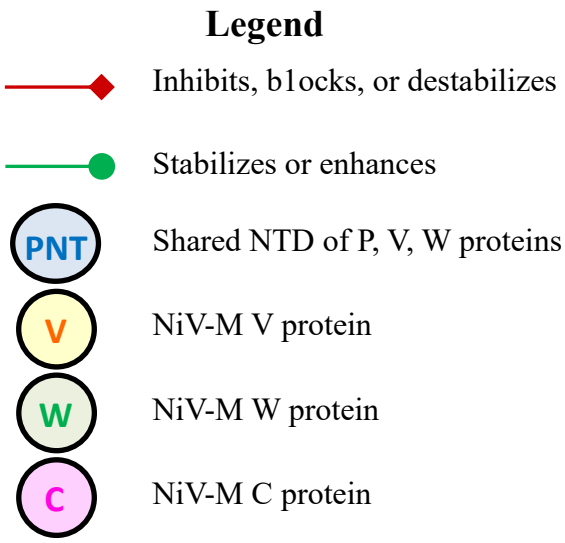

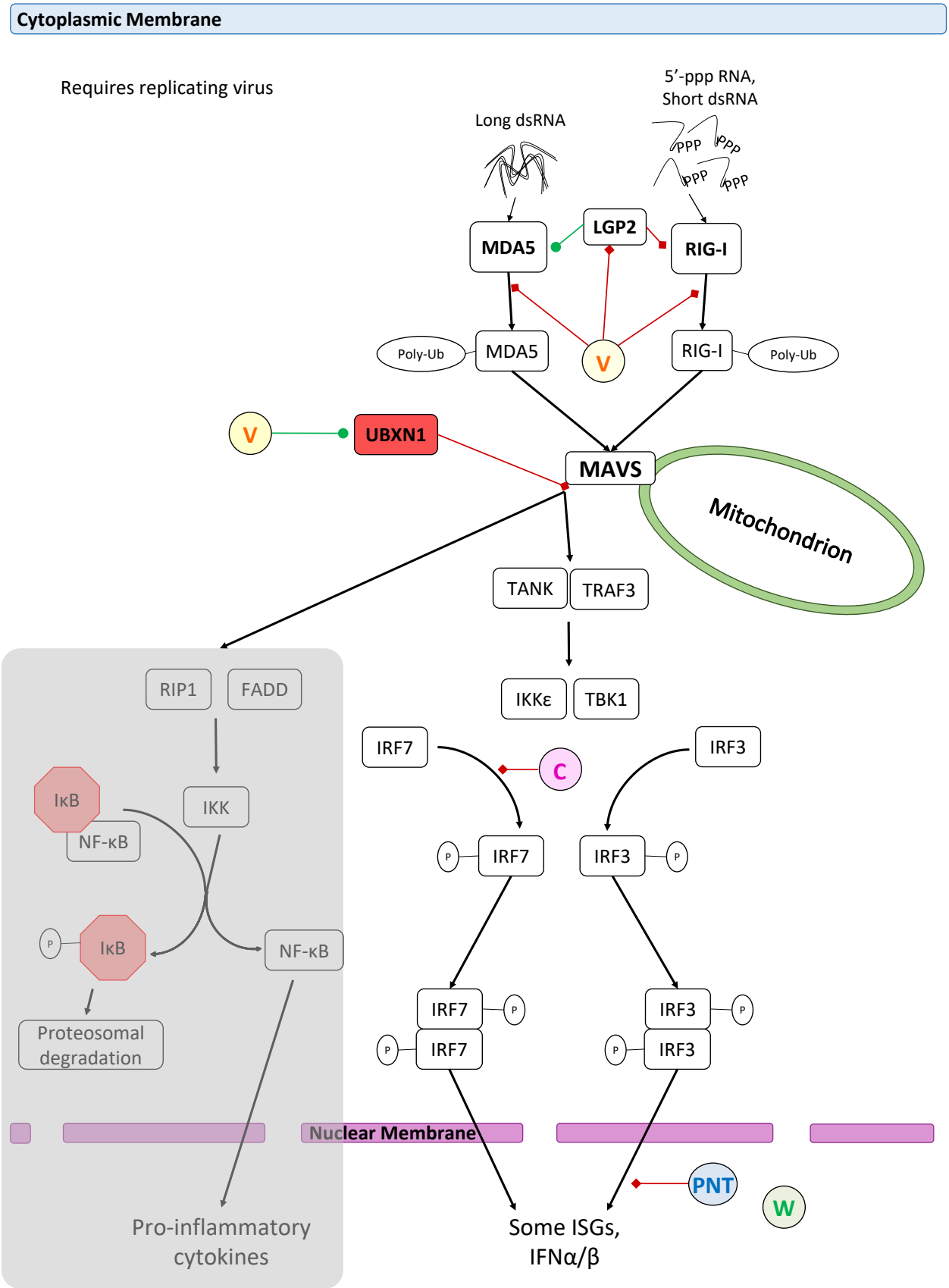
Cytoplasmic Membrane
Requires replicating virus
Long dsRNA
5'-ppp RNA,
Short dsRNA
PPP
MDA5
LGP2
RIG-I
Poly-Ub
MDA5
V
RIG-I
Poly-Ub
V
UBXN1
MAVS
Mitochondrion
TANK
TRAF3
RIP1
FADD
IKKε
TBK1
IRF7
C
IRF3
IκB
IKK
NF-κB
P
IRF7
IRF3
P
IκB
NF-κB
Proteosomal
degradation
IRF7
IRF3
IRF7
IRF3
Nuclear Membrane
PNT
W
Pro-inflammatory
cytokines
Some ISGs,
IFNα/β

1.5.12 Transcription Factors in Type I IFN Induction

As described above, type I IFN induction signalling cascades converge on the phosphorylation of the interferon regulatory factors IRF3 and IRF7. Phosphorylated IRFs dimerize and translocate to the nucleus to activate type I IFN promoters. The nature of the IFNα/β response depends on the level of expression of IRF3 and IRF7 in the stimulated cell [Levy *et al* 2002].

IRF3 has a more restrictive promoter preference than IRF7 and will mainly induce expression of IFNβ. IRF7 has less discriminating promoter-binding activity and will induce both IFNβ and several IFNα subtypes [Lin *et al* 2000, Génin *et al* 2009, Honda *et al* 2006].

IRF3 and IRF7 also differ in their expression in different cell types, and their expression differences allow for temporal regulation of the type I IFN response [Levy *et al* 2002, Honda *et al* 2006]. IRF3 is broadly constitutively expressed in most cell types. Constitutive expression of IRF7 is restricted to immune cells and, in particular, to pDCs [Honda *et al* 2006, Kawai and Akira 2007]. However, IRF7 expression can be induced in all cells by type I IFN signalling as an interferon-stimulated gene (ISG) [Honda *et al* 2006]. IFN-dependent IRF7 expression results in a biphasic induction of type I IFN in response to virus infection: IFNβ is produced first, and subsequent production of multiple IFNα subtypes occurs only if the initial IFNβ response does not sufficiently remove the virus [Sato *et al* 1998]. The mechanism of the biphasic, IFNβ-dependent expression of IFNα is summarized in Figure 7. A large amount of IFNα produced in viral infections can be attributed to immune cells such as pDCs which constitutively express IRF7 and thus can respond immediately to viral PAMPs with IFNα production [Prakash *et al* 2005, Fitzgerald-Bocarsly *et al* 2008, Kumagai *et al* 2007].

Figure 7. IFNβ-dependent induction of IFNα. Type I IFN can activate IFNARs in a paracrine (green- and yellow-bordered cells are different cells) and autocrine (yellow-bordered cell is the green-bordered cell after responding to type I IFN) manner. The grey box around TLR7 indicates that TLR7 is a PRR found in some immune cell types but in most other cell types it is neither present at steady-state nor inducible by IFN signalling. Numbers indicate the sequential order of steps for the production of IFNα by a non-IRF7-expressing cell upon the cell's detection of virus.

(1) Cellular PRRs recognize the presence of viral PAMPs and become activated.
(2) The resultant signalling cascade phosphorylates constitutively expressed IRF transcription factors (IRF3 only in steady-state cells).
(3) Phosphorylated IRF3 upregulates transcription of IFNβ.
(4) Upregulated IFNβ is secreted by the cell and binds to IFNARs in an autocrine or paracrine manner.
(5) IFNAR activation initiates a JAK/STAT signalling cascade that forms the ISGF3 transcription factor complex.
(6) ISGF3 binds to ISREs to initiate transcription of ISGs involved in the antiviral state.
(7) ISG proteins mediate the antiviral state: now, primed cells are more sensitive to PAMPs and express IRF7.
(8) The presence of viral PAMPs (continued or newly introduced) is recognized by the cellular PRRs. As in step (2), the subsequent signalling results in the phosphorylative activation of expressed IRF transcription factors. In the IFN-primed cell, this includes IRF3 and IRF7. In certain specific immune cell types, namely pDCs, TLR7 and IRF7 are present in the steady-state: the production of IFNα and IFNβ by such cells only requires steps (8) through (10).
(9) Transcription of both type I IFN subtypes is upregulated. IRF3 upregulates IFNβ while IRF7 upregulates both IFNβ and IFNα.
(10) IFNα and IFNβ are secreted and can initiate IFNAR receptor signalling in responding cells. The signalling cycle continues until viral PAMPs are no longer detected unless the pathway is blocked.

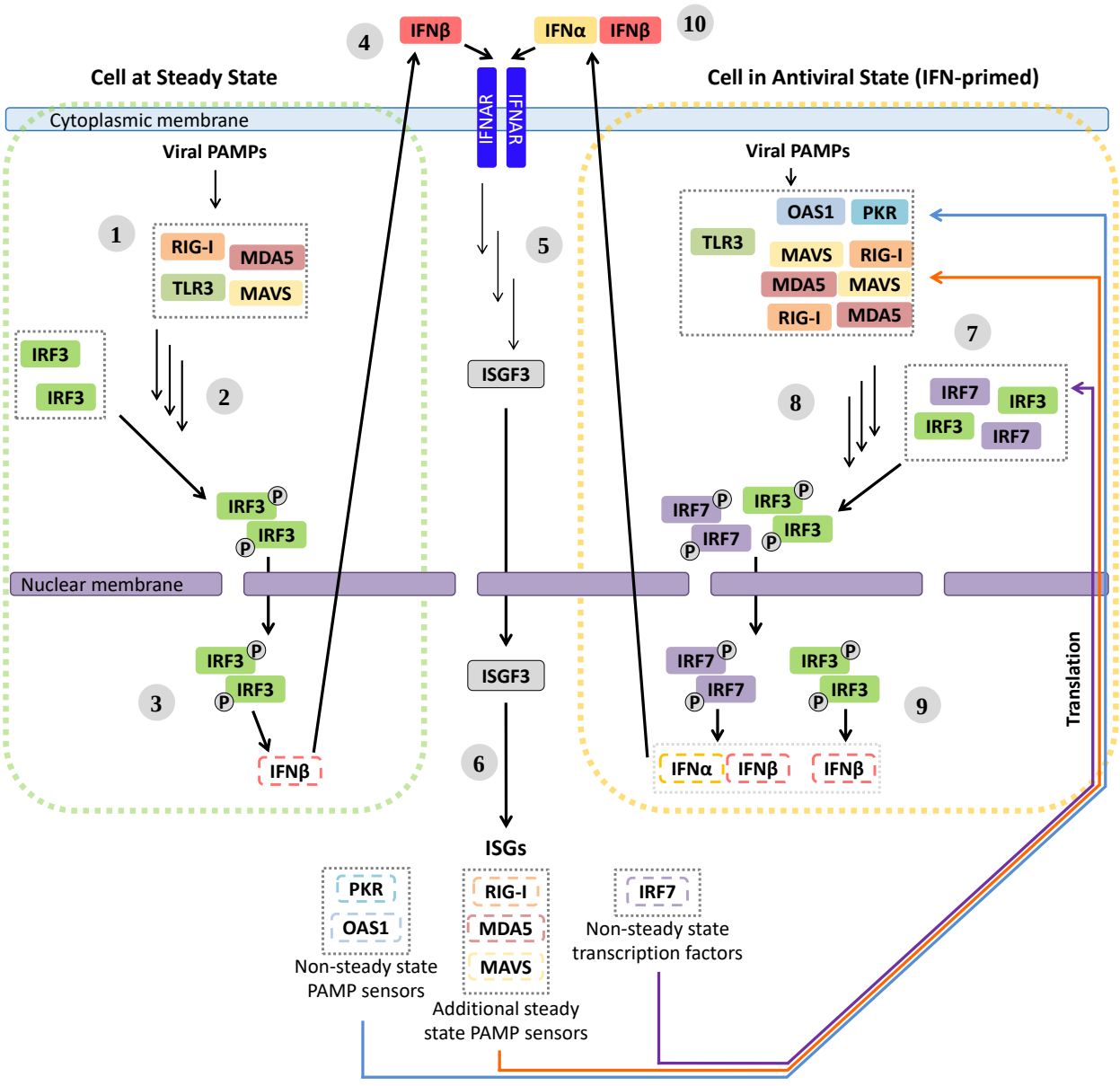
Cell at Steady State
Cell in Antiviral State (IFN-primed)
Cytoplasmic membrane
Viral PAMPs
Viral PAMPs
IFNβ
IFNα
IFNβ
IFNAR
IFNAR
RIG-I
MDA5
TLR3
MAVS
IRF3
IRF3
ISGF3
OAS1
PKR
TLR3
MAVS
RIG-I
MDA5
MAVS
RIG-I
MDA5
IRF7
IRF3
IRF3
IRF7
Nuclear membrane
IRF3
IRF3
IRF7
IRF3
IRF7
IRF3
ISGF3
IRF7
IRF7
IRF3
IRF3
IFNβ
IFNα
IFNβ
IFNβ
Translation
ISGs
PKR
OAS1
Non-steady state
PAMP sensors
RIG-I
MDA5
MAVS
Additional steady
state PAMP sensors
IRF7
Non-steady state
transcription factors
1
2
3
4
5
6
7
8
9
10

1.5.13 Negative regulators of type I IFN induction and signalling

Control of type I IFN production and signalling also involves negative regulators that limit type I IFN responses [Ivashkiv and Donlin 2014]. Both induction of and signalling by type I IFN can be suppressed by proteins or noncoding RNAs (e.g micro (mi)RNAs) upregulated in the type I IFN response. Protein suppressors of the type I IFN response system have various mechanisms by which they can block PRR or JAK/STAT signalling, including by direct interaction, dephosphorylation, ubiquitination, or deubiquitination of signalling pathway members [Arimoto *et al* 2018].

1.6 Auxiliary Functions of the NiV-M P Gene Products

The P gene products are implicated in a number of auxiliary functions that are not strictly necessary for replication but are important for pathogenesis, including evading the induction and signalling of type I IFN. As mentioned above, the amino-terminal domains (NTDs) of the P, V, and W proteins are identical; and although they share a nuclear export sequence (NES) in the NTD [Rodriguez *et al* 2004], these three proteins mediate their effects from different subcellular compartments. The V protein shuttles dynamically into and out of the nucleus with a net localization in the cytoplasm [Rodriguez *et al* 2002]. The P protein does not appear to interact with nuclear export machinery at all and is found entirely in the cytoplasm [Audsley *et al* 2016]. The W protein contains a nuclear localization sequence (NLS) in its unique CTD (requiring amino acids 439, 440, and 442) and is distributed to the nucleus in certain cell types, likely by interaction with karyopherin-α proteins [Shaw *et al* 2005]. Interestingly, the W protein does not appear to localize to the nucleus in all cell types: notably, it localizes to the cytoplasm in human endothelial cells and in a variety of porcine cell lines [Lo *et al* 2010, Bocskowzka 2014, Goolia

2009]. As mentioned above, the NiV-M C protein lacks any protein level homology with any other NiV-M P gene product and has both nuclear localization (NLS) and nuclear export (NES) signals that cause it to shuttle between the nucleus and cytoplasm [Horie *et al* 2016].

1.6.1 P Gene Product Transfection Studies

The limitations of work with BSL4 viruses has confined most research into the mechanisms of auxiliary P gene products' functions to transfection studies, which can provide indications of the actual functions of these proteins but whose biological relevance should be investigated. The auxiliary functions of the P gene products will be reviewed here in two separate sections: those that are attributed to the common NTD of P, V, and W proteins, and those that are attributable uniquely to different P gene products. The review of the functions unique to a single product will address neither the P protein (because its known unique roles are the necessary functions described above for viral replication) nor the W protein (because the only truly unique role determined for the W protein thus far is its nuclear localization, discussed above). The known roles of the P gene products in blocking type I IFN signalling and induction are indicated in Figures 4, 5, and 6.

1.6.1.1 Transfection Studies Revealing Shared Functions of P Gene Product N-terminal Domain (NTD)

Despite differences in their subcellular localization, the common NTD of the P, V, and W proteins causes the three proteins to share certain functions. Regions of interest in the P, V, and W NTDs are represented in Figure 1B and summarized in Table 2.

The shared STAT1 binding domain of the P, V, and W proteins allows them to prevent the nuclear translocation of STAT1 complexes, thereby blocking type I and type II IFN signalling. [Rodriguez *et al* 2004, Shaw *et al* 2004]. The P and V proteins colocalize with STAT1 in the cytoplasm, while the W protein has been seen to mainly mediate STAT accumulation and signalling block at the level of the nucleus. When the W protein localizes to the nucleus, it creates a stronger IFN signalling block than either P or V; the P protein creates the weakest IFN signalling block [Shaw *et al* 2004, Ciancanelli *et al* 2009]. Less is known about the 'strength' of the W protein-mediated IFN signalling block when the W protein localizes to the cytoplasm, and it may be equal or redundant to that of the V and P proteins in cells with cytoplasmic localization of W protein [Ciancanelli *et al* 2009, Shaw 2009].

The shared NTD seems to be able to limit genome replication: transfected P gene products, including the NTD alone, were found to inhibit NiV-M minigenome replication. This inhibition could also be mediated by the unique CTD of the V protein [Sleeman *et al* 2008, Goodbourn and Randall 2009].

1.6.1.2 V Protein Transfection Studies

NiV-M V protein transfection studies have indicated that the V protein's CTD allows it to evade RLR-mediated signalling in multiple ways. The CTD of the V protein has been implicated in mediating interference of the cytosolic RNA sensors MDA5, LGP2, and RIG-I [Childs *et al* 2007, 2009, 2012; Parisien *et al* 2009, Davis *et al* 2014, Rodriguez and Horvath 2013, 2014; Sánchez-Aparicio *et al* 2018]. The V protein has also been found to inhibit RLR signalling at the level of MAVS activation by stabilizing UBXN1 (a suppressor of MAVS), thereby inhibiting the RLR signalling pathways [Uchida *et al* 2018, Wang *et al* 2013].

1.6.1.3 C Protein Transfection Studies

The NiV-M C protein C inhibits type I IFN signalling but more weakly than the other P gene products, with a stronger ability to mediate this block when it is localized to the cytoplasm [Park *et al* 2003, Horie *et al* 2016]. The mechanism of this inhibition is unclear. The C protein also appears to be important for promoting efficient budding of NiV-M from infected cells [Park *et al* 2016]. There is some indication that the C protein may block IFNβ induction by inhibiting IKKα phosphorylation of IRF7, but the biological relevance of this is uncertain [Yamaguchi *et al* 2014].

1.6.2 P Gene Product Live Virus (*In Vitro*) Studies

The functions of the NiV P gene products have been investigated using recombinant viruses whose expression of V, W, or C are abrogated by single nucleotide substitutions introducing stop codons in the reading frame specific to one of these proteins. Recombinant NiV-M lacking expression of each non-structural protein have been used for investigation of the role of the non-structural proteins in during live infections [Ciancanelli *et al* 2009, Yoneda *et al* 2010, Mathieu *et al* 2012a, Lo *et al* 2012, Satterfield *et al* 2016, 2015]. In this thesis, recombinant NiV-M lacking expression of the V, W, or C protein will be referred to as NiV-ΔV, NiV-ΔW, and NiV-ΔC, respectively.

The W protein was not found to have a role in NiV-M replication *in vitro* and NiV-ΔW recombinants have been consistently found to replicate similarly to the wild-type NiV-M [Yoneda *et al* 2010, Lo *et al* 2012, Satterfield *et al* 2015, 2016]. In primary human endothelial cell lines, the W protein is important for the cellular antiviral response 24 hpi and later and its

absence *in vitro* led to strong upregulation of multiple pro-inflammatory cytokines and chemokines at 24 to 72 hpi [Lo *et al* 2012, Satterfield *et al* 2015].

In vitro, NiV-ΔV has been seen to replicate to lower titers than the wild-type NiV-M, although not in every cell type and not consistently at the same time points [Yoneda *et al* 2010, Lo *et al* 2012, Satterfield *et al* 2015]. A reduction in P gene mRNA editing was seen for NiV-ΔV, possibly implicating the V protein in control of P gene mRNA editing [Lo *et al* 2012].

In human primary endothelial cells, the V protein appears to be important to evasion of antiviral state and IFNβ induction at later time points post-infection (24 hpi and later) [Lo *et al* 2012], similar to what was seen for the W protein (see above). The V protein was found to block the production of certain pro-inflammatory cytokines and chemokines in human primary endothelial cells, although to a lesser extent than the W protein [Satterfield *et al* 2015].

The C protein likely has some role in viral replication and growth, as NiV-ΔC recombinants replicate to lower titers than wild-type NiV-rM [Lo *et al* 2012, Yoneda *et al* 2010, Satterfield *et al* 2016, Ciancanelli *et al* 2009, Mathieu *et al* 2012a]. Using NiV-ΔC, the C protein has also been implicated in blocking the production of IFNβ in infected primary human endothelial cells, although at earlier time points than the V and W proteins [Mathieu *et al* 2012a, Lo *et al* 2012].

1.6.3 P Gene Product *In Vivo* Pathogenesis Studies

In vivo studies of NiV-ΔV and NiV-ΔW have been performed to investigate the roles of the V and W proteins in pathogenesis in animal models of human NiV-M infection. The two models used for these investigations to date are the golden hamster model [Yoneda *et al* 2006, 2010; model developed by Wong *et al* 2003] and the ferret model [Satterfield *et al* 2015, 2016; model developed by Bossart *et al* 2009].

In infections of golden hamsters, the W protein was found to have no role in pathogenesis: the absence of the W protein did not reduce clinical signs or improve survival compared to the wild-type rNiV [Yoneda *et al* 2010]. In ferrets, the presence/absence of the W protein was irrelevant to lethality; however, the absence of the W protein led to a delayed time to death (8-11 dpi), reduced respiratory signs of disease, and aggravated neurological signs of disease. Satterfield *et al* suggest that during NiV-M infection, the W protein blocks production of inflammatory cytokines and chemokines which would otherwise reduce damage to the lung and cause damage to the central nervous system. Interestingly, NiV-ΔW-infected ferrets did not develop neutralizing antibodies even though their time to death was delayed [Satterfield *et al* 2015, 2016].

Although the V protein was found to create a weaker *in vitro* block of inflammatory mediator production in human primary cells, it appears to be a much greater contributor to NiV-M pathogenesis than the W protein. All golden hamsters infected with NiV-ΔV survived challenge and had no detectable virus in any organs despite the development of anti-NiV antibodies [Yoneda *et al* 2010]. In the ferret model, NiV-ΔV-infected ferrets all survived challenge with significantly reduced or absent detection of NiV in tissues. NiV-ΔV infection of ferrets led to the production of neutralizing antibodies by 10 dpi [Satterfield *et al* 2015].

In vivo, the C protein was found to be important for pathogenesis and virulence in golden hamsters. In its absence, golden hamsters survived challenge; had reduced detection of NiV in tissues; and had reduced inflammation in the brain despite increased inflammation in the lungs [Yoneda *et al* 2010, Mathieu *et al* 2012a]. In infected ferrets, NiV-M C was less important to virulence. No ferrets infected with NiV-ΔC survived challenge and all succumbed over a similar

timeline to the wild-type NiV-M, although the C protein's absence led to a reduction in respiratory signs of disease [Satterfield *et al* 2016].

1.7 Rationale

The roles of the NiV-M non-structural proteins V and W have been primarily investigated using transfection systems, and few virus infection studies into their roles have been performed to date. Despite differences in the pathogenesis of NiV-M disease between humans and swine and despite the impact of swine on the NiV-M outbreak, very little is known about the contributions of the NiV-M non-structural proteins to infections of swine.

The observations that IFNα mRNA is downregulated in NiV-infected porcine T cells [Stachowiak and Weingartl 2012] and indications that the non-structural proteins play a role in preventing type I IFN induction [Rodriguez and Horvath 2014, Childs *et al* 2009, Sánchez-Aparicio *et al* 2018] together suggest that NiV infection of important IFNα/β-producing cells early in infection may lead to a reduced IFNα/β response. This could be a contributing factor to the transient immunosuppression observed in NiV-M-infected pigs.

1.8 Hypothesis

Nipah virus (NiV) delays the immune response in swine in part by blocking type I IFN (IFNα/β) production in important innate immune cells of myeloid origin with its non-structural proteins.

1.9 Aim

Explore the role of the V and W proteins in NiV replication and the antiviral response in swine cells of myeloid origin.

1.10 Objectives

Objective 1: Determine if the V or W proteins are important for NiV replication in porcine immune cells of myeloid origin.

Objective 2: Determine if the role of the V protein is in genome replication and virion release or in reducing the antiviral activity of infected swine cell supernatants.

Objective 3: Determine whether *de novo* synthesis of the NiV-M V protein is required for the block of type I IFN induction or if the V protein is entering with the NiV virions.

Materials and Methods

2.1 Removal of Samples from CL4

Samples to be removed from CL4 to CL3 for analysis were inactivated according to the CFIA Special Pathogens Unit standard operating protocols. Samples for RNA extraction were removed in TriPure Isolation Reagent (Roche Diagnostics, Manheim, Germany, Cat# 11 667 165 001). Samples containing virus-infected cells were fixed with 10% formalin buffered phosphate (Fisher Chemical, Waltham, MA, USA, Cat. No. SF100-4), which contains formaldehyde at a concentration of 4% v/v**,** for 24 hrs before removal from CL4. Cells on plates were formalin fixed as well and kept for 24 hrs in a hermetically sealed secondary container containing 10% phosphate-buffered formalin. Samples for immunoblot analysis were removed in minimum 2% SDS (Millipore-Sigma, Burlington, MA, USA, Cat. No. 71736), denatured for 10 min at 98°C in CL4 before removal and then for 2 min at 98°C in CL3. Samples to be removed from CL4 were kept in secure tubes which were entirely internally inactivated by any of the above-described methods. These tubes were placed in sealable primary containers which were then filled with 5% Micro-Chem Plus^{TM} disinfectant (National Chemical Laboratories, Inc., Philadelphia, PA, USA, Cat. No. 0255) to completely submerge the sample tubes and coat the entire interior of the primary containers. Primary containers were then placed in sealable secondary containers also completely filled with 5% Microchem disinfectant. The entire secondary container was removed from CL4 to CL3 by submerging completely in 5% Microchem for a minimum of 15 minutes. Formalin-filled containers containing formalin-fixed cells were considered to be secondary containers and were dunked out after the 24 hr inactivation period accordingly.

2.2 Cell Lines

MDBK (Madin-Darby bovine kidney epithelial), ST (swine testis, fibroblast) and Vero 76 (African green monkey kidney epithelial) cells were maintained in Dulbecco's modified Eagle medium (DMEM) (Wisent Bioproducts, Saint-Jean-Baptiste, QC, Cat. No. 319-005-CL) supplemented with 10% fetal bovine serum (FBS) (HyClone Laboratories Inc., Omaha, NE, Cat. No. SH3007103**)**; IPAM31 (immortalized porcine alveolar macrophages, 3D4/31) were maintained in DMEM supplemented with 10% FBS, 1X MEM non-essential amino acids and 1X penicillin-streptomycin (Wisent Bioproducts, Cat. No. 450-201-EL). MRC5 (human lung fibroblast) cells were maintained in Eagle's Minimum Essential Medium (EMEM) (Wisent Bioproducts, Cat. No. 320-005-CL) supplemented with 10% FBS and 1X MEM non-essential amino acids (Wisent Bioproducts, Cat. No. 321-011-EL). All cells were maintained in a 37°C, 5% CO_2 cell culture incubator. Maintenance cells were passaged every 1-4 days by washing with Dulbecco's phosphate-buffered saline (PBS; Wisent Bioproducts, Cat. No. 311-425-CL) followed by trypsinization with 0.25% Trypsin/EDTA (Wisent Bioproducts, Cat. No. 325-043-CL) for 2 to 15 minutes until detached. To determine cell counts for seeding density and multiplicity of infection (MOI) calculations, a Nexcelom Cellometer Auto T4 automated cell counter (Nexcelom Bioscience, Lawrence, MA) was used. Trypan blue dye exclusion (Invitrogen, Waltham, MA, USA, Cat. No. 15250061) was used for live/dead cell discrimination.

2.3 Viruses

Wild type Nipah virus - Malaysia genotype (NiV-M-WT) (4^{th} passage on Vero 76 cells of a pig lung isolate) and recombinant Nipah viruses (rNiVs) designed and provided by Dr. Misako Yoneda and Dr. Chieko Kai [Yoneda *et al* 2010] and previously rescued at the NCFAD were

amplified on Vero 76 cells. For NiV stocks to be used in infection studies, Vero 76 cells were infected at an MOI of 0.01with virus in serum-free DMEM for 1 hr, followed by a 2 day incubation in 2% FBS DMEM. Virus produced for infection studies was aliquoted and stored at -150°C. All handling of infectious NiV was performed under BSL4 conditions.

Vesicular stomatitis virus (VSV) was amplified on Vero 76 cells. VSV stock was diluted to an MOI of 0.01 in serum-free DMEM and incubated with Vero 76 cells for 1 hr, followed by a 2 day incubation in 2% FBS DMEM. At 2 dpi, flasks of VSV-infected Vero 76 cells were freeze-thawed at -70°C before collection and clarification of the supernatant at 1600 rcf, 4°C for 20 minutes. VSV stocks were then aliquoted and stored at -70°C until use. Handling of VSV alone was performed in CL3.

2.4 Polyethylene Glycol (PEG) Precipitation of NiV

NiV used for polyethylene glycol (PEG) precipitation and structural analysis was amplified in serum-free DMEM. At 2 dpi, supernatants were harvested and clarified by centrifugation at 1015 rcf, 4°C for 20 minutes before use. PEG precipitation of NiV was performed using the PEG Virus Precipitation Kit (Abcam, Cambridge, UK, Cat. No. ab102538) as per directions included in the kit. Briefly, newly amplified and clarified virus stocks were incubated with PEG solution overnight at 4°C and then centrifuged at 1600 rcf for 30 min at 4°C. Precipitated virus was then resuspended and stored as appropriate for downstream applications.

2.5 Plaque Assays

Titers of infectious virus in stocks and in supernatants were determined by plaque assay on 48 well plates. NiV titrations were performed on confluent Vero 76 cells; VSV titrations were

performed on confluent MDBK cells. Virus stocks or test samples to be titrated were serially diluted in serum-free DMEM. Cells were washed with serum-free DMEM and then incubated with 100 µl of each dilution of sample/stock in triplicate wells for 1 hr in a 5% CO_2, 37°C in a humidified cell incubator. After this adsorption period, 0.5 ml of 1.75% carboxymethylcellulose (CMC) overlay (see Appendix A.1 for the formulation) was added to each well and plates were incubated for two days at 37°C, 5% CO_2. At 2 dpi, plates were fixed with 10% phosphate-buffered formalin. VSV-only plates in CL3 were fixed for minimum 3 hrs; plates in CL4 were fixed for 24 hrs (as described above). Fixed cells were washed and then stained with 0.5% crystal violet (Ricca Chemical, Arlington, TX, USA Cat. No. 3235-4) for 30 min, then washed again before counting plaques in the monolayer. Infectious titers of NiV determined using Vero 76 plaque assays were used to standardize the number of infectious particles in inocula for infections of all cell types with each of the (r)NiVs used; thus, all MOIs used are based on infectious titers of NiV-M on Vero 76 cells.

2.6 RNA Isolation

The TriPure Isolation Reagent separates RNA from DNA and protein on the basis of differential solubility in phenol, chloroform, and water. Extraction of the RNA was performed as described by the manufacturer's protocol. Briefly, the sample from which the RNA was to be extracted was added to the isolation reagent. Then, 200 µl of chloroform (Fisher Chemical, Cat. No. BP1145-1) was added to the isolation reagent, vortexed, and centrifuged to separate the aqueous layer from the phenol-chloroform. The aqueous layer was collected, mixed with 750 µl of isopropanol (Fisher Chemical, Cat. No. A464-4) and 3 µl of GlycoBlue™ Coprecipitant (Invitrogen, Cat. No. AM9515), and then left for a minimum of 30 minutes at -20°C. The RNA

was pelleted, washed with 70% ethanol (Commercial Alcohols, Toronto, ON, Canada, Cat. No. P006EAAN) in nuclease-free water (Ambion, Cat. No. AM9932), air-dried at room temperature, and resuspended. For RNA used for quantification of NiV, RNA pellets were washed once with 70% ethanol and resuspended in RNAsecure Resuspension Solution (Ambion, Foster City, CA, USA, Cat. No. AM7010). For cell pellet RNA, RNA pellets were washed twice with 70% ethanol and resuspended in nuclease-free water (Ambion, Cat**.** No. AM9932). Resuspended RNA was stored at -70℃ until use. TriPure to be used for collecting RNA for NiV-N detection was spiked with Armored RNA Enterovirus (Asuragen, Austin, TX, USA, Cat. No. 42050) as an extraction and reaction control prior to sample collection. TriPure for cell pellet samples was not spiked with Armored Enterovirus; the cyclophilin housekeeping gene acted as an extraction and reaction control.

2.7 Cell Pellet RNA DNase Treatment

Isolated cell pellet RNA in nuclease-free water was quantitated using a NanoDrop One Microvolume UV-Vis Spectrophotometer (ThermoFisher Scientific, Waltham, MA, Cat. No. ND-ONE-W) which measures sample absorbance at 260 nm (A260) to calculate RNA concentration. Cell pellet RNA concentrations were then individually adjusted to 150 ng/µl by adding nuclease-free water in order to be within the concentration range recommended in the TURBO DNA-free Kit ThermoFisher Scientific, Cat. No. AM1907) for DNase treatment. For samples with RNA concentrations lower than 150 ng/µl, no volume adjustments were made. DNase treatment was performed on 26 µl aliquots of the extracted and adjusted RNA using the TURBO DNA-free Kit according to the instructions included in the kit. Briefly, RNA was incubated with 1X TURBO DNase buffer and 1 µl of TURBO DNase for 30 min at 37°C and

then inactivated with 1X DNase inactivation reagent for 5 min at room temperature. Inactivation reagent was removed by centrifugation for 2 min at 10,000 rcf and DNased RNA samples were stored at -70°C until analysis by real-time semi-quantitative (r)RT-PCR.

2.8 Agarose Gel Electrophoresis for cDNA products

Gels were prepared by heating the appropriate amount of solid agarose (Invitrogen, Cat. No. 16500-500) in 0.5X TBE buffer (Life Technologies, Carlsbad, CA, USA, Cat. No. AM9864) to dissolve at the desired concentration. SYBR Safe DNA Gel Stain (Invitrogen, Cat. No. S33102) was mixed in at a 1:50,000 dilution before casting the gel. BlueJuice Gel Loading buffer (Invitrogen, Cat. No. 10816015) was added to 1X concentration and mixed into each sample under analysis before loading into the gel. Gels were run in 0.5X TBE buffer at 100 V. Each gel included either a 1 kbp (Invitrogen, Cat. No. 10787018) or 100 bp (Invitrogen, Cat. No. 15628019) DNA ladder as appropriate for the expected target size. Completed gels were visualized using a Bio-Rad Gel Doc 2000 transilluminator (Hercules, CA, USA, Cat. No. 170-8100).

2.9 Semi-quantitative, real-time (r)RT-PCR

For all rRT-PCR and PCR reactions, primer and probe sources, sequences, targets, product sizes, and purposes are described in Appendix A.2. All primers were synthesized by Invitrogen Life Technologies Custom DNA Primer Synthesis (Invitrogen). Sample master mixes for each of the PCR reactions are found in Appendix A.3. All semi-quantitative, real-time (r)RT-PCR reactions and analyses were performed using the Qiagen Rotor-Gene Q and associated Rotor-Gene Q Series Software (Qiagen, Hilden, Germany, Cat. No. 9001640); conventional PCR

reactions were performed using the Applied Biosystem's GeneAmp PCR System 9700 (Applied Biosystems, Foster City, CA, USA, Cat. No. N805-0200). For all RT-PCR and PCR reactions, reaction conditions are in Appendix A.4.

2.9.1 NiV-N Probe-based rRT-PCR

rRT-PCR targeting NiV-N was used for quantitation of NiV-Malaysia N RNA using primers and probe described by Guillaume *et al* [2004] in which the forward and reverse primers amplify a 105 bp fragment that is annealed to by the probe with a 5' end 6-carboxyfluorescein (6-FAM) dye and a 3' end 6-carboxy-tetramethyl-rhodamine (TAMRA) quencher [Guillaume *et al* 2004]. Detection of the enterovirus internal control added to the samples was performed using primers amplifying a 76 bp fragment with a probe containing a 5' end 6-carboxy-1,4-dichloro-2',7'-dichlorofluorescein (TET) dye and a 3' end Minor Groove Binding Non-Fluorescent Quencher (MGB NFQ), as per Pickering *et al* [2016]. rRT-PCR reactions were set up using the Rotor-Gene Multiplex RT-PCR Kit (Qiagen, Cat. No. 204974). For quantification of NiV-N RNA, a plasmid containing the NiV-N sequence was serially diluted in 10-fold steps to create a standard curve of known plasmid copy numbers, as described in Weingartl *et al* [2005]. Cycling threshold (C_T) values of the standard curve were used to interpolate copy numbers of NiV-N RNA in tested samples.

2.9.2 NiV-N vs NiV-L SYBR Green rRT-PCR

SYBR Green RT-PCR targeting NiV-N used the same primers as for NiV-N probe-based rRT-PCR [Guillaume *et al* 2004] (see above and Appendix A.2). Primers for NiV-L detection were designed using Primer3 web 4.0.0, targeting the NiV-Malaysia L gene coding sequence

(base pairs 11412-18146 from NCBI reference sequence NC_002728.1). Reactions were set up using the QuantiNova SYBR Green RT-PCR Kit (Qiagen, Cat. No. 20154). L primers were designed to have similar melting temperatures to the N primers already in use with the probe-based rRT-PCR assay. The SYBR Green rRT-PCR cycling conditions were designed by altering the NiV-N probe-based rRT-PCR reaction conditions for compatibility with the SYBR Green methodology, including the addition of a melt analysis at the end of the reaction. Both the N and L primers were evaluated for efficiency and specificity under the new reaction conditions by running melt analysis and gel electrophoresis of products from amplification of 10-fold serial dilutions of wild-type NiV-M stock RNA. Based on the cycle threshold (C_T) values seen on the NiV-N probe based rRT-PCR, some supernatant samples were predicted to be below the range of C_T values for which efficiency was evaluated. To avoid extrapolating outside of this range of C_T values, all test samples were diluted 1:10 in RNAsecure resuspension solution.

The RNA samples evaluated in the N vs L SYBR Green assay were the same as those from NiV-rM and NiV-ΔV-infected cell supernatants that had already been extracted and run on the NiV-N probe-based rRT-PCR. For each single supernatant RNA sample, the N and L reactions were run in separate reactions because SYBR Green non-specifically dyes DNA and cannot be used in multiplexed rRT-PCR reactions when it is important to distinguish between the products. As a result, each supernatant RNA sample was run in duplicate for both sets of primers for a total of four reactions per sample. Melt curves for all reactions were used to confirm product specificity. Select samples were run on agarose gel electrophoresis (described above) alongside a 100 bp DNA ladder to confirm melt curve results by product size analysis. Before the use of C_T values in calculations, all values from the reaction were confirmed to fall within the range for

which efficiency was determined. The C_T values used in the calculations were the averages of technical duplicates run for each sample and primer pair.

N to L C_T ratios from the reaction were calculated by a modified Livak and Schmittgen $2^{-\Delta\Delta Ct}$ method. A cellular internal control was not used because determining the amounts of N and L mRNA relative to each other was sufficient, and because the RNA samples were derived from clarified supernatants in which limited cellular RNA would be present. For statistical and graphical purposes, the data were best represented in the logarithmic (base 2) scale that is intrinsic to the methodology that produced it (cycle thresholds): as a result, linear transform of the data was not performed and the data for both NiV-rM and NiV-ΔV were graphically represented (rather than using $\Delta\Delta C_T$ to compare the two rNiVs). This amounts to a "ΔC_T" analysis rather than a "$2^{-\Delta\Delta Ct}$" analysis [Livak and Schmittgen 2001]. A sample calculation is included in Appendix A.5.4.

The ratio of N to L C_T values (ΔC_T N-L) was determined by subtracting the L C_T value from the N C_T value for a given sample. Subtraction of the C_T values provides a ratio comparison because unit differences in C_T values represent $\log_2$ changes, and the difference between log-transformed data points is equal to the log-transformation of the ratio of linear data. For example, a C_T difference (ΔC_T) of 1 is a two-fold difference and a ΔC_T of 3 is an eight-fold difference.

For the interpretation of the data, it is important to highlight that a lower C_T value indicates a greater abundance of the targeted RNA. This is because C_T values indicate the PCR cycle at which amplified product becomes detectable, and more abundant RNA species are amplified to detectable levels at earlier cycles. In the context of N to L C_T ratios (ΔC_T N-L), a preponderance of N RNA is represented as a negative ΔC_T; a preponderance of L RNA is represented as a positive ΔC_T; and equal amounts of N and L RNA is represented as a ΔC_T of zero.

2.9.3 IFNα and IFNβ SYBR Green rRT-PCR

Primers targeting porcine IFNα [Dawson *et al* 2005] and cyclophilin [Stachowiak and Weingartl 2012] are as described by Stachowiak and Weingartl [2012]. Primers for IFNβ detection were designed using Primer3 web 4.0.0, targeting *Sus scrofa* IFNβ1 mRNA (NCBI reference sequence NM_001003923.1). Reactions were set up using the QuantiNova SYBR Green RT-PCR Kit (Qiagen, Cat. No. 20154). Prior to running on IFNα/β SYBR Green rRT-PCR, samples were DNase treated as described above. Each sample was run in duplicate per primer pair for a total of six reactions per sample. C_T values obtained for all reactions were analyzed based on the Livak and Schmittgen $2^{-\Delta\Delta Ct}$ method [Livak and Schmittgen 2001]: fold change in target mRNA expression was determined by normalizing C_T values to cyclophilin as the reference mRNA for each sample, then by comparing the obtained ΔC_T value for each target mRNA (IFNα or IFNβ) and sample (NiV-ΔV-, NiV-ΔW- or NiV-rM-infected at 0, 1, 2, 4, 24, or 48 hpi) to the same target mRNA species in the mock-treated sample at the same time point ($\Delta\Delta C_T$). Where appropriate (i.e. to show decreased mRNA expression), data is represented in both linearized form ($2^{-\Delta\Delta Ct}$) and in the $\log_2$ expression ($-\Delta\Delta C_T$): a sample calculation is included in Appendix A.5.5. For all reactions, melt curve data were used to verify that the correct product had been detected in all reactions. Select samples were run on agarose gel electrophoresis (described above) alongside a 100 bp DNA ladder to confirm melt curve results by product size analysis.

2.10 P Gene Sequencing

Primers designed (using Primer3web 4.0.0) to amplify the whole P gene are described in Appendix A.2. NiV copy numbers in RNA isolated from stocks of NiV-rM, NiV-ΔV, and NiV-

ΔW were quantitated on NiV-N probe-based rRT-PCR and RNA concentrations were determined using the NanoDrop (described above). All rNiVs were adjusted to $1x10^6$ copies/µl in nuclease-free water; $1x10^7$ copies total were run for each virus in each reaction. The SuperScript II One-Step RT-PCR for Long Templates Kit (Invitrogen, Cat. No. 11922010) was used with the whole P gene primers (Appendix A.2) to amplify the P genes of all three rNiVs; as controls, a NiV-rM sample without reverse transcriptase and a non-template control (NTC) were included. A sample master mix formulation is included in Appendix A.3. Amplification was performed on an Applied Biosystems GeneAmp PCR System 9700 (Applied Biosystems, Foster City, CA, USA). After amplification, cDNA products were subjected to gel electrophoresis in a 0.8% agarose gel alongside 1 kbp DNA ladder to confirm the presence of the product at the expected size (2,467 bp) as well as the absence of other non-specific products.

Clean-up of the remaining amplified cDNA was performed using the QIAquick PCR Purification Kit (Qiagen, Cat. No. 28104) as per the instructions provided in the kit, eluting into nuclease-free water. The recovered product from each rNiV sample was quantitated by NanoDrop to determine the volume to use for cycle sequencing.

Cycle sequencing was performed using the BigDye Terminator v3.1 Cycle Sequencing Kit (Applied Biosystems, Cat. No. 4337455) on the GeneAmp 9700. Cycle sequencing was performed on all three NiVs using two opposite-sense primers flanking the P gene editing site. Additional coverage of the entire P gene of NiV-ΔV was also obtained using three additional forward and reverse sequencing primers. All primers used are listed in Appendix A.2.

Cycle sequencing products were cleaned using a DyeEx 2.0 spin kit (Qiagen, Cat. No. 63204) according to the instructions included in the kit, then vacuum dried for 30 min at 60°C using an Eppendorf Vacufuge plus (Eppendorf, Hamburg, Germany, Cat. No. 022820168). Dried PCR

products were resuspended in 25 µl of hot formamide and run on an ABI 3130xl Genetic Analyzer (ThermoFisher Scientific, Waltham, MA, USA, Cat. No. 4359571).

Sequence analysis was performed using DNASTAR's SeqMan Pro software (DNASTAR Inc., Madison, WI, USA), using the Clustal Omega Multiple Sequence Alignment free online software to compare sequences to a wild-type NiV-Malaysia reference sequence (NCBI reference sequence NC_002728.1).

2.11 Virus Growth Studies

Vero 76, IPAM31, MRC5, and ST cells were seeded on 24 well plates and used once confluent. On the day of infection, duplicate wells from each of the targeted cell types were trypsinized and counted using the automated cell counter; the average count was used to prepare inocula of each recombinant NiV to a Vero 76 equivalent MOI of 0.1. Cells were washed with serum-free DMEM and then infected for 1 hr at 37°C, 5% CO_2 on a plate rocker with 100 µl of the target rNiV diluted to an MOI of 0.1 in DMEM. After the 1 hr incubation, inocula were removed and cells were washed three times with PBS. Cells were then incubated in DMEM 2% FBS. Supernatants were collected at 1 hpi (directly after addition of the incubation media), 24 hpi, and 48 hpi; centrifuged at 1000 rcf, 4°C for 5 minutes to remove cellular material; and then stored at -70°C until processing. Each time point for each repeat of the experiment was performed in duplicate. Duplicate mock-infected cell conditions were included in each repeat. For MRC5 cells, the experiment was conducted identically except that EMEM with 1X non-essential amino acids was used as the base medium instead of DMEM.

After samples from all time points were collected, supernatants were assayed by plaque assay (as described above) and collected in TriPure to assay supernatants by NiV-N rRT-PCR (as described above).

2.12 Collection and Preparation of Porcine PBMC

Blood from 5 week-old weaned pigs was collected into 8 ml BD Vacutainer CPT Mononuclear Cell Preparation tubes with sodium citrate (BD Biosciences, San Jose, CA, Cat. No. 362761) and PBMCs were prepared according to the protocol associated with the tubes. CPT tubes use FICOLL-Hypaque solution and a polyester gel plug to separate low-density mononuclear cells from denser blood components such as erythrocytes and granulocytes. Briefly, CPT tubes were centrifuged at 1600 rcf for 20 minutes at room temperature in order to collect the interphase layer of mononuclear cells. PBMCs were washed twice in PBS by centrifugation at 450 rcf for 15 minutes, counted by haemocytometer, and then plated in RPMI 1640 (Wisent Bioproducts, Cat. No. 350-007-EL) with 10% FBS and 1X penicillin-streptomycin at $1x10^6$ cells/well into 24 well plates, 1 ml/well. After harvesting and plating, PBMCs were incubated at 37°C, 5% CO_2 overnight before use.

The collection of blood from uninfected pigs for use in the *in vitro* infection experiments was performed as per animal use documents approved by the Canadian Science Centre for Human and Animal Health (CSCHAH) Animal Care Committee for various experimental studies in pigs.

2.13 Infection and Harvesting Samples from Porcine PBMCs

Prior to infection, PBMCs from sample wells were removed and counted for MOI determination. Suspension cells were collected by pipetting supernatant multiple times; adherent

cells were collected by a combination of trypsinization and cell scrapers. Cells were washed with serum-free RPMI prior to infection. To infect, suspension PBMCs were centrifuged at 700 rcf for 5 minutes at room temperature to remove the wash and resuspended in the appropriate virus diluted to an MOI of 0.1 in serum-free RPMI. These virus-PBMC preparations were replaced in the same 24 well plates to simultaneously infect the adherent fraction of the PBMCs. Virus was allowed to adsorb for 1 hr at 37°C, 5% CO_2. After adsorption, both the adherent and suspension fractions were washed five times with PBS before finally resuspending cells in RPMI 1640 with 2% FBS and 1X penicillin-streptomycin. For the purposes of infection, all steps were performed without removing the adherent fraction of PBMCs from any wells; instead, the suspension fraction of cells was always placed back in the well containing the cognate adherent fraction. Cells were incubated in the incubation media until the harvesting of the samples at 1, 24, 48, and 72 hpi. 1 hpi samples were collected immediately after resuspending the PBMCs in 2% FBS RPMI post-washing.

At harvesting time points, supernatants of infected PBMCs (containing suspension cell fractions) were collected and centrifuged at 700 rcf, 4°C for 5 min. The clarified supernatant fractions were stored at -70°C until they could be titrated by plaque assay on Vero76 cells. Supernatant aliquots were also collected in TriPure for NiV-N rRT-PCR.

To collect the cell fraction for IFNα/β rRT-PCR, the cell pellet from the supernatant clarification (consisting of the pelleted suspended cells) was resuspended in TriPure. The adherent cell fraction was collected by using the TriPure sample of a particular set of non-adherent PBMCs to collect the adherent fraction from the same well.

2.14 rNiV Induction of Type I IFN in IPAM31 cells

Confluent IPAM31 on 12 well plates were infected with NiV-rM or NiV-ΔV, mock-infected, or treated with 200 ng/ml of high molecular weight (HMW) PolyI:C (InvivoGen, San Diego, CA, Cat. No. tlrl-pic). The number of cells per well was determined by trypsinizing and counting the cells from a single well. This count was used to prepare inocula of each rNiV at a Vero 76 equivalent MOI of 1. Cells were washed once in serum-free DMEM and then infected for 1 hr at 37°C, 5% CO_2 with 1 ml of NiV-rM or NiV-ΔV diluted to MOI of 1 in serum-free DMEM. After the 1 hr adsorption, the inoculum was removed and cells were washed three times with PBS. Cells were incubated for 1, 2, 4, and 24 hpi in 1 ml of serum-free DMEM with 1X penicillin-streptomycin before sampling. The 1 hpi time point was collected immediately after the addition of incubation medium post-wash. As a negative control for type I IFN production, Vero76 cells were infected and harvested alongside the IPAM31 cells in the same manner.

At indicated time points, supernatants were collected and clarified by centrifugation at 700 rcf for 5 min at 4°C and then stored at -70°C until their use in the type I IFN bioassay (described below). Cell pellet RNA was collected by washing wells in 1 ml of TriPure; these samples were stored at -70°C until RNA isolation in CL3.

2.15 Pre-stimulation of IPAM31 cells

IPAM31 cells plated for 80% confluence on 12 well plates were washed with serum-free DMEM and then treated 24 hrs after plating with either high molecular weight (HMW) PolyI:C alone; HMW PolyI:C and recombinant porcine (rp)IFNβ (Kingfisher Biotech, St Paul, MN, Cat. No. RP0011S-025); rpIFNβ alone; or transfection with HMW PolyI:C. For non-transfected cells,

HMW PolyI:C was added to cells in 200 ng/ml and/or rpIFNβ in 20 ng/ml in 1 ml per well of serum-free DMEM with 1X penicillin-streptomycin.

Transfection of IPAM31 cells with HMW PolyI:C was performed using the Lipofectamine® LTX with Plus™ Reagent system (ThermoFisher Scientific, Cat. No. 15338100) according to the protocol included in the kit, transfecting 100 ng of HMW PolyI:C per well. Briefly, IPAM31 cells were washed and media was replaced with serum-free DMEM supplemented with 1X penicillin-streptomycin to remove FBS. OptiMEM media **(**Gibco by Life Technologies, Cat. No. 51985-034**)** was used to prepare PolyI:C and Lipofectamine LTX reagents separately. Lipofectamine LTX was used at 6 µl per well. The polyI:C and LTX mixtures were incubated individually for 5 minutes at room temperature and then mixed together at a 1:1 ratio. This mixture was incubated a further 5 minutes at room temperature and then added in 150 µl volumes to each well. Mock-transfected IPAM31 cells received the same treatment but without the addition of HMW PolyI:C.

All pre-stimulated IPAM31 cells were incubated for 18 hrs at 37°C, 5% CO_2. Cell fractions from duplicate wells of each stimulation type were collected after the 18 hr pre-stimulation in 1 ml TriPure to serve as a pre-infection control. Duplicate wells were also trypsinized and counted to determine cell count for MOI calculations. NiV-rM, NiV-ΔV, and NiV-ΔW inocula were prepared to Vero76 equivalent MOI of 1 in serum-free DMEM with 1X penicillin-streptomycin (mock inoculum consisted of serum-free DMEM with no virus). Cells were washed once with PBS and then incubated with each inoculum in duplicate for 1 hr at 37°C, 5% CO_2. After the 1 hr incubation, inocula were removed and 1ml of TriPure was added to each well to collect the cell RNA fraction; these were stored at -70°C until RNA isolation.

2.16 Porcine IFNα and IFNβ ELISA

ELISAs specific to porcine IFNα (Kingfisher Biotech, Swine IFN alpha Do-It-Yourself ELISA, Cat. No. DIY0724S-003) and IFNβ (Kingfisher Biotech, Swine IFN beta Do-It-Yourself ELISA, Cat. No. DIY065S-003) were tested for sensitivity to type I IFN. These kits used 96 well plates, Streptavidin-horseradish peroxidase (HRP), 3,3',5,5'-tetramethylbenzidine (TMB), and 0.18 M Sulfuric Acid stop solution from the recommended ELISA Accessory Pack (Kingfisher Biotech, Cat. No. AR0133-002).

The ELISAs were carried out according to the protocols included with the ELISA kits. Dilutions of antibodies and of streptavidin-HRP were selected based on several optimization tests of the ELISAs, selecting the highest dilution of reagent that did not lead to a loss of sensitivity.

Briefly, 96 well plates were coated overnight at 4°C with capture antibody diluted 1:800 in PBS. Plates were washed five times with washing buffer (PBS-Tween-20) and then blocked with 4% BSA-PBS blocking buffer for 1 hr at room temperature. Known amounts of standard recombinant porcine (rp)IFNα or (rp)IFNβ (included in kits) were diluted in 2% FBS DMEM to mimic cell culture supernatants and incubated for 1 hr at room temperature; plates were then washed five times with washing buffer. Plates were incubated for 1 hr at room temperature with the biotinylated detection antibody (0.5 µg/ml) in blocking buffer and then washed five times with washing buffer. Streptavidin-HRP was added to each well at a 1:30,000 dilution and incubated for 30 min at room temperature, followed by five washes and then development with TMB substrate. Plates were developed for 10 min in the dark at room temperature at which point the reaction was stopped with stop solution**.** Plates were read at 450 nm on an Epoch Microplate Spectrophotometer (BioTehdk Instruments, Winooski, VT, USA).

2.17 MDBK-VSV Plaque Reduction Type I Interferon Bioassay

rNiV-infected IPAM31 and Vero 76 supernatant samples to be assayed on MDBK cells were treated for 1 hr at 60°C with shaking and then allowed to cool to room temperature. Supernatants selected for neutralizing anti-type I IFN antibody treatment were incubated for 1 hr at 37°C with polyclonal anti-porcine IFNα (Kingfisher Biotech, Anti-Swine IFNα1 Polyclonal Antibody, Cat. No. KP1122S-100) or polyclonal anti-porcine IFNβ (Kingfisher Biotech, Anti-Swine IFNβ Polyclonal Antibody, Cat. No. PB0124S-100) at a 1:100 dilution, or were mock-treated with an equivalent volume of PBS.

Confluent MDBK cells in 48 well plates were washed with serum-free media before 200 µl of each sample undiluted and at 1:2, 1:4, and 1:8 dilutions were applied to these cells in triplicate. MDBK cells with samples were incubated for 20 hrs at 37°C, 5% CO_2 before removing samples from wells and washing cells twice with PBS. VSV diluted in serum-free DMEM was then applied to the cells at 100 PFU/well in 100 µl volumes and cells with virus were incubated 1 hr at 37°C, 5% CO_2 on a plate rocker. After the incubation period, the assay was carried out as a plaque assay (described above). Plaque counts for VSV were used to determine the relative antiviral activity of each supernatant by standardizing a 50% reduction of plaques as 1 antiviral unit.

2.18 SDS-PAGE and Immunoblot

2.18.1 Sample Collection for Immunoblot

Infected adherent Vero 76 cell fractions in 6 well plates to be analyzed by immunoblot were collected by removing media from cells, washing three times with PBS, adding 100 µl of 2% SDS-HALT (Millipore Sigma, Cat. No. 71736) with 1X HALT™ protease and phosphatase

inhibitor cocktail (Thermo Scientific, Cat. No. 78440), and using a cell scraper to collect the entire fraction. PEG-precipitated virus for analysis by immunoblot was resuspended in 250 µl of 2% SDS-HALT directly using vigorous pipetting to solubilize the pellet.

All BSL4 samples in 2% SDS-HALT were vortexed, centrifuged to collect at the bottom of the tube, then heat inactivated as described above for removal of material from BSL4. Samples were equilibrated to room temperature before quantitation.

2.18.2 Protein Quantitation and Concentration Adjustment

Protein concentrations in 2% SDS were quantified using a BioDrop µLite UV-Vis Spectrophotometer (SERVA Electrophoresis GmbH, Heidelberg, Germany, Cat. No. 80-3006-51.01) which uses absorbance at 280 nm to determine protein concentrations. 2% SDS-HALT was used as a blank. Samples were adjusted to an equal concentration of 1.54 µg/µl for whole cell lysates or 3.85 µg/µl for PEG-precipitated virus by the addition of 2% SDS-HALT, or by acetone precipitating the protein (described below) and re-dissolving in 2% SDS-HALT. At these concentrations, there is 1.0 or 2.5 µg/µl of protein per sample of whole cell lysate or PEG-precipitated virus, respectively, after the addition of loading buffers for SDS-PAGE (described below). Sample calculations are included in Appendix A.5.3. Once adjusted to the appropriate concentration for use, samples were aliquoted and stored at -70°C until use.

2.18.3 Acetone Precipitation of Protein from SDS

Four volumes of acetone cooled to -20°C were added to one volume of the SDS-protein mixture and then left at -20°C for 1 hr. Samples were then centrifuged at 14,000 rcf for 10 min at 4°C and the supernatant was discarded. The protein pellets were allowed to dry for 10 min and

then resuspended in the appropriate volume of 2% SDS 1X HALT. Protein concentration was confirmed by spectrophotometry as described above.

2.18.4 SDS-PAGE and Blotting/Transfer

Samples to be separated by SDS-PAGE were mixed with 1X NuPAGE™ LDS Sample Buffer (Invitrogen, Cat. No. NP0007) and 1X NuPAGE™ Sample Reducing Agent (Invitrogen, Cat. No. NP0009) then denatured for 10 minutes at 70°C. Samples were allowed to cool to room temperature and loaded into pre-cast 10% Bis-Tris Gels (Invitrogen, Cat. No. NP0302BOX). For whole cell lysates, 20 µg of protein in 20 µl was loaded per well; for PEG-precipitated virus, 50 µg of protein in 20 µl was loaded per well. Example calculations are included in Appendix A.5.3. For size determination of protein bands, SeeBlue Plus2 Pre-stained Protein Standards (Invitrogen, Cat. No. LC5925) were included in each gel. Gels were run in 1X MOPS SDS Running Buffer (Invitrogen, Cat. No. NP0001) with NuPAGE antioxidant (Invitrogen, Cat. No. NP0005). Gels were run at 4°C overnight at a constant current of 0.01 mA using a PowerPac™ 200 (Bio-Rad, Cat. No. 165-5052). The minimum constant current was used to ensure the minimum voltage across the gel for the duration of the overnight run: a stable low voltage cannot be run overnight using the PowerPac™ 200 because the necessarily decreasing current eventually passes the minimum current the power source can provide, prematurely terminating the separation.

Gel transfer onto nitrocellulose membranes was performed using the iBlot™ Gel Transfer device (Invitrogen, Cat. No. IB21001**)** and iBlot™ nitrocellulose transfer stacks (Invitrogen, Cat. No. IB301001), which uses a dry blotting procedure. A transfer program at 20 V for 7 minutes was used for all transfers.

2.18.5 Immunoblot Staining and Visualization

Post-transfer, membranes were blocked in 1% alkali-soluble casein (Millipore-Sigma, Cat. No. 70955) in Tris-buffered saline with Tween® 20 (TBS-T) (Caledon Laboratory Chemicals, Georgetown, ON, Canada, Cat. No. CAL1301-40) blocking buffer overnight (18 hrs) at 4°C. Membranes were then incubated in primary antibody diluted in blocking buffer to concentrations indicated in Appendix A.6 at 4°C overnight (18 hrs). Membranes were washed five times for 5 minutes each in TBS-T and then incubated for 1 hr at room temperature with HRP-conjugated recombinant protein G (Invitrogen, Cat. No. 101223) diluted 1:4000 in blocking buffer. Protein G is produced naturally by Group G *Streptococcus* species [Fahnestock *et al* 1986] and is capable of binding immunoglobulin Gs (IgGs) of multiple species. Membranes were again washed five times for 5 minutes each in TBS-T then incubated for 2 minutes with Enhanced Chemiluminescent (ECL) Primer Western Blotting Detection Reagent system (GE Healthcare/Amersham, Chicago, IL, USA, Cat. No. RPN2232) and imaged with Azure Biosystems C400 (Dublin, CA, USA) using the Azure Biosystems cSeries Capture Software.

2.18.6 Immunoblot Stripping and Re-probing

For blots that were stripped and re-probed, stripping was performed using Re-Blot Plus Mild solution (Millipore-Sigma, Cat. No. 2502) by incubating membranes in a 1X solution of antibody stripping solution for 15 minutes at room temperature. Stripped membranes were re-blocked at 4° overnight before re-probing with the primary antibody.

2.19 Immunoelectron Microscopy (IEM)

BEI inactivated, sucrose gradient purified-NiV was graciously provided by Y. Berhane. The fraction used represented a lower band on the sucrose gradient, containing primarily herringbone structures instead of intact NiV particles [Berhane *et al* 2006]. The loading, immunogold labelling, and viewing of the grids were performed by A. Dufresne using rabbit polyclonal anti-V and anti-W primary antibodies as described in Appendix A.6. Secondary staining was performed using a goat anti-rabbit IgG antibody conjugated to a 10 nm gold particle (Electron Microscopy Sciences, Hatfield, PA, USA Cat. No. 25108) at a 1:10 dilution. Control grids received no primary antibody and the same dilution of the gold-conjugated secondary. Samples were fixed using 2% glutaraldehyde/2% paraformaldehyde (made with 8% Paraformaldehyde Aqueous Solution, EM Grade, Electron Microscopy Sciences, Cat. No. 157-8; and Glutaraldehyde 25% Solution, EM Grade/Distillation Purified, Electron Microscopy Sciences, Cat. No. 12220) in PBS.

2.20 Statistics

GraphPad Prism version 7.0 (GraphPad Software Inc., San Diego, CA, USA) was used for data analysis and to generate plots. Group means were compared using the Student's t-test. P values less than 0.05 were considered indicative of statistical significance.

Results

3.1 Growth of Recombinant Viruses

3.1.1 Recombinant Nipah virus (rNiV) system

The roles of the V and W protein in infections of porcine immune cells were investigated using three recombinant Nipah viruses (rNiVs), designed and provided by Dr. Misako Yoneda and Dr. Chieko Kai [Yoneda *et al* 2010]:

(1) NiV-rM, which has a wild-type genome sequence except for genome alterations made to accommodate the rescue system;

(2) NiV-ΔV, which has a nonsense mutation in the reading frame of the V protein (+1) immediately after the P editing site and lacks expression of the unique portion of the V protein;

(3) NiV-ΔW, which has a nonsense mutation in the reading frame of the W protein (+2) and lacks expression of the unique portion of the W protein.

All three recombinants were previously rescued in the NCFAD CL4 laboratory. Stocks of these recombinant viruses were produced from and titrated on Vero 76 cells.

3.1.2 Confirmation of rNiVs' expected P gene editing site sequences

The P gene editing sites of the three rNiVs were sequenced using the Sanger method to confirm that the viruses rescued from the plasmid rescue system [Yoneda *et al* 2006, Yoneda *et al* 2010] had the expected P gene editing site sequences. Sequencing confirmed the nonsense mutations of the NiV-ΔV and NiV-ΔW viruses and the presence of a stop codon in the +1 (V) and +2 (W) reading frames after each editing site, respectively (Fig. 8A). The three recombinants did not otherwise differ in nucleotide sequence from the NiV Malaysia reference

A

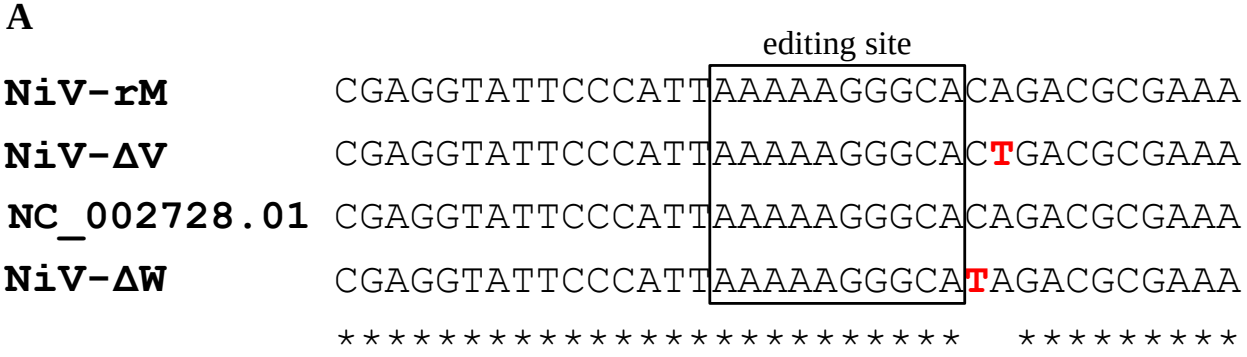

B

Protein	NC_002728.01	In rM	In ΔV	In ΔW
P	…PIKKGTDAKY…	PIKKGTDAKY…	PIKKGTDAKY…	PIKKGIDAKY…
V	…PIKKGHRREIS…	PIKKGHRREIS…	PIKKGH•REIS…	PIKKGHRREIS…
W	…PIKKAQTRNI…	PIKKAQTRN…	PIKKALTRN…	PIKKA•TRN…

Figure 8. Sequences of recombinant NiVs at P gene editing site. (A) The nucleotide sequence of recombinant NiVs editing sites obtained by Sanger sequencing of each recombinant compared to NCBI reference sequence (NC_002728.01). Editing site is indicated by the black box; Highlighted in red are the single base pair mutations introduced by Yoneda *et al* [2010] to create the NiV-ΔV and NiV-ΔW. (B) The amino acid sequence of P, V, and W proteins around editing site of each recombinant as well as reference sequence NC_002728.01, predicted from their nucleotide sequences. Stop codons are denoted by •. Amino acids that differ from the reference sequence for a given protein are in red and underlined.

(NC_002728.01) in the sequenced region. However, the single amino acid base pair changes in the NiV-ΔV and NiV-ΔW created a unique off-target missense mutation in one of the other reading frames in both of the recombinants (Fig. 8B): in NiV-ΔV, there is a Q408L substitution in the W protein; and in NiV-ΔW, there is a T407I substitution in the P protein. Off-target mutations are present in all the recombinant NiV-M systems for studying the V and W protein published to date. In most of these other systems, the off-target amino acid substitutions are the same as in the current investigation and are not thought to impact the proteins' structures or functions [Yoneda *et al* 2010, Lo *et al* 2012, Satterfield *et al* 2015].

3.1.3 Expression of V and W proteins in NiV-M-infected cells

To confirm the lack of V or W protein expression by NiV-ΔV and NiV-ΔW, whole cell lysates of Vero 76 cells infected at an MOI of 0.1 with NiV-rM, NiV-ΔV, NiV-ΔW, or with pig lung isolate (4^{th} passage) NiV-Malaysia were harvested at 24 hpi and analyzed by immunoblot (Fig. 9). Although three different rabbit polyclonal anti-V specific antibodies were tested, none were capable of recognizing the V protein in denaturing immunoblots. Non-denaturing immunoblots were not attempted due to the difficulties with performing such assays inside BSL4. To compensate for the lack of an anti-V antibody, V protein expression was evaluated by contrasting immunoblots probed with the anti-W antibody in conjunction with those probed with the monoclonal anti-P antibody (P58), which recognizes the common PNT of the P, V, and W proteins (see Fig. 1B for antibody-binding sites).

Blots of infected Vero cell lysates proteins probed with the P58 anti-P antibody revealed multiple bands (Fig. 9A), a pattern typical of immunoblots of NiV-M cell lysates probed with anti-P antibodies [Lo *et al* 2009, Satterfield *et al* 2015]. The distinct P protein band is at

Figure 9. Immunoblots of Vero 76 whole cell lysates harvested 24 hpi with NiV stocks at an MOI of 0.1. Cell lysate preparations were separated on a 10% Bis-Tris gel and transferred blots were probed for (A) the common N-terminus of the P, V, and W proteins and a histone H3 loading control or (B) the unique C-terminus of the W protein. Bands at 78 kDa correspond to the expected size of the P protein; bands at 51 kDa correspond to the expected size of the complete V and/or W proteins; and bands at 17 kDa are at the expected size of histone H3 protein**.** Predicted protein sizes based on SeeBlue Plus2 Pre-stained Protein Standards are listed adjacent to each blot. Asterisks (*) are placed just above the expected location of a W protein band in the NiV-ΔV cell lysate. “>” indicates the band corresponding to the (hypothesized) tP product. Blots were probed with the anti-W antibody, then stripped and reblotted with the anti-P/V/W and anti-histone H3 antibodies.

A

Anti-P (P58) antibody

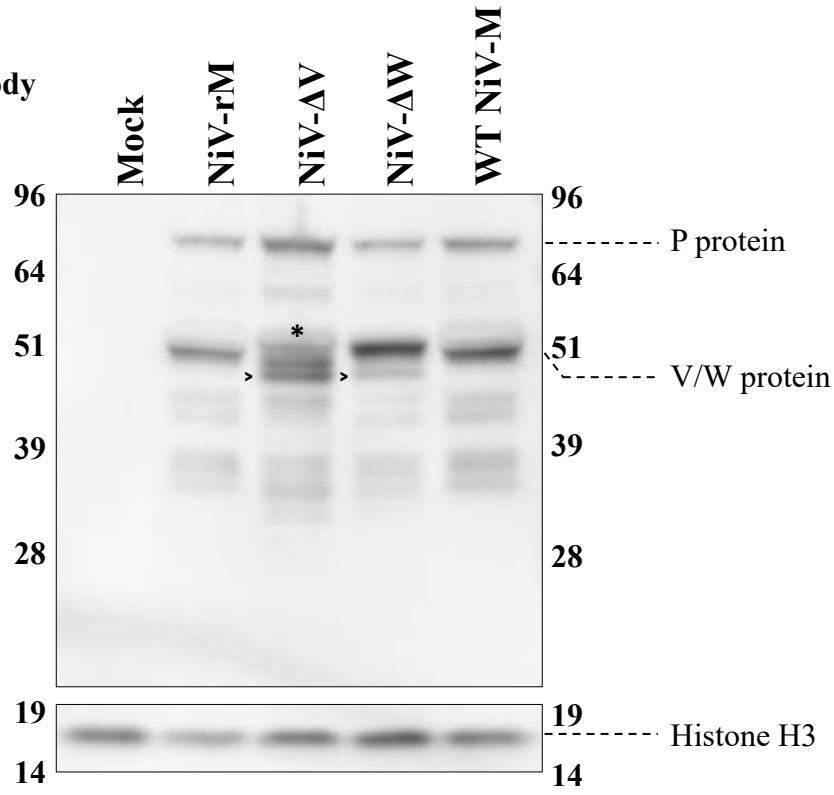

B

Anti-W antibody

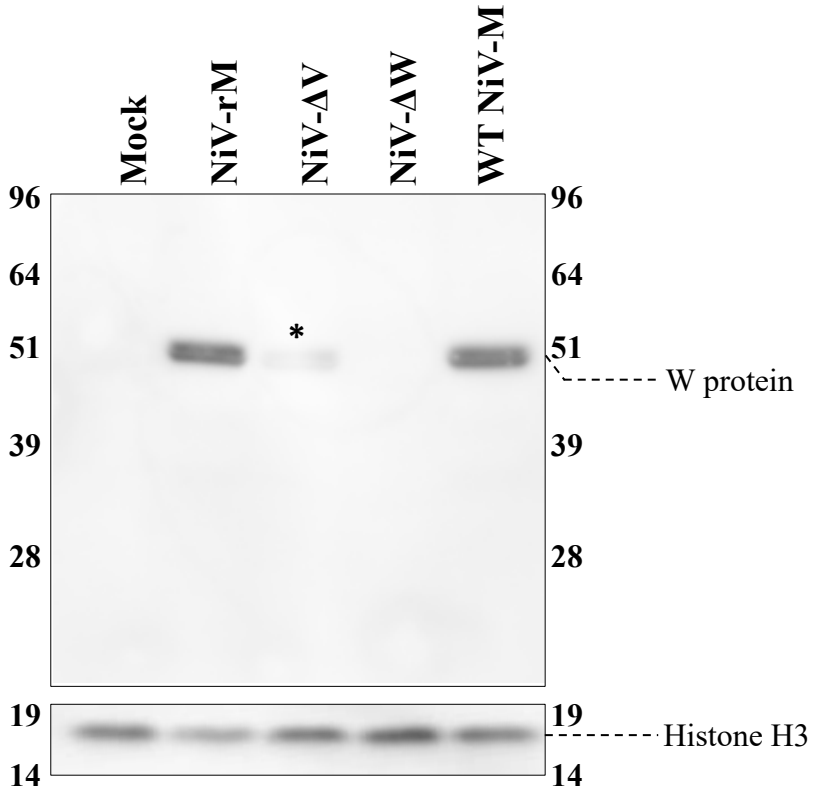

approximately 78 kDa, while the V and W proteins appear as bands of almost equal apparent size at around 51 kDa. The remaining bands are thought to be either different phosphorylation or acetylation states of the P, V and/or W proteins [Kulkarni *et al* 2009, Shiell *et al* 2003] or degradation products of the phosphoprotein [Lo *et al* 2009]. Interestingly, the anti-P immunoblots of the cell lysates from both NiV-ΔV- and NiV-ΔW-infected cells (but not of wild-type NiV-M- or NiV-rM-infected cells) showed an additional band slightly smaller in size than the V/W protein band that has not been previously reported (Fig. 9A, designated with >). These smaller bands might represent truncated P proteins (tP) consisting of the translated portions of the V protein in NiV-ΔV-infected cells or the W protein in NiV-ΔW-infected cells and would correspond to the common PNT of the P, V, and W proteins. This product was hypothesized by Yoneda *et al* [2010] to be produced by NiV-ΔV and NiV-ΔW, but have not previously been observed.

In NiV-ΔW cell lysates, there was a clear band at the V/W protein size in the anti-P blot (Fig. 9A), but no band at the W protein size on the anti-W blot (Fig. 9B), confirming the absence of expression of the W protein and indicating normal expression of the V protein by NiV-ΔW.

In NiV-ΔV cell lysates, there was a faint band at the expected V/W protein size on the anti-P blot (Fig. 9A) and a matching faint band at the W protein size on the anti-W blot (Fig. 9B). This confirmed that the NiV-ΔV had no expression of the V protein and indicated reduced expression of the W protein in infected Vero 76 cells, despite no genetic block of the synthesis of the W protein. This had not been observed using the rNiV system by Yoneda *et al* [2010], who assessed the expression of the V and W proteins only qualitatively. However, Satterfield *et al* [2015] detected noticeably less W protein in their NiV-ΔV compared with their wild-type NiV-M in

Vero 76 cells, and Lo *et al* [2012] observed this for their NiV-ΔV in a human endothelial cell line (HMVEC-L), but not in their Vero cells.

3.1.4 Growth of rNiVs in immortalized cell lines

The growths of the recombinants NiV-ΔV and NiV-ΔW were compared to the growth of the NiV-rM in Vero 76, IBRS-2, MRC5, IPAM31, and ST cells in order to evaluate the relative importance of the V and W proteins to NiV replication. Table 4 provides a summary of these cell lines and some of their major characteristics.

Vero 76 cells were chosen because they are incapable of producing interferon and would reflect the ability of NiV to replicate with minimal interference of host cell IFN [Desmyter *et al* 1968, Mosca and Pitha 1986]. IPAM31 were chosen to provide insight into the role of NiV V and W proteins in porcine immune cells of myeloid lineage [Weingartl *et al* 2002]. ST cells were chosen as a non-immune porcine cell type capable of interferon production [Lin *et al* 2013]. MRC5 cells were chosen as an interferon-producing primate cell line so that the species difference between Vero 76 and the two porcine cell lines could be partially accounted for [Markušić *et al* 2014]. A porcine kidney epithelial cell line incapable of producing type I IFN, IBRS-2 [Ahl and Rump 1976], was tested initially as a porcine analog to Vero 76 cells; its use was discontinued when the cells were determined to be unable to support replication of NiV-M. A human myeloid cell type was not used because it had been previously determined that NiV-M does not infect human monocytes or leukocytes [Mathieu *et al* 2011], in contrast to NiV-M infection of swine.

To assess the growth of the NiV-M recombinants, the Vero76, IPAM31, MRC5, and ST cells were infected with each of the recombinants at an MOI of 0.1. MOI calculations in this

Table 4: Characteristics of immortalized cell lines used for studies of the growth of NiV recombinants.

Cell Line	Full Name	Species	Type	Produces type I IFN?
Vero 76	N/A	African Green Monkey (*Cercopithecus aethiops*)	Kidney epithelial	No [Desmyter *et al* 1968; Mosca and Pitha 1986]
IPAM31	Immortalized porcine alveolar macrophages	Porcine (*Sus scrofa*)	Alveolar macrophages	Yes [Singh and Ramamoorthy 2016a,b]
ST	Swine testis	Porcine (*Sus scrofa*)	Testis fibroblast	Yes [Lin *et al* 2013]
MRC5	N/A	Human (*Homo sapiens*)	Lung fibroblast	Yes [Markušić *et al* 2014]
IBRS2	Instituto Biologico rim suino [House *et al* 1988]	Porcine (*Sus scrofa*)	Kidney epithelial	No [Ahl and Rump 1976]

investigation were based on (r)NiV titration in Vero 76 cells. Virus produced in the supernatants over time was quantitated by plaque assay and by NiV-N rRT-PCR (Fig. 10).

NiV-ΔW did not replicate differently than NiV-rM in any cell type tested by either quantitation of live virus or NiV genome copies in the supernatant (Fig. 10A-D), consistent with previous findings that the unique role of the W protein requires its nuclear localization [Shaw *et al.* 2005]. Previous studies in our lab demonstrated that the W protein did not localize to the nucleus in MRC5, ST, or IPAM31 cells [Escaffre 2009; Bodmer 2011].

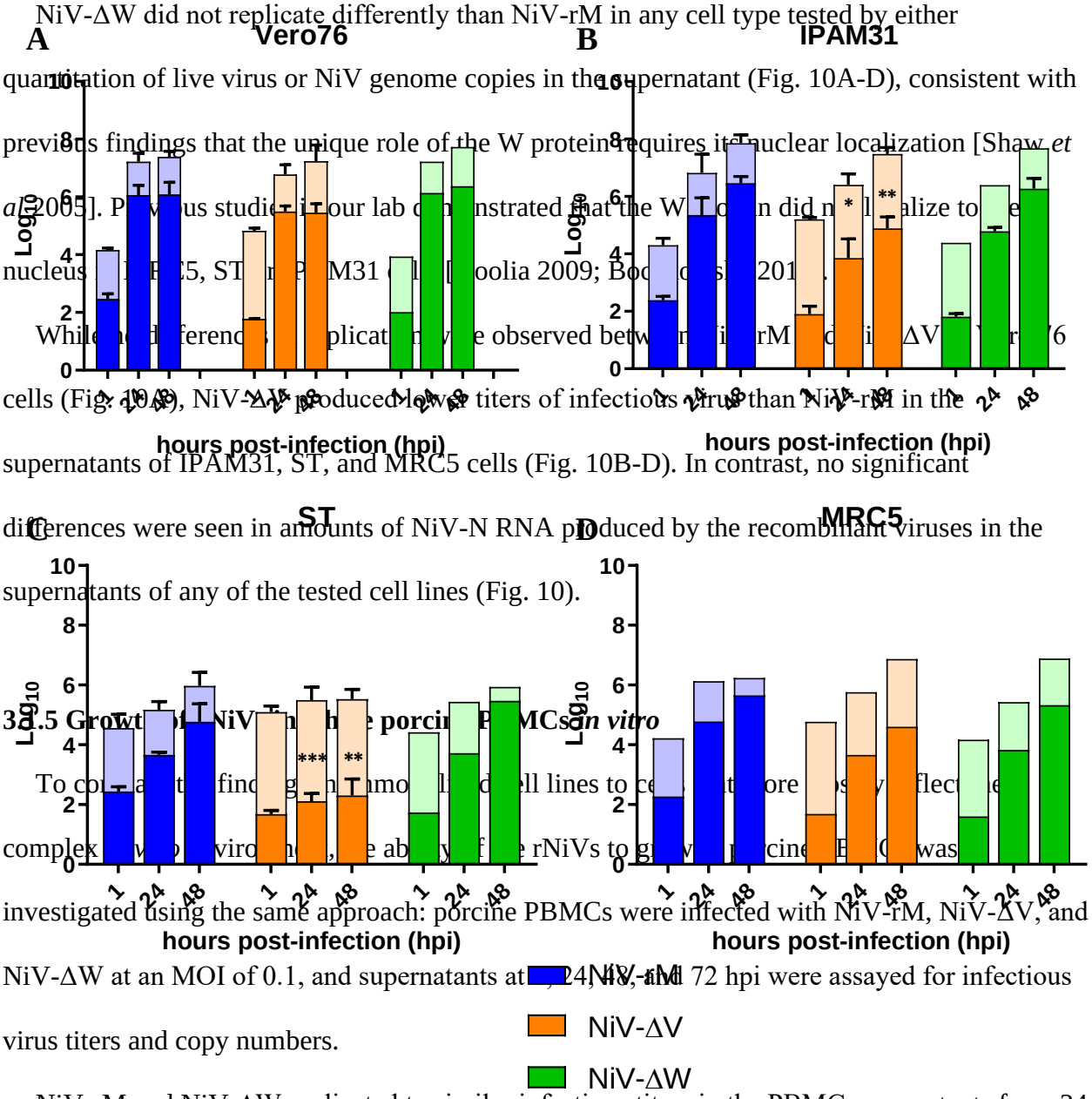

While no differences in replication were observed between NiV-rM and NiV-ΔV in Vero76 cells (Fig. 10A), NiV-ΔV produced lower titers of infectious virus than NiV-rM in the supernatants of IPAM31, ST, and MRC5 cells (Fig. 10B-D). In contrast, no significant differences were seen in amounts of NiV-N RNA produced by the recombinant viruses in the supernatants of any of the tested cell lines (Fig. 10).

3.2.5 Growth of NiV mutants in porcine PBMCs *in vitro*

To confirm findings in immortalized cell lines to ensure results more closely reflect the complex in vivo environment, the ability of the rNiVs to grow in porcine PBMCs was investigated using the same approach: porcine PBMCs were infected with NiV-rM, NiV-ΔV, and NiV-ΔW at an MOI of 0.1, and supernatants at 1, 24, 48, and 72 hpi were assayed for infectious virus titers and copy numbers.

NiV-rM and NiV-ΔW replicated to similar infectious titers in the PBMC supernatants from 24 to 72 hpi. NiV-ΔV also reached similar plaque titers to NiV-rM at 24 hpi but these titers more rapidly declined than those of NiV-rM and were significantly lower at 48 ($p<0.05$) and 72 hpi ($p<0.01$) (Fig. 11). The pattern of NiV-ΔV infectious virus production in porcine PBMCs

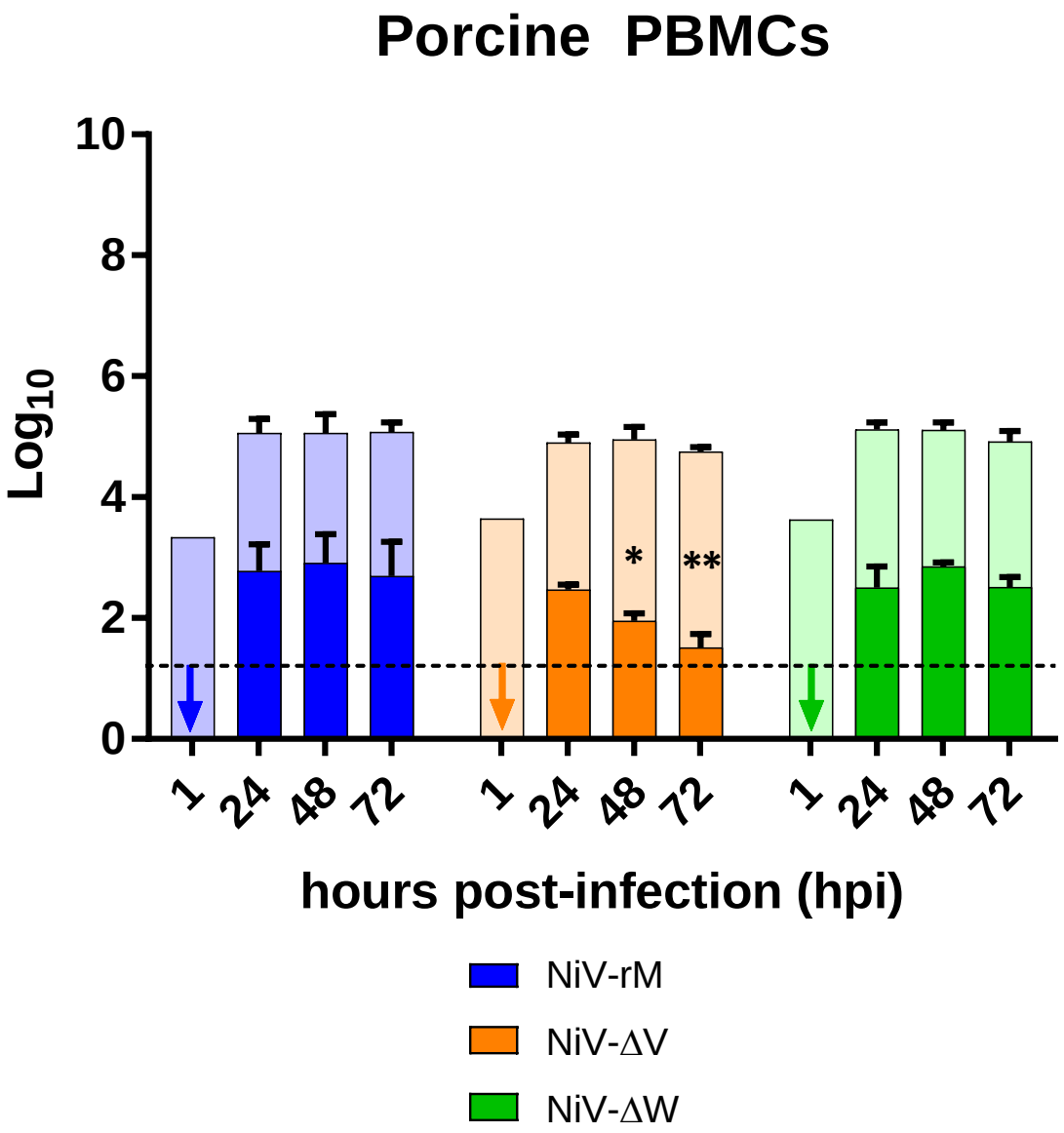

Figure 10. Replication of recombinant NiVs *in vitro* over 48 hpi in multiple immortalized cell lines. Cells were infected with NiV-rM (blue), NiV-ΔV (orange), or NiV-ΔW (green) at an MOI of 0.1. Clarified supernatants from (A) Vero76, (B) IPAM31, (C) ST, and (D) MRC5 cells at 1, 24, and 48 hpi were assayed by plaque assay for infectious titer (dark-coloured, overlying bars) in Log_{10}(PFU/mL); and by NiV-N –specific rRT-PCR for copy numbers (light-coloured, subjacent bars) in Log_{10}(copy numbers/mL). Results with error bars are means of three independent experiments (n=3); error bars represent standard deviation. Results without error bars represent data from a single repeat (n=1). Significance indicates a significant difference in infectious titer or genome copies compared to the NiV-rM in the same cell type (*$p<0.05$, **$p<0.01$, ***$p<0.001$).

Figure 11. Replication of recombinant NiV in porcine PBMC *in vitro* over 72 hpi. Whole PBMC were infected at an MOI of 0.1 with NiV-rM (blue), NiV-ΔV (orange), or NiV-ΔW (green). Clarified supernatants collected at 1, 24, 48, and 72 hpi were assayed by plaque assay for infectious titer (dark-coloured, overlying bars) in Log_{10}(PFU/mL); and by NiV-N-specific rRT-PCR for copy numbers (light-coloured, subjacent bars) in Log_{10}(copy numbers/mL). Results are from three independent repeats (n=3) of the experiment. Arrow represents a titrated sample that was undetected; the limit of detection for the plaque assay is indicated by the dotted line. Bars represent means replicates, error bars represent standard deviation, and significance refers to a significant difference in infectious titer or copy number of a sample compared to the NiV-rM at the same time point (*p<0.05, **p<0.01).

(Fig. 11) was different from the pattern in immortalized cell lines (Fig. 10): the difference between NiV-ΔV and NiV-rM manifested in the PBMCs as a more rapid decline in NiV-ΔV

infectious titers after 24 hpi. That NiV-ΔV reached comparable infectious titers to NiV-rM at 24 hpi in the supernatants porcine PBMCs (Fig. 11) indicated that the absence of the V protein does not affect early replication of NiV-M in porcine PBMCs. The decline in infectious titers of NiV-ΔV after 24 hpi in porcine PBMCs suggested that the V protein is important for the maintenance of infectious titers in the supernatants at later time points.

Similar to what was seen for genome copy numbers of the rNiVs in the supernatants of the immortalized cell lines, genome copy numbers in the PBMC supernatants as (quantitated by NiV-N rRT-PCR) were similar for all three rNiVs and did not change from 24 to 72 hpi (Fig. 11).

In all infected cell supernatant samples tested (from cell lines or PBMCs), the NiV RNA copy numbers were considerably higher than the plaque forming units. The NiV-N probe-based rRT-PCR cannot distinguish between mRNA and full-length genomic RNA; consequently, detection of NiV-N mRNA can artificially increase the number of detected NiV-M genome copies. This was a concern especially for the NiV-ΔV infectious titers in the supernatants of cells producing IFN such as IPAM31 or PBMC because these data demonstrated a reduction in infectious titer without a commensurate reduction in genome copy numbers measured by the NiV-N probe-based rRT-PCR. To determine whether the detected viral RNA represents viral genomes and presumably virus particles, the copy numbers for the NiV-M N and L genes were compared.

3.1.6 Verifying genome copy numbers in supernatants with NiV N vs NiV L SYBR Green rRT-PCR

The N vs L gene rRT-PCR was designed on the premise that equal amount of N gene to L gene sequences would be present in the infected cell supernatants if copies of genomic RNA (and hence virions) were being detected. The L gene was selected for comparison with the N gene because the L gene is at the opposite (5') end of the NiV genome and is the least abundant mRNA species produced due to the 3' to 5' transcription gradient of paramyxoviruses [Rima and Duprex 2009, Lamb and Parks 2013]. The rRT-PCR assay used SYBR Green for detection of amplified targets, which allowed the relative amounts of the N and L genes of NiV-M in supernatants to be compared.

The efficiencies of the N and L primers' amplification of NiV RNA were evaluated and found to be similar (Fig. 12A), indicating that it was appropriate to use the primers and determined reaction conditions to compare N and L RNA amounts over the evaluated range of NiV-M RNA concentrations [Livak and Schmittgen 2001]. Additionally, the primer pairs were found to amplify the same amount of target RNA at similar C_T values and the lines of best fit of the C_T values of serially diluted NiV-M RNA between both primer pairs were not significantly different ($p = 0.1$) (Fig. 12A), altogether demonstrating that the primer pairs had similar sensitivities.

Supernatants taken at 48 hpi from Vero 76, IPAM31, and ST cells infected with NiV-ΔV and NiV-rM were analyzed by the NiV-L and NiV-N SYBR Green rRT-PCR in parallel with the analysis by the probe-based NiV-N rRT-PCR reported in Fig. 10A-C. The ratio of the amount of the N RNA to L RNA was determined by a modified Livak and Schmittgen $2^{-\Delta\Delta Ct}$ analysis [Livak and Schmittgen 2001] and plotted as the N to L ratio (ΔC_T N-L) on a $\log_2$ scale (Fig. 12B).

Figure 12. Differences between C_T values detected by NiV-N vs NiV-L SYBR Green rRT-PCR. (A) The differences between NiV-N and NiV-L C_T values (ΔC_T N-L) in clarified 48 hpi supernatants of Vero 76, IPAM31, and ST cells infected with NiV-ΔV (orange) or NiV-rM (blue). Each point represents the average of the differences between the C_Ts for NiV-N and NiV-L (ΔC_T N-L) of samples from three independent repeats of the experiment (n=3). Error bars represent standard deviation. Refer to Appendix A.5.4 for sample data analysis calculations. (B) C_T values of N vs L primers' amplification of 10-fold serially diluted NiV-M RNA by the SYBR Green L and N amplification method. C_T values from the L primer pair are in blue and C_T value from the N primer pair are in red. Each data point represents the average of three technical replicates (three separate rRT-PCR amplifications, each run in duplicate) of the same RNA dilution series. Error bars on data points represent the standard deviations of these replicates. The line of best fit (black) for the data determined using the extra sum of squares F test (GraphPad Prism), which tests the null hypothesis that the line of best fit for two data sets is not different: the null was not rejected ($p = 0.1$). Dotted lines represent the 95% confidence interval for the standard curve.

A

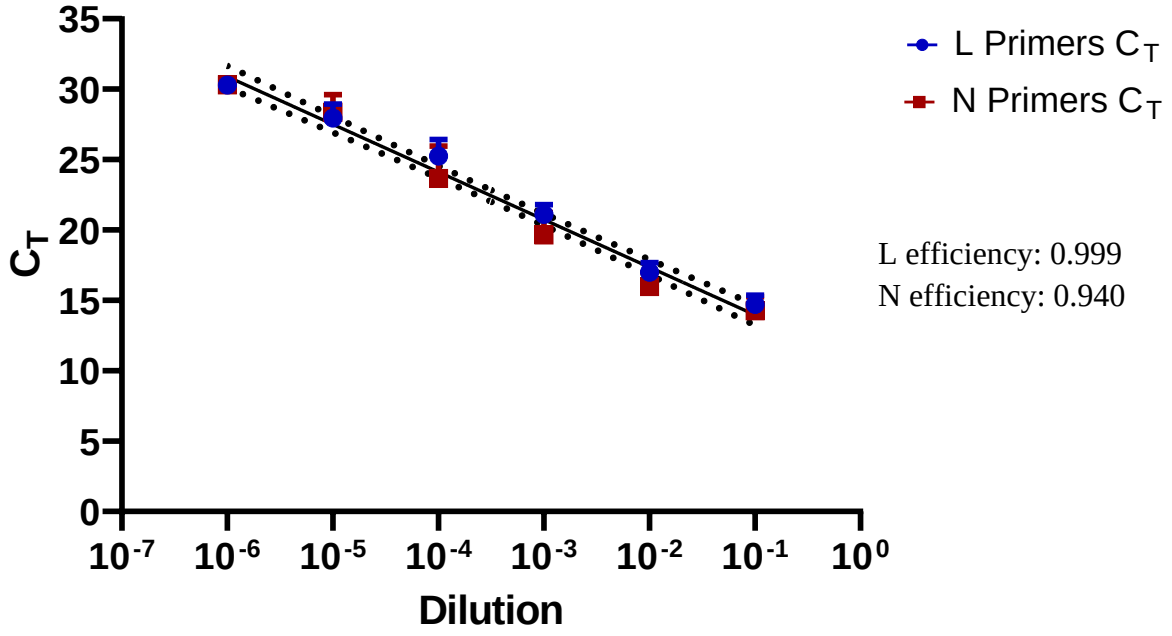
35
30
25
20
15
10
5
0
C_T
10^{-7} 10^{-6} 10^{-5} 10^{-4} 10^{-3} 10^{-2} 10^{-1} 10^{0}
Dilution
L Primers C_T
N Primers C_T
L efficiency: 0.999
N efficiency: 0.940

B

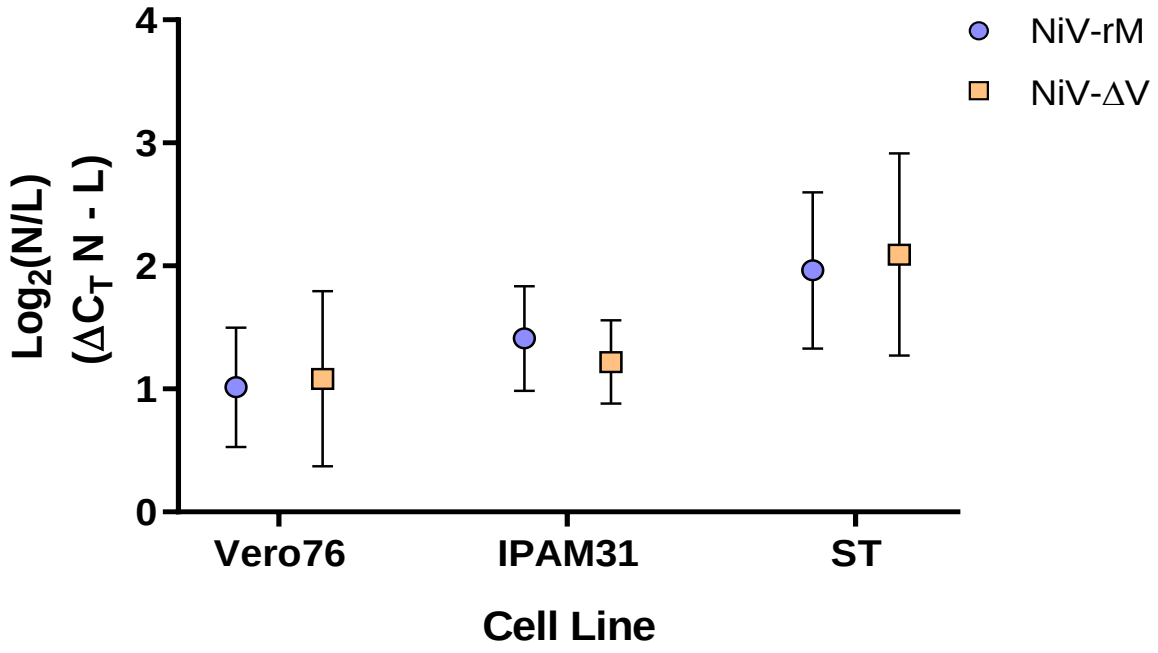
4
3
2
1
0
$Log_2(N/L)$
$(\Delta C_T$ N - L)
Vero76
IPAM31
ST
Cell Line
NiV-rM
NiV-ΔV

Within each tested cell type, ratios of N to L RNA in the supernatants of NiV-rM- and NiV-ΔV-infected cells were not significantly different. Interestingly, the ΔC_T N-L was not zero for any of the rNiVs in any cell type, as would be expected for equal detection of N and L RNA; instead, the ΔC_T values were all positive, indicating a greater amount of L RNA than N RNA. (Fig. 12B). See Appendix A.5.4 for sample data analysis calculations and interpretation.

The N vs L rRT-PCR assay verified that detection of mRNA was not contributing to the high ratio of copy numbers to infectious particles and could not account for differences in this ratio between NiV-rM- and NiV-ΔV-infected cells. The lack of difference between NiV-ΔV and NiV-rM or NiV-ΔW infectious virus titers in Vero 76 cells indicated that the V protein does not play a significant role in viral replication. The reduced infectious titers of NiV-ΔV compared to NiV-rM and NiV-ΔW in the IFN-producing cells (IPAM31, ST, MRC5, and PBMC) instead indicated a role for the V protein in preventing the production of type I IFN.

3.2 Type I IFN induction in the presence and absence of the V protein

3.2.1 Antiviral activity of rNiV-infected IPAM31 supernatants

To determine antiviral activity in the supernatants of IPAM31 infected with the recombinant viruses, a plaque reduction bioassay with Madin-Darby bovine kidney (MDBK) cells and vesicular stomatitis virus (VSV) was used. This assay is classically used to titrate type I IFN activity [Familletti and Pestka 1981; Meager 2002]. Attempts were made to optimize the available anti-porcine IFNα and IFNβ ELISAs (Fig. 13), but the bioassay was more sensitive.

In order to inactivate NiV without abolishing the antiviral activity of the supernatants, it was necessary to test several approaches to the assay. Initially, supernatants were treated at low pH to inactivate NiV and isolate IFNα/β based on their acid resistance. This method was abandoned

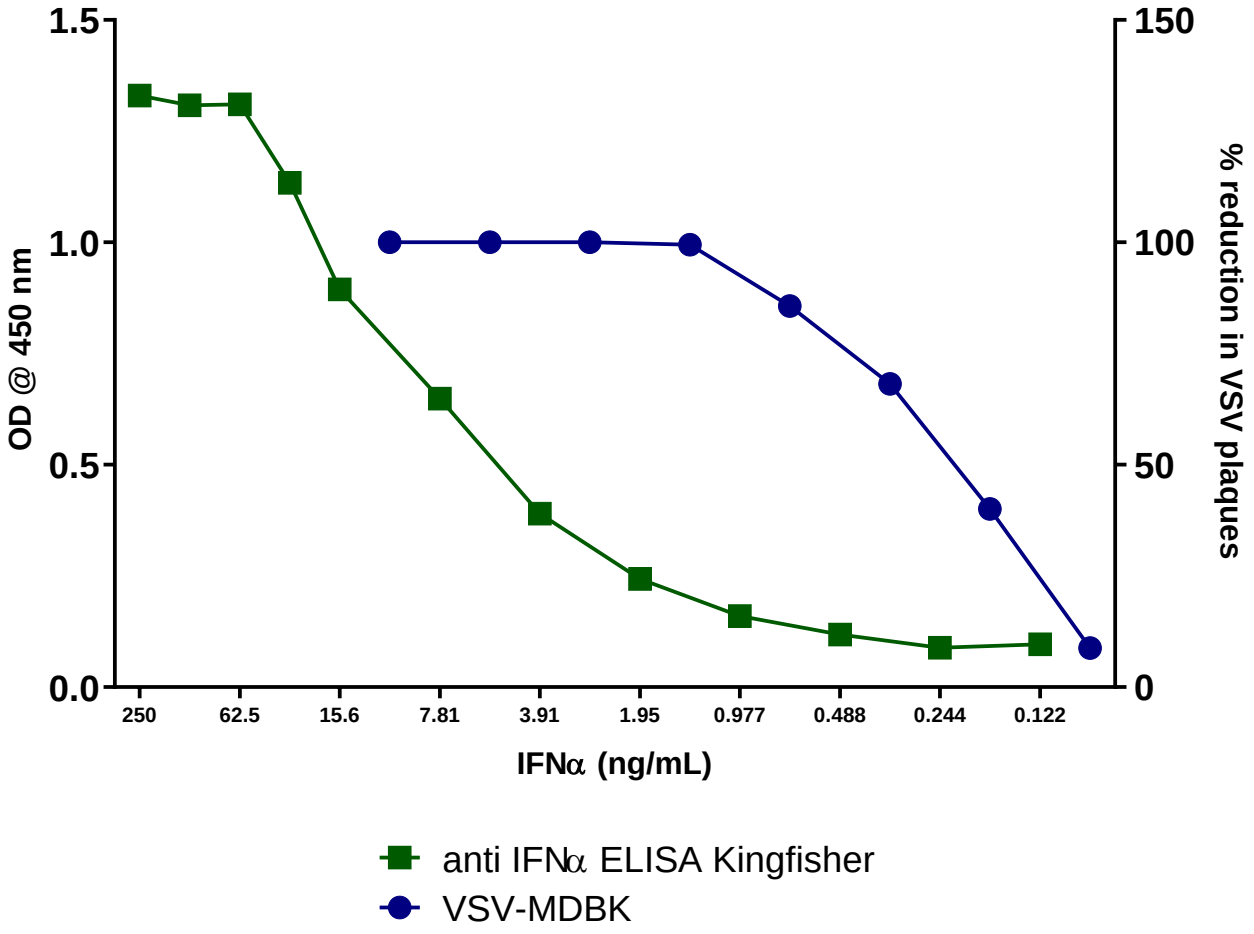

Figure 13. Comparison of the sensitivity of MDBK cells to IFNα in cell culture media (blue, in percent reduction in VSV plaques) to the sensitivity of an optimized commercial anti-porcine IFNα ELISA (green, in optical density at 450nm).

due to difficulties in maintaining the correct pH for the supernatants in all steps of the assay.

Subsequently, centrifugal filtration of the supernatants through 50 kDa molecular weight cut-off (MWCO) filters was tested to exclude large proteins and NiV particles on the basis of size: porcine IFNα and IFNβ are approximately 21 and 22 kDa, respectively. This method required a very large input of sample supernatant; the size exclusion filters did not reliably exclude NiV; and it was suspected that retention of type I IFN was leading to a loss of antiviral activity during the assay.

Finally, virus heat inactivation was employed. Type I IFNs are highly heat-stable at temperatures up to 60°C [Rentsch and Zimmer 2011] and at that temperature, NiV and other factors with antiviral activity potentially released by infected cells were expected to be inactivated.

Supernatants collected from Vero 76 and IPAM31 cells at 24 and 48 hpi with NiV-rM or NiV-ΔV (at an MOI of 1) alongside supernatants from mock-infected (control) cells were analyzed by the MDBK-VSV bioassay (Fig. 14A). Each supernatant was also tested undiluted to ensure that the supernatants had no residual live NiV. There were no differences in antiviral activities between NiV-rM, NiV-ΔV, or mock-inoculated cells at 24 hpi in either cell line. However, while supernatants of NiV-ΔV-infected IPAM31 cells had the same level of antiviral activity as the control cells at 48 hpi, antiviral activity in NiV-rM-infected IPAM31 was significantly reduced at this time point (NiV-ΔV vs NiV-rM, $p<0.001$). No differences were observed in the antiviral activities of the Vero 76 cell supernatants at that time (Fig. 14A**)**.

Pre-treatments of supernatants with polyclonal anti-porcine IFNα or IFNβ antibodies were used to analyze the relative contribution of the two type I IFN subtypes to the antiviral activity in the NiV-rM-infected IPAM31 supernatants. The use of polyclonal antibodies provided evidence

Figure 14. Analysis of the antiviral activity rNiV-infected IPAM31 supernatants. (A) The ratio of the antiviral activity of 24 and 48 hpi supernatants of cells infected with NiV-rM (blue) or NiV-ΔV (orange) to the antiviral activity of supernatants of mock-infected cells of the same type (grey). The magnitude of antiviral activity in each sample was based on the ability of these supernatants to reduce VSV plaques on MDBK cells in an antiviral bioassay. Bars represent the average antiviral activity ratio to mock of two independent repeats of the experiment (n=2); error bars represent standard deviation. (**$p<0.01$, ***$p<0.001$). (B) Percent reduction of VSV plaques on MDBK cells after pre-treatment with IPAM31 supernatants prepared for the assay using centrifugal filtration and anti-IFN neutralizing antibody treatment. Grey bars represent non-antibody-treated supernatants; yellow bars represent supernatants with IFNα activity neutralized; and red bars represent supernatants with IFNβ activity neutralized. Bars represent the average of three technical replicates from a single biological repeat of the experiment.

A

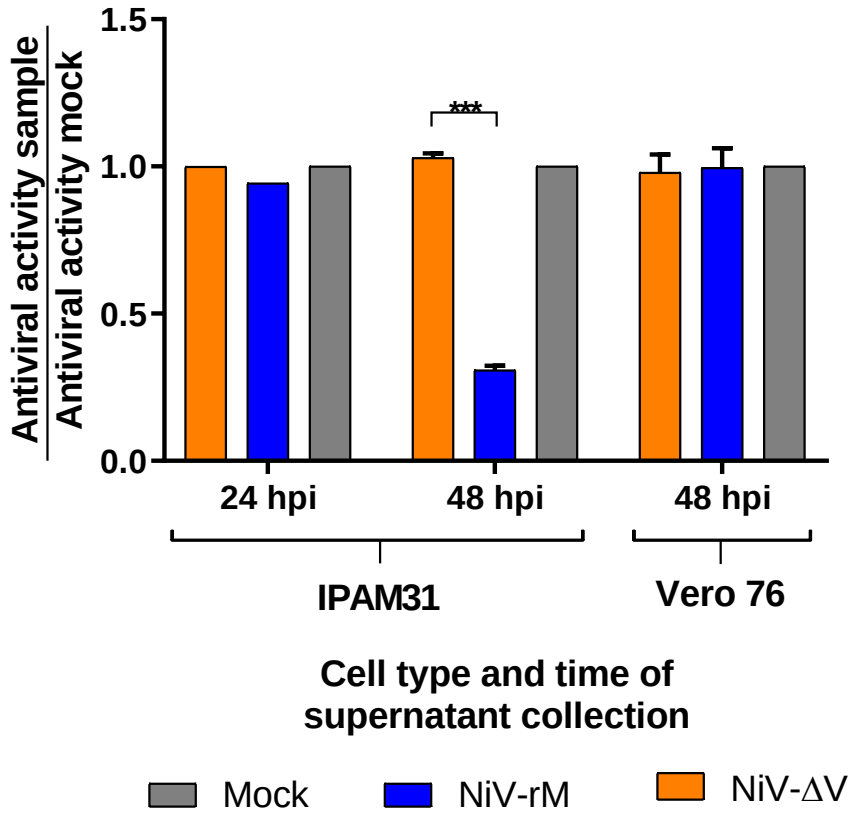
Antiviral activity sample
Antiviral activity mock
1.5
1.0
0.5
0.0
***
24 hpi
48 hpi
48 hpi
IPAM31
Vero 76
Cell type and time of supernatant collection
Mock
NiV-rM
NiV-ΔV

B

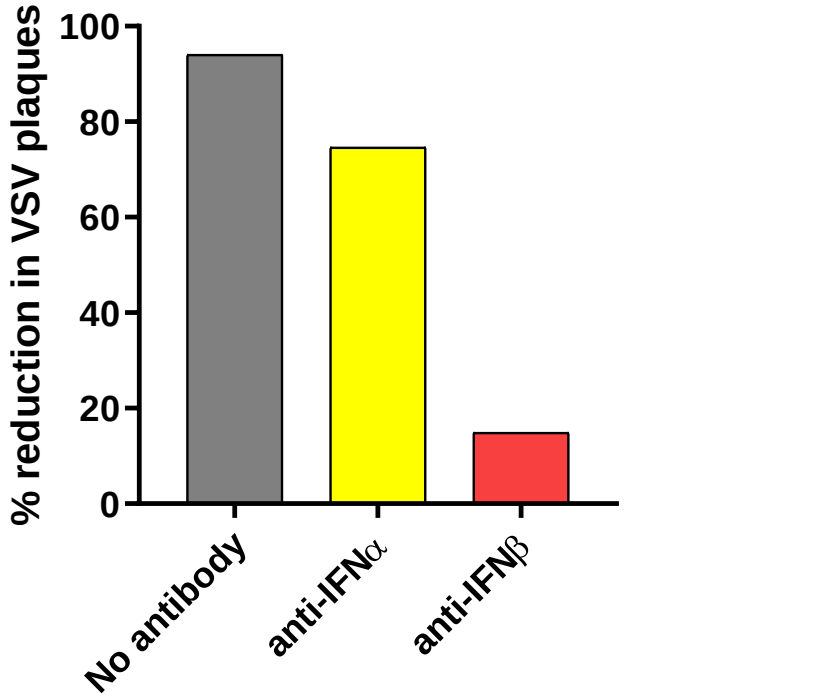
% reduction in VSV plaques
100
80
60
40
20
0
No antibody
anti-IFNα
anti-IFNβ
Antibody pre-treatment of IPAM31 supernatant

that IPAM31 cells can produce type I IFN during rNiV infection and that this type I IFN is primarily IFNβ: the supernatants had high antiviral activity (94.0% reduction in VSV plaques) which was diminished after treatment with anti-IFNβ (by 79.1%) but not by anti-IFNα antibodies (diminished only by 19.4%) (Fig. 14B).

3.2.2 IFNα/β mRNA expression in rNiV-infected IPAM31 cells

The findings that the supernatants from NiV-ΔV-infected IPAM31 cells had significantly greater antiviral activity than those infected with NiV-rM and that the V protein was important for the production of infectious virus from type I IFN-producing cells indicated that the V protein's major role might be in type I IFN evasion.

To determine whether the V protein prevents type I IFN induction, IPAM31 cells were infected with NiV-rM or NiV-ΔV at an MOI of 1 and expression of IFNα and IFNβ mRNA was evaluated at time points up to 24 hpi by a SYBR Green rRT-PCR method.

Fold change in expression of IFNα and IFNβ mRNA was calculated using Livak and Schmittgen's $2^{-\Delta\Delta Ct}$ method [Livak and Schmittgen 2001], normalizing to the expression of cyclophilin as the housekeeping gene and comparing to mock-infected cells at the same time points (Fig. 15). Neither NiV-rM nor NiV-ΔV induced significantly different amounts of IFNα from the mock-infected IPAM31 (Fig. 15A). However, IPAM31 cells infected with NiV-ΔV did express significantly more IFNβ mRNA than those infected with NiV-rM at 24 hpi only (Fig. 15B, $p<0.001$), despite a lack of detectable antiviral activity in the supernatants of NiV-ΔV- or NiV-rM-infected IPAM31 cells at 24 hpi (see Fig. 14A).

In NiV-ΔV-infected IPAM31, there was an upregulation of IFNβ mRNA at 2 hpi followed by a downregulation at 4 hpi (Fig. 15B). No firm conclusions can be drawn from this because only

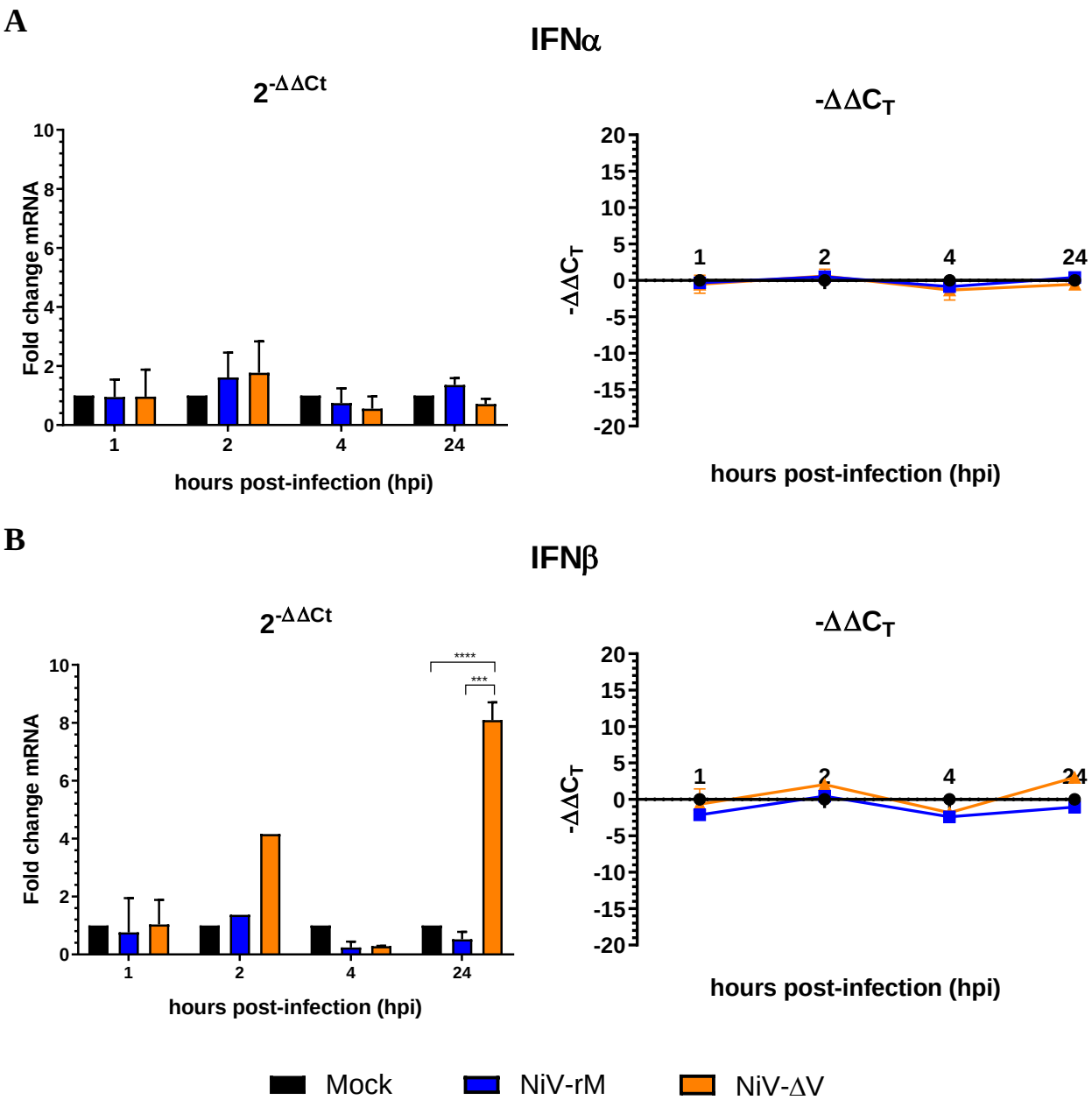

Figure 15. Fold change in expression of (A) IFNα and (B) IFNβ mRNA in IPAM31 cells over time after infection with NiV-rM (blue) or NiV-ΔV (orange) at an MOI of 1. $-\Delta\Delta C_t$ values were calculated using the Livak and Schmittgen method [Livak and Schmittgen 2001] normalizing to cyclophilin as the reference gene; fold change is expressed as relative to the mock-infected cells (black) at the same time point; see Appendix A.5.5 for sample calculations. The same data is represented as both $-\Delta\Delta C_t$ (left) and $2^{-\Delta\Delta Ct}$ (right). Bars/points represent the average fold change of three independent replicates of the experiment (n=3); error bars represent standard deviation. (***p<0.001, ****p<0.0001).

one biological replicate of the 2 hpi time point was performed for IFNβ, precluding the proper application of descriptive statistics.

3.2.3 IFNα/β mRNA expression in rNiV-infected whole porcine PBMCs

To evaluate the effect of NiV infection on an immune response model that is closer to the *in vivo* environment, IFNα and IFNβ mRNA expression in porcine PBMCs inoculated with either rNiV-M or NiV-ΔV was evaluated. Porcine PBMCs were chosen because they are a more complex immune cell population and more closely reflect the *in vivo* environment.

A decrease in both IFNα and IFNβ mRNA expression at the 1 and 24 hpi time points from the high level of expression by the mock-infected PBMCs was observed in porcine PBMCs infected with either the NiV-rM or NiV-ΔV (Fig. 16). For both type I IFN subtypes, the mRNA downregulation was greater in NiV-rM-infected PBMCs than in NiV-ΔV-infected PBMCs (Figure 16A and B, particularly the $-\Delta\Delta C_T$ panels).

The high expression of type I IFN in the mock-infected PBMCs was not surprising, as porcine immune cells can produce type I IFN independently of infection in order to maintain balance [Wattrang *et al* 1998, Razzuoli *et al* 2011, Amadori 2007]. However, the block of type I IFN expression by 1 hpi was unexpected. Although 1 hr is enough time for NiV-M to attach to and enter the cells, it is too early for the production of new non-structural viral proteins (see Fig. 3) [Kulkarni *et al* 2009, Noton and Fearns 2015, Boczkowska 2014].

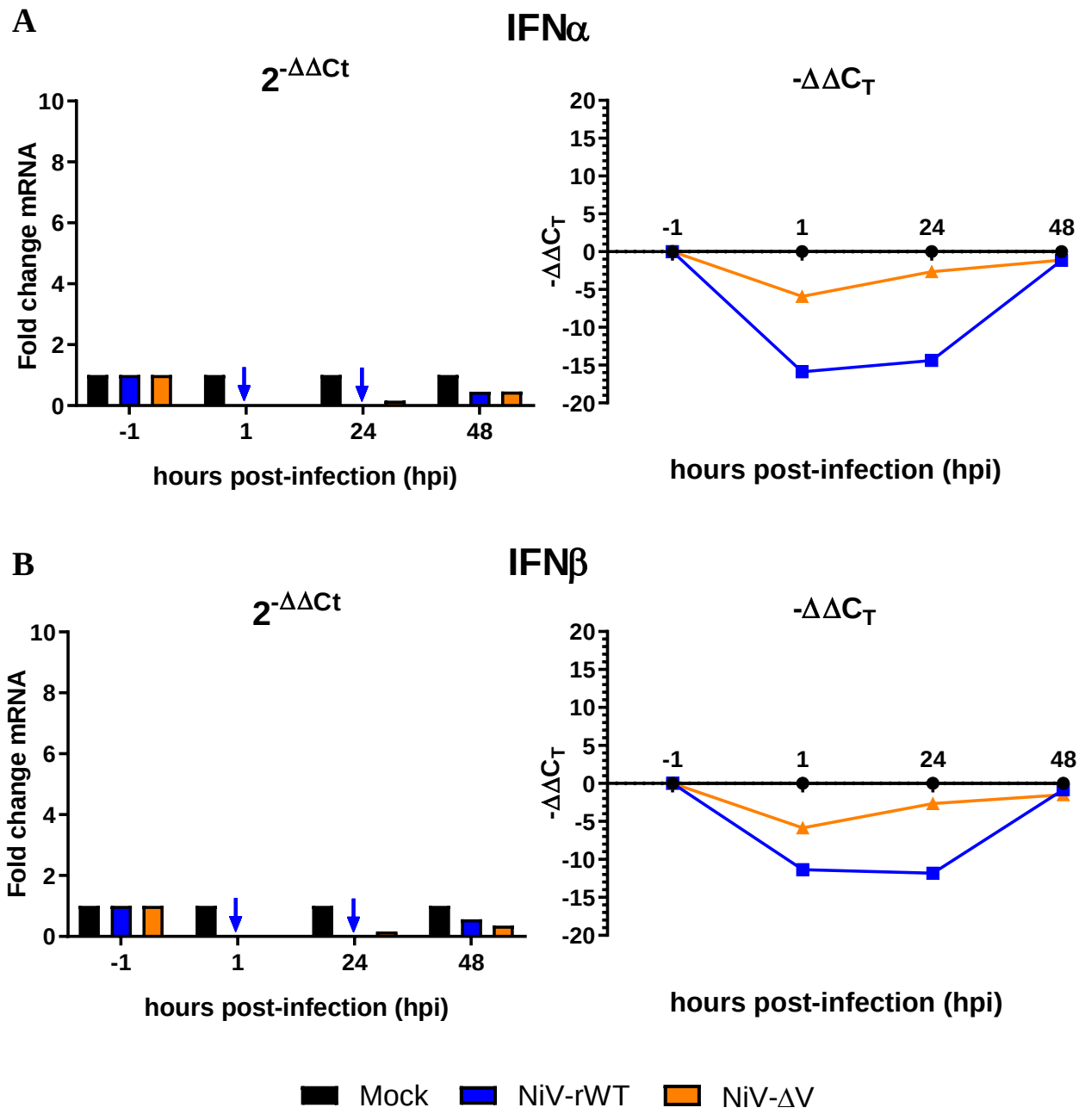

Figure 16. Fold change in expression of (A) IFNα and (B) IFNβ mRNA in whole porcine PBMCs over time after infection with NiV-rM (blue) or NiV-ΔV (orange) at an MOI of 0.1. -$\Delta\Delta C_t$ values were calculated using the Livak and Schmittgen method [Livak and Schmittgen 2001] normalizing to cyclophilin as the reference gene; fold change is expressed as relative to the mock-infected cells (black) at the same time point. See Appendix A.5.5 for sample calculations. The same data are represented as both -$\Delta\Delta C_t$ (left) and $2^{-\Delta\Delta Ct}$ (right). Bars/points represent the average fold change of duplicate samples from one replicate of the experiment (n=1). Arrow indicates samples that were assayed but the target was not detectable.

3.2.4 Early induction/block of IFNα/β mRNA expression by rNiV infection of stimulated IPAM31 cells

To confirm that NiV-rM and NiV-ΔV differ in their ability to block type I IFN expression as early as 1 hpi, IPAM31 were pre-stimulated with either transfected HMW PolyI:C; HMW PolyI:C and recombinant porcine (rp)IFNβ; or rpIFNβ alone in order to mimic the high basal level of expression of type I IFN observed in the porcine PBMCs. After 18 hrs of pre-stimulation, these IPAM31 were mock-infected or infected with NiV-ΔV, NiV-ΔW, or NiV-rM at an MOI of 1 for 1 hr, at which time cell pellets were collected and analyzed for IFNα/β mRNA expression (compared to the mock-infected cells) (Fig. 17). While NiV-rM and NiV-ΔW did not differ in IFNα/β expression from each other and were similar to the mock, NiV-ΔV induced substantial IFNα and IFNβ mRNA within 1 hpi in all IPAM31 pre-stimulated cells. The priming of the IPAM31 cells seemed to sensitize the cells, leading to greater fold-induction of type I IFN than at any time point in the non-pre-stimulated IPAM31 (Fig. 17 vs Fig. 15).

A block of type I IFN mRNA expression by the NiV-M within an hour of exposure to the virus would suggest a blocking mechanism related either to attachment or entry or to a block mediated by components of the incoming viral particles. The difference in the magnitude of the block between NiV-ΔV and NiV-rM indicates that a difference between these two viruses exists before new V protein can be made. Since it is unlikely that the NiV-rM and NiV-ΔV differ in their entry mechanism, a component of the incoming wild-type NiV virion that is absent in the NiV-ΔV must mediate this early block of type I IFN induction. Previously, the non-structural proteins of NiV have been identified in purified preparations of the virions [Lo *et al* 2009]. We hypothesized that virion-incorporated V protein may be responsible for mediating most of this early post-infection block.

Figure 17. Fold change in expression of (A) IFNα and (B) IFNβ mRNA in pre-stimulated IPAM31 cells infected for 1 hour with NiV-rM, NiV-ΔV, or NiV-ΔW. IPAM31 were pre-stimulated for 18 hrs with transfected HMW PolyI:C (white), IFNβ and HMW PolyI:C (black), or IFNβ alone (grey) and then infected with one of the rNiVs at an MOI of 1. Fold change values ($2^{-\Delta\Delta Ct}$) were calculated using the Livak and Schmittgen method [Livak and Schmittgen 2001], normalizing to cyclophilin as the reference gene and then expressed relative to 1 hpi mock-infected cells subjected to the same pre-stimulation. See Appendix A.5.5 for a sample calculation. Bars represent the average fold change of three independent experiments; error bars represent standard deviation.

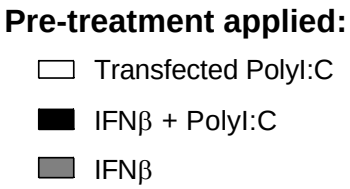

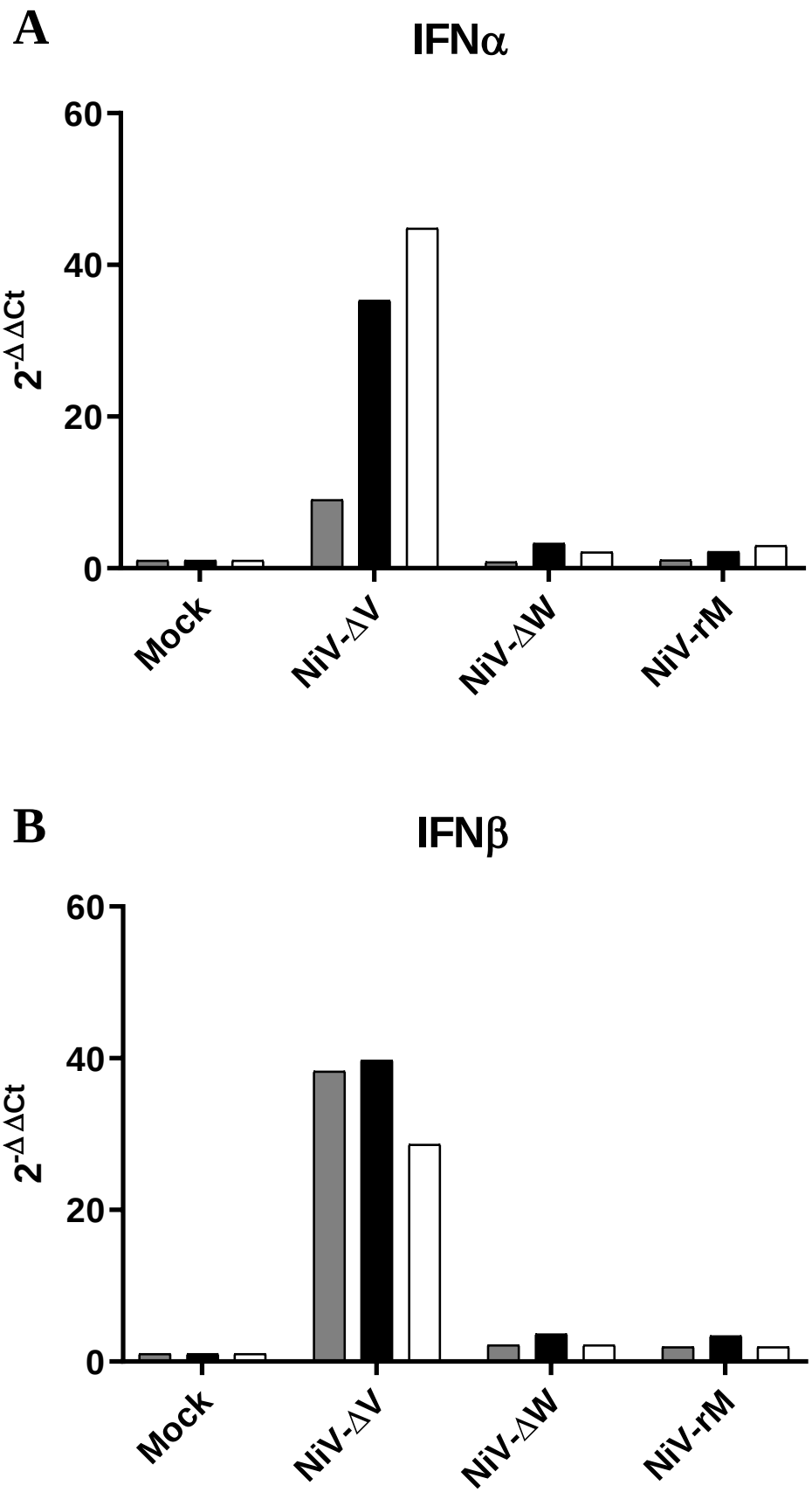
A
IFNα
60
40
20
0
2-ΔΔCt
Mock
NiV-ΔV
NiV-ΔW
NiV-rM
B
IFNβ
60
40
20
0
2-ΔΔCt
Mock
NiV-ΔV
NiV-ΔW
NiV-rM

3.3 NiV non-structural proteins in virions

3.3.1 Immunoblot comparisons of non-structural proteins in rNiV virions

To confirm that the V protein is included in the NiV virion, immunoblots were performed on virions of all three recombinants and a wild-type NiV Malaysia stock (pig lung isolate, passage 4 on Vero 76 cells) that had been isolated and concentrated by polyethylene glycol (PEG) precipitation (Fig. 18). The immunoblots correspond well with those reported for NiV-M concentrated by sucrose gradient centrifugation [Lo *et al* 2009]. Blots were probed with an anti-P/V/W monoclonal antibody P58 (Fig. 18A) or a rabbit polyclonal anti-W antibody (Fig. 18B).

All four NiVs had a similar band at 78 kDa on the anti-P/V/W blot corresponding to the P protein (Fig. 18A), indicating that each virus preparation had similar amounts of the phosphoprotein. The 51 kDa band corresponding to the V and W proteins was similar in intensity in the NiV-Malaysia, the NiV-rM and NiV-ΔW, but fainter in the NiV-ΔV. Although the NiV-ΔW virions contained wild-type amounts of the V protein, the NiV-ΔV virions did not have wild-type amounts of V or W protein. Probing the blot with anti-W antibodies (Fig. 18B) confirmed that the NiV-ΔV virus preparation had markedly less W protein than the wild-types. Considering the reduced expression of the W protein in NiV-ΔV infected Vero 76 cell lysates (Fig. 9B), the lack of the W protein in NiV-ΔV virions is probably secondary to its low level of expression.

Interestingly, the putative tP protein initially observed in the cell lysates of NiV-ΔV and NiV-ΔW (Fig. 9A) was detected in the NiV-ΔV virion but not the other virion preparations (Fig. 18A, designated with >). As mentioned previously, this band may correspond to the PNT of the P protein without a specific V, W, or P protein C-terminus. If this is the case, it appears to be incorporated into the virion of at least NiV-ΔV. The absence of this product in NiV-ΔW virions may indicate that either its incorporation occurs or is detectable by immunoblot only if there are

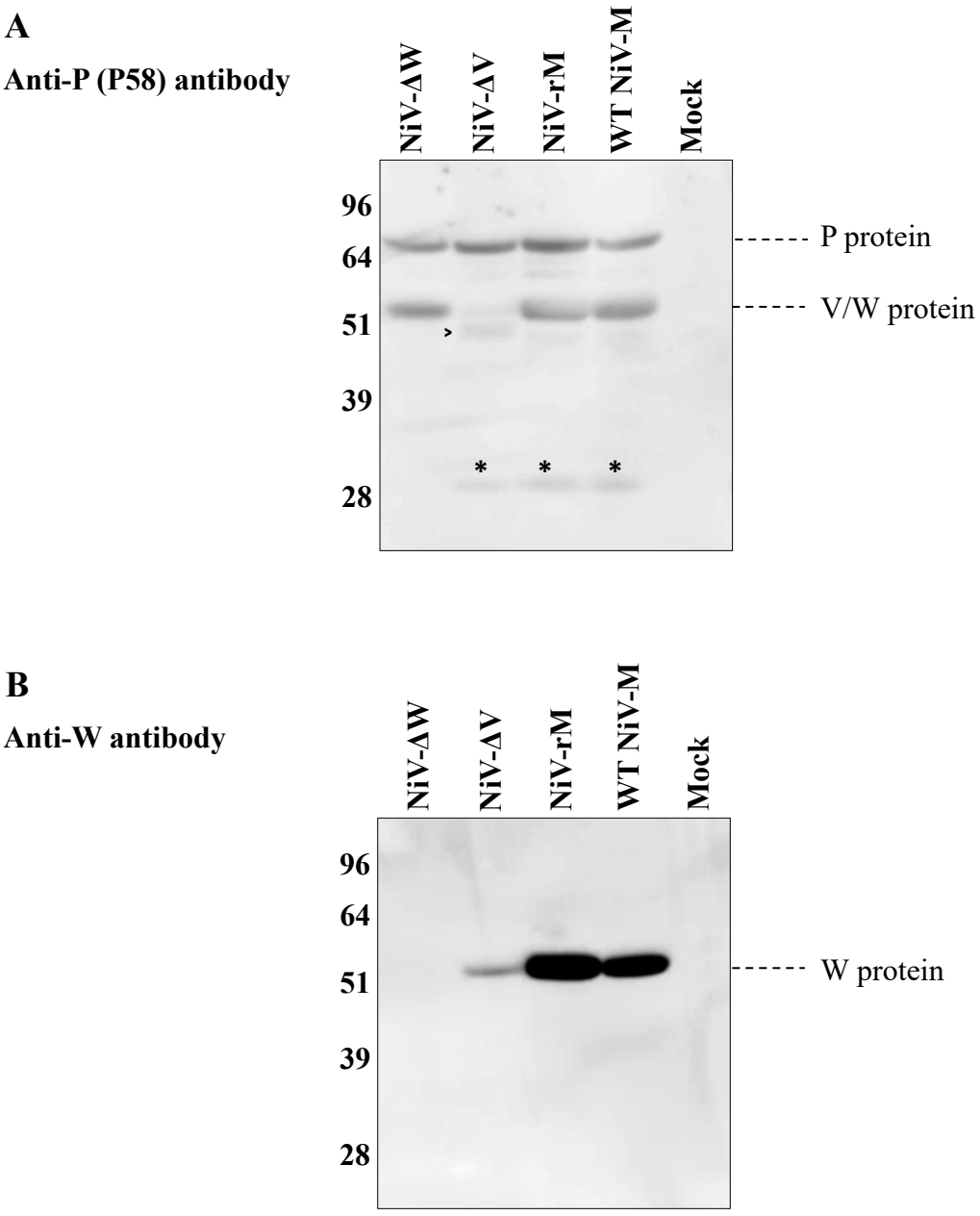

Figure 18. Immunoblots for P gene products in polyethylene glycol (PEG)-precipitated NiV stock preparations. Virus preparations were separated on a 10% Bis-Tris gel, and transferred blots were probed for (A) the common N-terminus of the P, V, and W proteins and (B) the unique C-terminus of the W protein. Bands at 78 kDa correspond to the expected size of the P protein, and bands at 51 kDa correspond to the expected size of the complete V and/or W proteins. Predicted protein sizes based on SeeBlue Plus2 Pre-stained Protein Standards are listed adjacent to each blot. "**>**" indicates the band corresponding to the (hypothesized) tP product. Asterisks (*) are placed just above the ~28 kDa cellular protein.

low levels of both V and W protein.

An unexpected ~28 kDa product was also detected in the anti-P protein-probed virions of NiV-ΔV, NiV-rM, and wild-type NiV-M, but not of NiV-ΔW (Fig. 18A). It is unlikely a degradation product of the W protein because most degradation products seen in the cell lysates are not also seen in the virions (Fig. 9A vs 18A), and because it is present in the NiV-ΔV virion at similar levels to the wild-type despite the reduced expression and incorporation of the W protein by NiV-ΔV. It is possible that this is a cellular protein incorporated into the NiV-M virion with or by the W protein.

3.3.2 Immunoelectron microscopy confirmation of non-structural protein incorporation into NiV virions

To determine whether the V and W protein are incorporated into the NiV virion by an attachment to the nucleocapsid, immunoelectron microscopy (IEM) was performed on a sucrose-gradient purified preparation of binary ethylenimine (BEI)-inactivated, wild-type NiV-M stock (prepared by Y. Berhane [Berhane *et al* 2006]). Rabbit polyclonal antibodies against the NiV-M W protein or V protein were used to probe the samples. One set of anti-V polyclonal antibodies was found to be compatible with samples fixed for IEM in glutaraldehyde-formaldehyde.

The preparation of NiV used for this was a fraction enriched for NiV nucleocapsids. Preparation of grids and imaging was performed by A. Dufresne. Gold particles localized to NiV herringbone structures in grids stained with both anti-V (Fig. 19A) and anti-W (Fig. 19B) antibodies, whereas control grids had very few gold particles visible and distributed in an apparently random fashion (Fig. 19C). Some gold labelling not associated with the nucleocapsid

Figure 19. Immunoelectron microscopy (IEM) of sucrose-gradient purified wild-type NiV-Malaysia nucleocapsids labelled with (A) polyclonal rabbit anti-V protein antibody; (B) polyclonal rabbit anti-W protein antibody; and (C) unlabelled controls. Goat anti-rabbit antibodies conjugated to 10 nm gold particles were used for detection of the labelling antibodies. Detailed views of selected structures are provided in separate, adjacent panels.

A

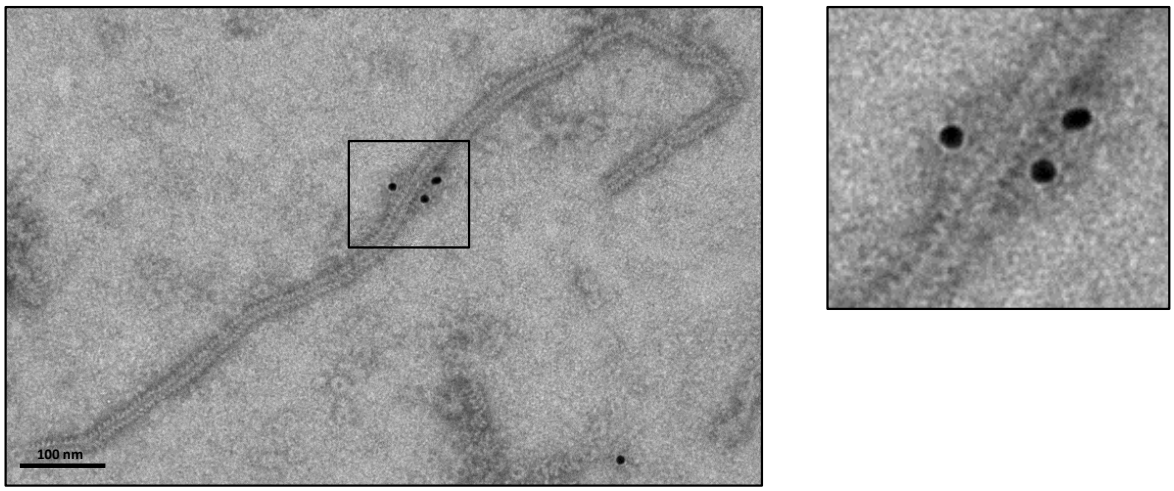

B

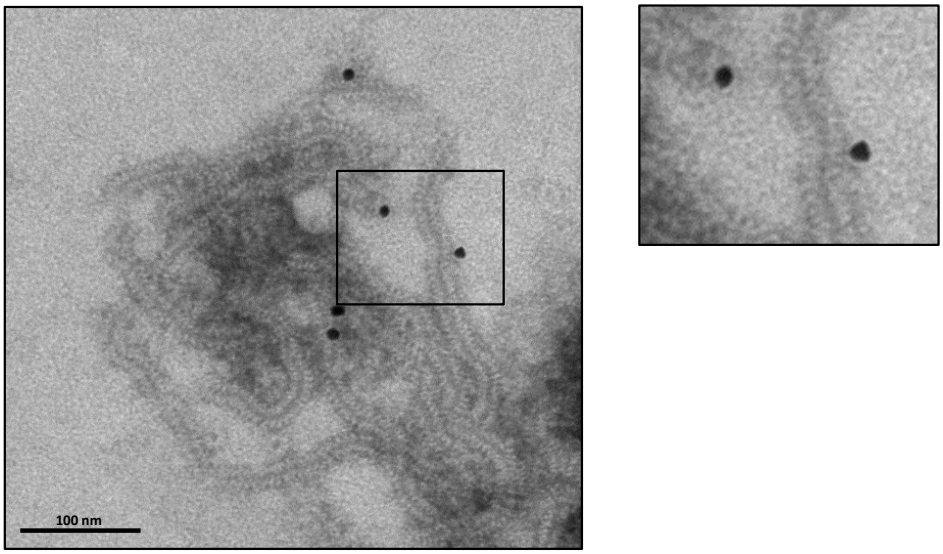

C

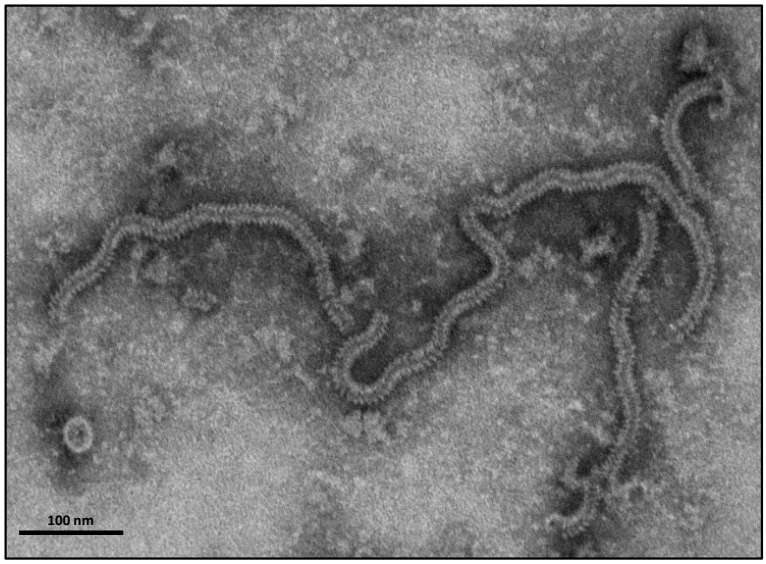

was also observed in the anti-V and anti-W stained samples. The appearance of gold labelling off the nucleocapsid could indicate V/W proteins stripped from the nucleocapsid by preparation procedures or may indicate V/W protein attached to broken nucleocapsid fragments, which were visible as rings in IEM preparations. It is also possible that along with the deliberate, nucleocapsid-bound incorporation of V/W protein, some incorporation of non-attached V/W protein could result from the non-specific envelopment of nearby proteins during NiV-M release.

Altogether, these data indicated that the V and W protein are found associated with the nucleocapsid in NiV virions. It is likely that this interaction is mediated by the common amino terminus of the V and W protein which mediates a binding interaction between the P and N proteins.

Discussion

The aim of this investigation was to explore the roles of the V and W proteins to NiV-M replication in swine cells of myeloid origin. It was determined that the W protein was not important for NiV-M replication in swine myeloid cells or PBMCs, but that the V protein was important for preventing induction of type I IFN in these cell types, with little to no direct role in viral replication. It was also determined that the V and W proteins are incorporated into the NiV-M virions through an attachment to the nucleocapsid, and that incorporated V protein is capable of blocking type I IFN induction immediately post-entry into porcine immune cells. These findings may have important implications in elucidating the immune response of swine to NiV-M infection.

4.1 Protein expression from the P gene open reading frame in cells infected with the recombinant viruses.

Examining the presence of the P, V, and W proteins in cell lysates by immunoblot confirmed lack of expression of the V or W protein by the NiV-ΔV or NiV-ΔW recombinant viruses, respectively. This study is the first to report the detection of the putative truncated P protein (tP) expressed by the NiV-ΔV or NiV-ΔW recombinant viruses (Fig. 9A) and observed also in the NiV-ΔV virions (Fig. 18A).

The existence of the tP protein was proposed by Yoneda *et al* [2010] but not observed in previous investigations with rNiVs because all previous investigations used antibodies that specifically targeted the unique C-terminal portions of the P, W or V proteins [Yoneda *et al* 2010, Lo *et al* 2012, Satterfield *et al* 2015]. The use of the P58 antibody that targets the common N-terminal region of the P, V and W proteins allowed the current investigation to directly

observe this product at approximately the predicted apparent size of 45 kDa. Although it would be interesting to confirm the identity of this protein as tP by amino acid sequencing and to determine whether the tP is also present as a low-frequency product of wild-type NiV-M infections, such investigation was considered beyond the scope of this project.

Relatively high expression of the tP protein in recombinant viruses lacking the V and W protein expression may theoretically affect the efficiency of virus replication as it could interfere with functions of the P protein, such as its viral polymerase cofactor functions [Ciancanelli *et al* 2009]. It might also be capable of affecting ribonucleocapsid assembly: the tP is likely able to bind cytoplasmic N^0 (a function of the PNT) but unable to efficiently bring it to the nucleocapsid (a function of the PCT), which could limit the pool of nucleoprotein available for nucleocapsid construction [Chan *et al* 2004, Yabukarski *et al* 2014]. However, there may not be enough tP produced to have a significant impact on virus replication. The tP product would not be expected to increase the total amount of PNT produced and so may not mediate an effect that does not already occur in the presence of the intended full-length P gene product. Additionally, large amounts of excess N protein are produced in NiV-infected cells, leading to the formation of cytoplasmic inclusion bodies (Berhane; unpublished data). Such excess N protein may be enough to overcome interference by the relatively smaller amount of tP.

Importantly, the presence of the tP in the rNiVs may counteract the loss of the type I IFN signalling block that might be expected by the reduced/absent expression of the V or W protein in NiV-ΔV and NiV-ΔW. Yoneda *et al* found that none of their recombinants differed from the wild-type NiV-M in their ability to block type I IFN signalling and suggested that this was because the total amount of PNT containing the P/V/W STAT binding site likely remained unchanged [Yoneda *et al* 2010]. Consistent with this, the unexpectedly low expression of the W

protein by NiV-ΔV in the current experiments (Fig. 9B) appears to be offset by the relatively greater expression of tP by NiV-ΔV than by NiV-ΔW (Fig. 9A). As Yoneda *et al* [2010] predicted, it appears that total PNT and likely the STAT block remain constant despite differences in V and W expression levels between the rNiVs.

The reduced W protein expression by NiV-ΔV would therefore only diminish the functions of the unique C terminal portion of the W protein along with that of the V protein in this recombinant. As the experiments conducted in this thesis research indicated no difference between NiV-rM and NiV-ΔW (see below), the low expression of the W protein in the NiV-ΔV virus was not deemed a limitation for the purposes of this study.

4.2 Growth of rNiVs in multiple cell lines

The growths of the recombinants NiV-ΔV and NiV-ΔW were compared to the NiV-rM in multiple cell lines and in porcine PBMCs to determine whether the V and/or W proteins were important in any aspect of NiV-M replication in porcine immune cells. Although porcine immune cells (represented by IPAM31 cells and PBMCs) were the cell types of interest, multiple other cell lines, described in Table 4, were included in the investigation in order to construct hypotheses regarding the function of these non-structural proteins.

4.2.1 Virus replication

In all tested cell types and for all rNiVs, there were large differences between the infectious titers and the viral RNA copy numbers in the cell supernatants. Viral RNA copy numbers in the supernatants were identified as being viral genomic RNA rather than mRNA by the N vs L gene SYBR Green assay. These data altogether suggested that the NiV-N rRT-PCR values roughly

approximate the number of NiV-M virions. The high ratio of genomic RNA to infectious particle number is likely due to the packaging of multiple genomes per particle and to the presence of a large number of defective particles containing rRT-PCR-detectable genomes [Goldsmith *et al* 2003, Jensen *et al* 2018, Chang *et al* 2006a,b; Manzoni and López 2018].

The ΔC_T N-Ls of the rNiVs in each cell type were all positive, indicating a greater presence of L RNA than N RNA (Fig. 12). It is possible that the production and packaging of 5' copy-back defective interfering (DI) particles could lead to detection of greater amounts of L RNA: these DI genomes contain two copies of the 5' end of the genome (the L gene end) and no 3' end of the genome (the N gene end) [Manzoni and López 2018**].**

4.2.2 The NiV-M W protein has no known unique role in porcine cells

NiV-ΔW did not differ from NiV-rM in any of the cells tested: no evidence was found in any of the cells tested that the W protein was important for NiV-M replication or production of infectious virus (Fig. 10, 11). This finding is consistent with previous data suggesting that the W protein has a unique anti-interferon effect if localized to the nucleus and that it does not localize to the nucleus in MRC5, IPAM31, and ST cells [Shaw *et al* 2005, Boczkowska 2014, Goolia 2009]. Furthermore, the similar blocks of type I IFN induction early post-infection by NiV-rM and NiV-ΔW (Fig. 17) indicated that the W protein is also unimportant to early antiviral evasion of NiV-M in porcine immune cells.

The similarity between NiV-rM and NiV-ΔW in this investigation is consistent with previous cell culture growth studies [Yoneda *et al* 2010, Lo *et al* 2012, Satterfield *et al* 2015]. The only cell types tested so far wherein NiV-M growth may have differed in the presence and absence of the W protein were primary human microvascular endothelial cells of the brain and lungs;

however, since the statistically significant differences were small in these cells, it is difficult to assess the biological relevance [Satterfield *et al* 2015].

Evidence exists that the W protein can be involved in blocking the production of pro-inflammatory cytokines and chemokines in certain cell types and host species and that it plays a role in disease presentation of NiV-M-infected ferrets [Lo *et al* 2012, Satterfield *et al* 2015, 2016]. However, the absence of the W protein in NiV-M-infected golden hamsters and ferrets led neither to reduced lethality nor to differences in antibody development compared to the wild-type NiV-M [Yoneda *et al* 2010, Satterfield *et al* 2015, 2016]. It has yet to be shown that the W protein has any impact on NiV-M infection of the porcine host at all.

4.2.3 The NiV-M V protein is not important for viral replication but affects infectivity in supernatants of infected IFN-producing cells

NiV-ΔV did not differ from NiV-rM in terms of genome copy numbers in any cell type tested and also did not differ from NiV-rM in the non-IFN-producing Vero 76 cells in terms of infectious titers (Fig. 10, 11), suggesting that the V protein is not directly involved in NiV replication, virion production, and release.

All previous investigations on recombinant NiV-M lacking expression of the V and W proteins have evaluated rNiV growth in cell culture only by infectious titer [Yoneda *et al* 2010, Lo *et al* 2012, Satterfield *et al* 2015]. In contrast to what was seen for Vero 76 cells in this investigation (Fig. 10A), each of these previous investigations found NiV-ΔV to have slower replication and/or to reach reduced peak titers in Vero cells compared to the wild-type. Since there were variations among these previous investigations in the time points at which the NiV-ΔV titers significantly differed and in the magnitudes of the reduction in titers from the NiV-M,

it is possible that the lack of significant difference between NiV-ΔV and NiV-rM infectious titers in Vero 76 cells in the current investigation results from variations between the Vero cell lines used by each group [Yoneda *et al* 2010, Lo *et al* 2012, Satterfield *et al* 2015].

The current investigation used an MOI of 0.1 rather than the MOI of 0.01 used in all the previous investigations, which could have reduced the time to maximum titer or the likelihood of detecting a significant difference in titer in Vero cells. The lack of a difference between NiV-ΔV and NiV-rM in Vero 76 cells in the current investigation was not considered to be a major limitation; instead, it indicated that the supposed role of the NiV-M V protein in viral replication observed in previous investigations is relatively minor compared to its auxiliary function in the IFN-producing cells.

The reduced infectious titers produced from NiV-ΔV-infected, IFN-producing cells (IPAM31, ST, or MRC5 cells) (Fig. 10B-D) and IFN-producing cell populations (PBMC) (Fig. 11) led to the conclusion that the major role(s) of the V protein are either unique to IFN-producing porcine cells or depend on the production of type I IFN. Here, the hypothesis tested was that the V protein is important for the production of infectious NiV-M in these cells because it blocks type I IFN induction.

4.3 The NiV-M V protein prevents type I IFN production by infected porcine immune cells

The major role of the V protein was hypothesized here to be in blocking type I IFN induction rather than in blocking type I IFN signalling because previous investigations had found (a) that NiV-ΔV and NiV-ΔW were as competent in blocking STAT signal transduction as the NiV-rM [Yoneda *et al* 2010]; (b) that the relevance of the STAT block to live NiV-M virus infections may not be as great as transfection studies indicated [Virtue *et al* 2011]; and (c) that there are

many potential interaction partners for the NiV-M V protein in IFN induction/virus sensing pathways indicated by protein-level studies [Childs *et al* 2012, Parisien *et al* 2009, Rodriguez and Horvath 2013, 2014; Davis *et al* 2014, Sánchez-Aparicio *et al* 2018, Uchida *et al* 2018].

4.3.1 NiV-M V protein inhibits type I IFN production in porcine myeloid cells

Wild type NiV-M-stimulated induction of type I IFN has been seen in some cell types, such as primary human microvascular lung endothelial cells (HMVEC-L) and in primary human umbilical vein cord endothelial cells (HUVEC); but not in other cell types, such as human small airway epithelial cells (SAEC), human bronchial/tracheal epithelial cells, and human moDCs [Lo *et al* 2012, Mathieu *et al* 2012b, Escaffre *et al* 2013b, Gupta *et al* 2013]. This is the first report on type I IFN induction in NiV-M-infection of a porcine myeloid immune cell line.

IPAM31 cells were used to model the monocyte type I IFN response to NiV-M infection. IPAM31 are porcine immune cells of the myeloid lineage which, as de-differentiated macrophages, are similar to monocytes [Weingartl *et al* 2002]. Monocytes are found in the peripheral blood; are important producers of type I IFN in response to virus infection; can differentiate into important type I IFN-producing cell types such as macrophages and DCs; and are known to be permissive to NiV-M infection [Swiecki and Colonna 2011, Kumagai *et al* 2007, Stachowiak and Weingartl 2012]. Thus, IPAM31 cells are a useful model for examining the type I IFN response of important type I IFN-producing porcine immune cells in a controlled manner.

The absence of induction of type I IFN by NiV-rM or NiV-ΔW in the infected IPAM31 cells (Fig. 15, 17) indicated that both viruses potently antagonized virus-stimulated type I IFN

induction. Induction of IFNβ mRNA at 24 hpi by NiV-ΔV indicated that NiV-M can initiate the induction of type I IFN, but that the V protein prevents the completion of this induction pathway.

The complete lack of IFNα mRNA induction in non-pre-stimulated IPAM31 cells infected with the recombinant viruses (including NiV-ΔV) (Fig. 15A) was unexpected, considering that IPAM31 cells are capable of responding to stimulus with IFNα expression (see Fig. 17A). A lack of IFNα mRNA upregulation at 24 hpi in the NiV-ΔV-infected IPAMs would be consistent with the model of the biphasic type I IFN response where most cells initially respond to virus with IFNβ, then respond to IFNβ by upregulating IRF7, which then permits the cell to respond to continued virus presence with IFNα [Sato *et al* 1998]. Refer to Figure 7 for a summary of IFNβ-dependent IFNα induction. Since no induction of antiviral activity by NiV-ΔV greater than the mock-infected cell was observed at 24 hpi or 48 hpi (Fig. 14A) and upregulation of IFNβ mRNA was detected only at a low level at 24 hpi (contrast Fig. 15 and 17), it is possible that there was no IFNβ protein in the supernatant of the NiV-ΔV-infected IPAM31 cells at 24 hpi to stimulate production of IFNα. It is also possible that IFNβ protein was produced and released at levels that were below the detection limit of the antiviral assay.

Together with the analysis of antiviral activity in the NiV-M-infected IPAM31 cells which indicated that approximately 80% of the antiviral activity was attributable to IFNβ and only 20% to IFNα (Fig. 14B), the data may imply that both NiV-M and NiV-ΔV have a competent STAT block that prevents IFNβ-dependent IRF7 upregulation and thereby IFNα induction (refer to Figure 7 for IFNβ-dependent IRF7 upregulation). As discussed above, the P58 antibody-probed immunoblots of infected cell lysates (Fig. 9A) demonstrated that all the rNiVs express approximately equal amounts of the PNT (containing the STAT1-binding region) in the form of the P, tP, V, or W protein. Consequently, all the rNiVs would be expected to mediate a wild-type

STAT1 block. This would be consistent with Yoneda *et al*'s [2010] previous findings that the NiV-ΔV STAT block is similar to that of the wild-type and their hypothesis attributing this to the tP product.

Early induction of type I IFN may be quite complex: the observed increase in IFNβ expression at 2 hpi in NiV-ΔV-infected IPAM31 may be evidence of the virion-incorporated V protein-mediated inhibition of type I IFN induction, although it is unclear why this would decrease by 4 hpi (Fig. 15B). However, because it was only collected once, the 2 hpi time point for IFNβ could simply represent a statistical outlier.

To determine why NiV-ΔV-infected, non-pre-stimulated IPAM31 cells appear to have a deficit in IFNβ protein production and lack an IFNα response despite IFNβ mRNA expression, future investigation should examine exactly which aspects of the antiviral state are permitted in NiV-ΔV-infected IPAM31 cells. Considering previous findings that NiV-M requires some activation of an antiviral state in infected porcine cells, it would be interesting to determine how NiV-M balances evasion of type I IFN induction and signalling with the appropriate level of antiviral state activation [Bocskowska 2014].

4.3.2 The NiV-M V protein silences steady-state and virus-stimulated IFNα/β expression in porcine PBMCs

To investigate the block of type I IFN by the NiV-M V protein in porcine immune cells, type I IFN mRNA expression was investigated in early post-wean porcine PBMCs. Porcine PBMCs were chosen as a porcine immune cell model that contains multiple interacting cell types and that more closely reflects *in vivo* immune cells than IPAM31 cells. High levels of expression of type I IFN mRNA by the immune cells of post-wean pigs is not unusual and can occur as a

homeostatic response to stress from a variety of non-infectious factors including weaning itself or transport [Wattrang *et al* 1998, Razzuoli *et al* 2011, Amadori 2007].

The V protein was confirmed to contribute substantially to the suppression of basal mRNA expression of both IFNα and IFNβ in NiV-M-infected PBMCs. NiV-ΔV did cause a reduction in type I IFN mRNA expression, but smaller than the reduction caused by NiV-rM (Fig. 16). Some block of type I IFN induction by NiV-ΔV early post-entry was not entirely unexpected: the C, W, and M proteins of NiV-M have also been implicated in blocking type I IFN responses, and these proteins were likely present (to some degree) throughout NiV-ΔV infection of the porcine PBMCs [Mathieu *et al* 2012a, Lo *et al* 2012, Satterfield *et al* 2015, Ciancanelli *et al* 2009, Bharaj *et al* 2016]. The ability of NiV-M to reduce type I IFN mRNA expression in porcine T cells infected with NiV-M has been seen previously [Stachowiak and Weingartl 2012]. Considering that porcine PBMCs contain many different cell populations (permissive and non-permissive to NiV-M) that can produce type I IFN, the summative response to NiV infection is highly complex.

Unexpectedly, the suppression of both IFNα and IFNβ mRNA occurred by 1 hpi (Fig. 16) this is approximately enough time for NiV to enter the cells but is prior to the synthesis of new V protein, which is unlikely to be in sufficient concentration to be active before 4 hpi [Plumet *et al* 2005, Lo *et al* 2009, Kulkarni *et al* 2009]. Such a rapid suppression of type I IFN by a paramyxovirus has (to the author's knowledge) not been reported before.

4.3.3 The NiV-M V protein inhibits IFNα/β induction in stimulated porcine myeloid cells immediately post-entry

To confirm and to at least partially elucidate the early block of type I IFN observed in the

porcine PBMCs, pre-stimulated IPAM31 cells were used to model porcine monocytes in the presence of type I IFN. Pre-stimulated IPAM31 cells were expected to more closely mimic the environment of porcine monocytes in the porcine PBMCs expressing high pre-infection levels of type I IFN (as seen in Fig. 16). IPAM31 cells were pre-stimulated with either IFNβ, IFNβ and polyI:C, or transfected polyI:C. After 18 hrs of this treatment, the pre-stimulated IPAM31 were infected with NiV-rM, NiV-ΔW, and NiV-ΔV. Increases in both IFNα and IFNβ mRNA expression at 1 hpi was observed only in NiV-ΔV-infected IPAM31 cells, and these increases were seen for NiV-ΔV-infected cells in each of the three pre-stimulation methods: this confirmed that the V protein plays a crucial role in preventing IFNα/β induction as early as 1 hpi post-infection.

The induction of type I IFN in by NiV-ΔV at 1 hpi in pre-stimulated (Fig. 17) but not non-pre-stimulated (Fig. 15) IPAM31 cells may help identify the interaction partners for the virion-incorporated V protein at this early time point. The lack of induction in non-pre-stimulated cells at 1 hpi (Fig. 15) seems to indicate that the V protein inhibits the IFN-induction cascade by interacting with a factor that is upregulated by IFN stimulation (i.e. an interferon-stimulated gene product). Examples of such factors include known V protein inhibition targets such as the viral RNA sensors MDA5, RIG-I, or LGP2, and related signalling molecules such as MAVS [Andrejeva *et al* 2004, Childs *et al* 2007, 2009, 2012, Motz *et al* 2013, Davis *et al* 2014, Sánchez-Aparicio *et al* 2018, Uchida *et al* 2018]. A summary of these signalling molecules can be found in Figures 5 and 6, and their IFN signalling-dependent upregulation is visualized in Figure 7.

However, the inhibition of type I IFN expression at 1 hpi only in pre-stimulated IPAM31 cells may instead indicate that the V protein inhibits other viral RNA sensors or signalling

components that are not typically present in steady state cells but are only expressed as ISGs (see Figure 7). Examples of this may include PKR or OAS1 [de Veer *et al* 2001, Soos and Szente 2003], for which possible inhibition by the V protein has not previously been reported. Future investigations should aim to determine which PRRs and related signalling components are expressed in resting state and IFN-pre-stimulated IPAM31 cells.

It is possible that the the V protein triggers or enhances the activity of negative regulators of type I IFN induction to rapidly reduce the levels and production of type I IFN. There are many negative regulators of type I IFN that are produced after type I IFN signalling which could be affected by the V protein [Arimoto *et al* 2018]: it may be valuable to identify potential V protein interaction partners in an unbiased way by using co-immunoprecipitation and shotgun mass spectroscopy to isolate and then identify V protein interaction partners in infected cells.

Considering the marked 1 hpi decrease in type I IFN mRNA in the NiV-rM-infected porcine PBMCs, it is possible that the V protein degrades or reduces the stability of type I IFN mRNA transcripts in a targeted fashion (as cyclophilin housekeeping mRNA was not reduced). Potentially, V protein-mediated activation of miRNAs that specifically target IFNα (e.g. miR-466I in mice/humans) or IFNβ (e.g. miR-26a, 34a, or 145 in humans) could lead to specific IFNα/β mRNA degradation [Arimoto *et al* 2018]. Alternatively, V protein-mediated induction of cytoplasmic RNA granules could lead to the degradation of certain mRNAs over others. Among paramyxoviruses, MeV has been observed to induce RNA granules; but whether IFNα/β mRNA is is specifically incorporated into such granules is unknown [Tsai and Lloyd 2016, Guo *et al* 2018, Okonski and Samuel 2013].

4.4 The early post-entry block of IFN production is mediated by the V protein incorporated into NiV-M virions.

The data thus far prompted investigation into the hypothesis that the early block of type I IFN observed in porcine immune cells is largely due to the inhibition of type I IFN-induction by NiV-M V protein that is incorporated into the NiV-M virion. Non-structural proteins have been detected in the virions of NiV-M before [Lo *et al* 2009]; however, there has been no indication or suggestion that these incorporated non-structural proteins might suppress type I IFN or have any effect at all.

4.4.1 The co-amino terminal P gene products are found in NiV-M virions

The immunoblots of the PEG-precipitated (r)NiV-M virions probed with antibodies targeting the PNT (P58) and the W protein confirmed previous reports that the V and W proteins are present in NiV-M virions, and provided evidence that the ability to block type I IFN induction early post-entry depended primarily on the presence of the V protein in the virions (Fig. 18). NiV-rM virions were found to contain the P, V, and W proteins, as well as a putative cellular protein of 28 kDa that reacted with the P58 antibody. NiV-ΔV virions were found to contain P, tP, and W proteins and a 28 kDa, P58-reacting putative cellular protein as well. NiV-ΔW virions were found only to contain the P and V proteins (Fig. 18). These immunoblots indicated that the early post-entry block of type I IFN induction is a role of virion-incorporated V protein and not of the W protein: although the W protein was also found to be incorporated in NiV-rM virions (Fig. 18B), the NiV-ΔW appeared to block IFNα/β induction as competently as the NiV-rM (Fig. 17).

It may be of interest to identify the putative cellular protein at 28 kDa by amino acid sequencing of the protein band in Fig. 18, or by mass spectroscopy investigations into the cellular contents of NiV-M (and possibly the rNiV-M) virions. Attempts were made to predict the identity of this 28 kDa protein *in silico* using the NCBI Standard Protein BLAST® to search for proteins (a) in primate databases; (b) with primary sequence similarity to the anti-P antibody P58's epitope (aa 211-221 in the NiV-M P, V, and W proteins); and (c) with molecular weights of approximately 28 kDa. The only proteins in the database found to fill all these criteria at least partially are certain potential isoforms of the transcription factor RFX4 (specifically, UniProtKB references B4DZB7 and F8VRD4). However, this was considered weak evidence: the RFX4 protein has significant similarity to but not identity with the P58 epitope; and the relevant (~28 kDa) RFX4 isoforms have been predicted computationally but not observed experimentally. Although there have been investigations into the cellular contents of NiV-M virions [Vera-Velasco *et al* 2018], these have been done using VLPs produced using the NiV-M F, G, and M protein. As they do not contain the majority of different NiV-M proteins that are important components of infectious NiV-M virions (P, V, W, N, L, and potentially C), VLPs are insufficient for identifying the cellular proteins incorporated into NiV-M virions.

4.4.2 Virion incorporation of the NiV-M V protein is mediated by interaction with the nucleocapsid

Immunoelectron microscopy of NiV-M nucleocapsids supported the hypothesis that the NiV-M V and W proteins are incorporated into the virions by attachment to the nucleocapsid, with gold particles clustering closely with the nucleocapsid structures (Fig. 19).

Previous IEM investigation by Paterson *et al* into V protein incorporation into virions of the paramyxovirus SV5 produced similar results: the SV5 V protein was found attached to the nucleocapsid in SV5 virions at an apparently similar frequency to what is seen for NiV-M here (compare Fig. 19A and B to the findings of Paterson *et al* [1995]). Paterson *et al* found that SV5 virions incorporated about 350 copies of the V protein, 315 of which were associated specifically with nucleocapsids [Paterson *et al* 1995]. NiV-M incorporation of V protein may be similar: likely, some V protein is incorporated into the virion adventitiously, while the majority is incorporated by interaction with the nucleocapsid. Binding to the nucleocapsid of the V protein may allow NiV-M virions to enrich their V protein content beyond what would occur by chance alone.

Relative to the amount of P protein, the V and W proteins are less abundant in the virion than in infected cells (Fig. 9A, 18A). This was also observed for sucrose gradient-purified NiV-M virions [Lo *et al* 2009]. If binding of the PNT of V/W to the nucleocapsid mediates the incorporation of these proteins into the virion, the reduced V/W protein in the virions despite their high prevalence in cells may be understood through the difference in affinity of the PNT and the PCT to bind the nucleocapsid (N^{NUC}). The PNT region is mainly responsible for binding the soluble, non-nucleocapsid N protein, so the V/W protein-N^{NUC} interaction would not be as favourable as the PCT-N^{NUC} interaction that recruits the P protein proper [Chan *et al* 2004, Yabukarski *et al* 2014]. This difference in affinity could ensure adequate incorporation of P protein despite a preponderance of intracellular V/W protein.

Conclusions and Future Directions

Perhaps the most unique finding in this investigation is that the non-structural V protein is not only incorporated within the virion but that it also mediates an auxiliary function immediately post-entry. In the tested cells, the V protein blocked type I IFN induction at two distinct time points: immediately after entry into the cell via virion-incorporated V protein, and later during viral replication via newly produced V protein.

The effects of virion-incorporated, "non-structural" viral proteins early post-infection have been previously investigated in arboviruses. In certain arboviruses, virion structure differs according to the cell of origin, and virions derived from insect cells can alter the ability of immune cells to induce a type I IFN response [Silva *et al* 2007, Shabman *et al* 2007, Nfon *et al* 2012, Weingartl *et al* 2014]. However, the insect cell-derived characteristics of these virions are lost after the first cycle of replication in the mammalian host cell. In contrast, the V protein of NiV-M is expected to be present throughout an infection with NiV-M and therefore would contribute to post-entry type I IFN suppression throughout an infection. Although some other paramyxoviruses are known to incorporate their non-structural proteins, no studies to date and to the author's knowledge have been performed attributing an incorporated non-structural protein of a paramyxovirus to the evasion of an early antiviral response [Paterson *et al* 1995, Takeuchi *et al* 1990, Shiell *et al* 2003].

Although NiV V protein appears to mediate the early block of type I IFN in porcine cells, it is possible that some of the effects are mediated by NiV C proteins, W proteins**,** or the M protein, all of which have been found to be incorporated into NiV-M virions and have some anti-IFN effects [Lo *et al* 2009, Satterfield *et al* 2015, 2016; Bharaj *et al* 2016]. It may be worth investigating the block of type I IFN immediately after entry in NiV-ΔC and NiV-ΔW

recombinants, or by NiV-M VLPs containing or missing the M protein. It is also possible that the NiV entry process itself is IFN-suppressive in some way, potentially as an effect of ephrin binding. This could be investigated as well, using VLPs containing different combinations of the NiV-M F, G, M proteins and/or the attachment/entry receptors of a different (ephrin-independent) virus.

This investigation has demonstrated that the V protein is important to NiV-M infection of porcine immune cells by blocking the production of type I IFN. The ability of NiV-M to compromise the type I IFN production response via the V protein in major interferon-producing cells may be important to its pathogenesis in swine and its observed ability to create transient immunosuppression in infected pigs.

The research in this thesis opens many avenues for future research. Investigation into the exact targets of the V protein in the NiV-M-inected IPAM31 cells would bolster the existing data from transfection studies [Childs *et al* 2007, 2009, 2012; Parisien *et al* 2009, Davis *et al* 2014, Rodriguez and Horvath 2013, 2014; Sánchez-Aparicio *et al* 2018, Uchida *et al* 2018] and identify the mechanism by which the V protein suppressed type I IFN induction in these cells. *In vitro* live infection studies assessing type I IFN expression in individual porcine immune cell subtypes infected with the different rNiVs could reveal the extent of the type I IFN suppression of the V protein among porcine immune cells: it might be of particular interest to determine whether NiV-M infects and blocks type I IFN in the major type I IFN-producing pDCs. Experimentally infecting swine with NiV-ΔV and NiV-rM would complement the *in vitro* data described in this thesis, allowing the assement of the effect of the absence of the V protein on the timing of the neutralizing antibody development in infected swine. Additionally, in light of the stark effects of incorporated V protein on type I IFN mRNA expression immediately post-

infection, it would be interesting to investigate if other non-essential virion components (especially host-derived) have measurable biological effects upon viral entry.

References

Aguilar, H. C., Aspericueta, V., Robinson, L. R., Aanensen, K. E., & Lee, B. (2010). A Quantitative and Kinetic Fusion Protein-Triggering Assay Can Discern Distinct Steps in the Nipah Virus Membrane Fusion Cascade. *Journal of Virology*, *84*(16), 8033–8041. https://doi.org/10.1128/JVI.00469-10

Aguilar, H. C., Ataman, Z. A., Aspericueta, V., Fang, A. Q., Stroud, M., Negrete, O. A., … Lee, B. (2009). A novel receptor-induced activation site in the Nipah virus attachment glycoprotein (G) involved in triggering the fusion glycoprotein (F). *The Journal of Biological Chemistry*, *284*(3), 1628–1635. https://doi.org/10.1074/jbc.M807469200

Ahl, R., & Rump, A. (1976). Assay of bovine interferons in cultures of the porcine cell line IB-RS-2. *Infection and Immunity*, *14*(3), 603–606.

Amadori, M. (2007). The Role of IFN-α as Homeostatic Agent in The Inflammatory Response: A Balance between Danger and Response? *Journal of Interferon & Cytokine Research*, *27*(3), 181–190. https://doi.org/10.1089/jir.2006.0110

Amadori, M., Cristiano, A., & Ferrari, M. (2010). Constitutive expression of interferons in swine leukocytes. *Research in Veterinary Science*, *88*(1), 64–71. https://doi.org/https://doi.org/10.1016/j.rvsc.2009.05.011

Arimoto, K.-I., Miyauchi, S., Stoner, S.A., Fan, J.-B., & Zhang, D.-E. (2018) Negative regulation of type I IFN signaling. *Journal of Leukocyte Biology*. 1-18. https://doi.org/10.1002/JLB.2MIR0817-342R

Audsley, M. D., Jans, D. A., & Moseley, G. W. (2016). Nucleocytoplasmic trafficking of Nipah virus W protein involves multiple discrete interactions with the nuclear import and export machinery. *Biochemical and Biophysical Research Communications*, *479*(3), 429–433. https://doi.org/10.1016/j.bbrc.2016.09.043

Berger Rentsch, M., & Zimmer, G. (2011). A Vesicular Stomatitis Virus Replicon-Based Bioassay for the Rapid and Sensitive Determination of Multi-Species Type I Interferon. *PLOS ONE*, *6*(10), e25858.

Berhane, Y., Weingartl, H. M., Lopez, J., Neufeld, J., Czub, S., Embury-Hyatt, C., … Czub, M. (2008). Bacterial infections in pigs experimentally infected with Nipah virus. *Transboundary and Emerging Diseases*, *55*(3–4), 165–174. https://doi.org/10.1111/j.1865-1682.2008.01021.x

Berhane, Y., Berry, J. D., Ranadheera, C., Marszal, P., Nicolas, B., Yuan, X., … Weingartl, H. (2006). Production and characterization of monoclonal antibodies against binary ethylenimine inactivated Nipah virus. *Journal of Virological Methods*, *132*(1–2), 59–68. https://doi.org/10.1016/j.jviromet.2005.09.005

Bharaj, P., Wang, Y. E., Dawes, B. E., Yun, T. E., Park, A., Yen, B., … Rajsbaum, R. (2016). The Matrix Protein of Nipah Virus Targets the E3-Ubiquitin Ligase TRIM6 to Inhibit the IKKε Kinase-Mediated Type-I IFN Antiviral Response. *PLOS Pathogens, 12*(9), e1005880.

Blocquel, D., Habchi, J., Gruet, A., Blangy, S., & Longhi, S. (2012). Compaction and binding properties of the intrinsically disordered C-terminal domain of Henipavirus nucleoprotein as unveiled by deletion studies. *Molecular BioSystems, 8*(1), 392–410. https://doi.org/10.1039/c1mb05401e

Boczkowska, B. (2014). *Aspects of porcine immunological response to Nipah virus*. University of Manitoba.

Bossart, K. N., Zhu, Z., Middleton, D., Klippel, J., Crameri, G., Bingham, J., … Broder, C. C. (2009). A neutralizing human monoclonal antibody protects against lethal disease in a new ferret model of acute nipah virus infection. *PLoS Pathogens, 5*(10), e1000642–e1000642. https://doi.org/10.1371/journal.ppat.1000642

Braun, D., Caramalho, I., & Demengeot, J. (2002). IFN-α/β enhances BCR-dependent B cell responses. *International Immunology, 14*(4), 411–419.

Bruhn, J. F., Barnett, K. C., Bibby, J., Thomas, J. M. H., Keegan, R. M., Rigden, D. J., … Saphire, E. O. (2014). Crystal structure of the nipah virus phosphoprotein tetramerization domain. *Journal of Virology, 88*(1), 758–762. https://doi.org/10.1128/JVI.02294-13

Cattaneo, R., Rebmann, G., Baczko, K., ter Meulen, V., & Billeter, M. A. (1987). Altered ratios of measles virus transcripts in diseased human brains. *Virology, 160*(2), 523–526.

Chan, Y. P., Koh, C. L., Lam, S. K., & Wang, L.-F. (2004). Mapping of domains responsible for nucleocapsid protein-phosphoprotein interaction of Henipaviruses. *The Journal of General Virology, 85*(Pt 6), 1675–1684. https://doi.org/10.1099/vir.0.19752-0

Chan, Y. K., & Gack, M. U. (2016). Viral evasion of intracellular DNA and RNA sensing. *Nature Reviews Microbiology, 14*, 360.

Chang, L.-Y., Ali, A. R. M., Hassan, S. S., & AbuBakar, S. (2006). Nipah virus RNA synthesis in cultured pig and human cells. *Journal of Medical Virology, 78*(8), 1105–1112. https://doi.org/10.1002/jmv.20669

Chang, L.-Y., Ali, A. R. M., Hassan, S. S., & AbuBakar, S. (2006). Quantitative estimation of Nipah virus replication kinetics in vitro. *Virology Journal, 3*, 47. https://doi.org/10.1186/1743-422X-3-47

Childs, K. S., Andrejeva, J., Randall, R. E., & Goodbourn, S. (2009). Mechanism of mda-5 Inhibition by paramyxovirus V proteins. *Journal of Virology, 83*(3), 1465–1473. https://doi.org/10.1128/JVI.01768-08

Childs, K., Randall, R., & Goodbourn, S. (2012). Paramyxovirus V Proteins Interact with the RNA Helicase LGP2 To Inhibit RIG-I-Dependent Interferon Induction. *Journal of Virology*, *86*(7), 3411 LP-3421. https://doi.org/10.1128/JVI.06405-11

Childs, K., Stock, N., Ross, C., Andrejeva, J., Hilton, L., Skinner, M., … Goodbourn, S. (2007). mda-5, but not RIG-I, is a common target for paramyxovirus V proteins. *Virology*, *359*(1), 190–200. https://doi.org/10.1016/j.virol.2006.09.023

Ching, P. K. G., de los Reyes, V. C., Sucaldito, M. N., Tayag, E., Columna-Vingno, A. B., Malbas Jr, F. F., … Foxwell, A. R. (2015). Outbreak of henipavirus infection, Philippines, 2014. *Emerging Infectious Diseases*, *21*(2), 328–331. https://doi.org/10.3201/eid2102.141433

Chong, H. T., Hossain, M. J., & Tan, C. T. (2008). Differences in epidemiologic and clinical features of Nipah virus encephalitis between the Malaysian and Bangladesh outbreaks. *Neurology Asia*, *13*, 23–26.

Chua, K. B., Bellini, W. J., Rota, P. A., Harcourt, B. H., Tamin, A., Lam, S. K., … Mahy, B. W. (2000). Nipah virus: a recently emergent deadly paramyxovirus. *Science (New York, N.Y.)*, *288*(5470), 1432–1435.

Chua, K. B., Goh, K. J., Wong, K. T., Kamarulzaman, A., Tan, P. S., Ksiazek, T. G., … Tan, C. T. (1999). Fatal encephalitis due to Nipah virus among pig-farmers in Malaysia. *Lancet (London, England)*, *354*(9186), 1257–1259. https://doi.org/10.1016/S0140-6736(99)04299-3

Chua, K. B. (2003). Nipah virus outbreak in Malaysia. *Journal of Clinical Virology*, *26*(3), 265–275. https://doi.org/https://doi.org/10.1016/S1386-6532(02)00268-8

Chua, K. B., Koh, C. L., Hooi, P. S., Wee, K. F., Khong, J. H., Chua, B. H., … Lam, S. K. (2002). Isolation of Nipah virus from Malaysian Island flying-foxes. *Microbes and Infection*, *4*(2), 145–151.

Ciancanelli, M. J., Volchkova, V. A., Shaw, M. L., Volchkov, V. E., & Basler, C. F. (2009). Nipah Virus Sequesters Inactive STAT1 in the Nucleus via a P Gene-Encoded Mechanism. *Journal of Virology*, *83*(16), 7828 LP-7841. https://doi.org/10.1128/JVI.02610-08

Clayton, B. A. (2017). Nipah virus: transmission of a zoonotic paramyxovirus. *Current Opinion in Virology*, *22*, 97–104. https://doi.org/https://doi.org/10.1016/j.coviro.2016.12.003

Cox, R. M., & Plemper, R. K. (2017). Structure and organization of paramyxovirus particles. *Current Opinion in Virology*, *24*, 105–114. https://doi.org/10.1016/j.coviro.2017.05.004

Crouse, J., Kalinke, U., & Oxenius, A. (2015). Regulation of antiviral T cell responses by type I interferons. *Nature Reviews Immunology*, *15*, 231.

Davis, M. E., Wang, M. K., Rennick, L. J., Full, F., Gableske, S., Mesman, A. W., … Gack, M. U. (2014). Antagonism of the phosphatase PP1 by the measles virus V protein is required for innate immune escape of MDA5. *Cell Host & Microbe*, *16*(1), 19–30. https://doi.org/10.1016/j.chom.2014.06.007

Dawson, H. D., Beshah, E., Nishi, S., Solano-Aguilar, G., Morimoto, M., Zhao, A., … Urban, J. F. J. (2005). Localized multigene expression patterns support an evolving Th1/Th2-like paradigm in response to infections with Toxoplasma gondii and Ascaris suum. *Infection and Immunity*, *73*(2), 1116–1128. https://doi.org/10.1128/IAI.73.2.1116-1128.2005

de Veer, M. J., Holko, M., Frevel, M., Walker, E., Der, S., Paranjape, J. M., … Williams, B. R. (2001). Functional classification of interferon-stimulated genes identified using microarrays. *Journal of Leukocyte Biology*, *69*(6), 912–920.

de Weerd, N. A., & Nguyen, T. (2012). The interferons and their receptors—distribution and regulation. *Immunology & Cell Biology*, *90*(5), 483–491. https://doi.org/10.1038/icb.2012.9

Desmyter, J., Melnick, J. L., & Rawls, W. E. (1968). Defectiveness of interferon production and of rubella virus interference in a line of African green monkey kidney cells (Vero). *Journal of Virology*, *2*(10), 955–961.

Diederich, S., Moll, M., Klenk, H.-D., & Maisner, A. (2005). The nipah virus fusion protein is cleaved within the endosomal compartment. *The Journal of Biological Chemistry*, *280*(33), 29899–29903. https://doi.org/10.1074/jbc.M504598200

Diederich, S., Thiel, L., & Maisner, A. (2008). Role of endocytosis and cathepsin-mediated activation in Nipah virus entry. *Virology*, *375*(2), 391–400. https://doi.org/10.1016/j.virol.2008.02.019

Earp, L. J., Delos, S. E., Park, H. E., & White, J. M. (2005). The many mechanisms of viral membrane fusion proteins. *Current Topics in Microbiology and Immunology*, *285*, 25–66.

Eaton, B. T., Broder, C. C., Middleton, D., & Wang, L.-F. (2006). Hendra and Nipah viruses: different and dangerous. *Nature Reviews Microbiology*, *4*, 23.

Edelmann, S. L., & Heissmeyer, V. (2014). Tfh cell differentiation: missing Stat3 uncovers interferons' interference. *Immunity*, *40*(3), 307–309. https://doi.org/10.1016/j.immuni.2014.02.008

El Najjar, F., Schmitt, A. P., & Dutch, R. E. (2014). Paramyxovirus glycoprotein incorporation, assembly and budding: a three way dance for infectious particle production. *Viruses*, *6*(8), 3019–3054. https://doi.org/10.3390/v6083019

Epstein, J. H., Field, H. E., Luby, S., Pulliam, J. R. C., & Daszak, P. (2006). Nipah virus: impact, origins, and causes of emergence. *Current Infectious Disease Reports*, *8*(1), 59–65.

Errington, W., & Emmerson, P. T. (1997). Assembly of recombinant Newcastle disease virus nucleocapsid protein into nucleocapsid-like structures is inhibited by the phosphoprotein. *The Journal of General Virology*, *78 (Pt 9)*, 2335–2339. https://doi.org/10.1099/0022-1317-78-9-2335

Escaffre, O., Borisevich, V., Carmical, J. R., Prusak, D., Prescott, J., Feldmann, H., & Rockx, B. (2013). Henipavirus pathogenesis in human respiratory epithelial cells. *Journal of Virology*, *87*(6), 3284–3294. https://doi.org/10.1128/JVI.02576-12

Fahnestock, S. R., Alexander, P., Nagle, J., & Filpula, D. (1986). Gene for an immunoglobulin-binding protein from a group G streptococcus. *Journal of Bacteriology*, *167*(3), 870–880.

Familletti, P. C., & Pestka, S. (1981). Cell cultures producing human interferon. *Antimicrobial Agents and Chemotherapy*, *20*(1), 1–4.

Fitzgerald-Bocarsly, P., Dai, J., & Singh, S. (2008). Plasmacytoid dendritic cells and type I IFN: 50 years of convergent history. *Cytokine & Growth Factor Reviews*, *19*(1), 3–19. https://doi.org/10.1016/j.cytogfr.2007.10.006

Geisbert, T. W., Daddario-DiCaprio, K. M., Hickey, A. C., Smith, M. A., Chan, Y.-P., Wang, L.-F., … Broder, C. C. (2010). Development of an acute and highly pathogenic nonhuman primate model of Nipah virus infection. *PloS One*, *5*(5), e10690. https://doi.org/10.1371/journal.pone.0010690

Geisbert, T. W., Feldmann, H., & Broder, C. C. (2012). Animal Challenge Models of Henipavirus Infection and Pathogenesis BT - Henipavirus: Ecology, Molecular Virology, and Pathogenesis. In B. Lee & P. A. Rota (Eds.) (pp. 153–177). Berlin, Heidelberg: Springer Berlin Heidelberg. https://doi.org/10.1007/82_2012_208

Genin, P., Lin, R., Hiscott, J., & Civas, A. (2009). Differential regulation of human interferon A gene expression by interferon regulatory factors 3 and 7. *Molecular and Cellular Biology*, *29*(12), 3435–3450. https://doi.org/10.1128/MCB.01805-08

Gitlin, L., Benoit, L., Song, C., Cella, M., Gilfillan, S., Holtzman, M. J., & Colonna, M. (2010). Melanoma differentiation-associated gene 5 (MDA5) is involved in the innate immune response to Paramyxoviridae infection in vivo. *PLoS Pathogens*, *6*(1), e1000734. https://doi.org/10.1371/journal.ppat.1000734

Goldsmith, C. S., Whistler, T., Rollin, P. E., Ksiazek, T. G., Rota, P. A., Bellini, W. J., … Zaki, S. R. (2003). Elucidation of Nipah virus morphogenesis and replication using ultrastructural and molecular approaches. *Virus Research*, *92*(1), 89–98.

Gombart, A. F., Hirano, A., & Wong, T. C. (1992). Expression and properties of the V protein in acute measles virus and subacute sclerosing panencephalitis virus strains. *Virus Research*, *25*(1), 63–78. https://doi.org/https://doi.org/10.1016/0168-1702(92)90100-N

Gommerman, J. L., Browning, J. L., & Ware, C. F. (2014). The Lymphotoxin Network: orchestrating a type I interferon response to optimize adaptive immunity. *Cytokine & Growth Factor Reviews*, *25*(2), 139–145. https://doi.org/10.1016/j.cytogfr.2014.02.002

Goodbourn, S., & Randall, R. E. (2009). The regulation of type I interferon production by paramyxoviruses. *Journal of Interferon & Cytokine Research : The Official Journal of the International Society for Interferon and Cytokine Research*, *29*(9), 539–547. https://doi.org/10.1089/jir.2009.0071

Goolia, M. N. (2009). *The Expression and Localization of the V and W Accessory Proteins in Porcine and Human Cells Infected with Nipah Virus*. University of Manitoba.

Gough, D. J., Messina, N. L., Clarke, C. J. P., Johnstone, R. W., & Levy, D. E. (2012). Constitutive type I interferon modulates homeostatic balance through tonic signaling. *Immunity*, *36*(2), 166–174. https://doi.org/10.1016/j.immuni.2012.01.011

Guillaume, V., Lefeuvre, A., Faure, C., Marianneau, P., Buckland, R., Lam, S. K., … Deubel, V. (2004). Specific detection of Nipah virus using real-time RT-PCR (TaqMan). *Journal of Virological Methods*, *120*(2), 229–237. https://doi.org/10.1016/j.jviromet.2004.05.018

Guo, L., Vlasova-St Louis, I., & Bohjanen, P.R. (2018) Viral manipulation of host mRNA decay. *Future Virology, 13*(3):211-223. https://doi.org/10.2217/fvl-2017-0106

Gupta, M., Lo, M. K., & Spiropoulou, C. F. (2013). Activation and cell death in human dendritic cells infected with Nipah virus. *Virology*, *441*(1), 49–56. https://doi.org/https://doi.org/10.1016/j.virol.2013.03.004

Habchi, J., & Longhi, S. (2015). Structural Disorder within Paramyxoviral Nucleoproteins and Phosphoproteins in Their Free and Bound Forms: From Predictions to Experimental Assessment. *International Journal of Molecular Sciences*, *16*(7), 15688–15726. https://doi.org/10.3390/ijms160715688

Habchi, J., Mamelli, L., Darbon, H., & Longhi, S. (2010). Structural Disorder within Henipavirus Nucleoprotein and Phosphoprotein: From Predictions to Experimental Assessment. *PLOS ONE*, *5*(7), e11684.

Habjan, M., Andersson, I., Klingstrom, J., Schumann, M., Martin, A., Zimmermann, P., … Weber, F. (2008). Processing of genome 5' termini as a strategy of negative-strand RNA viruses to avoid RIG-I-dependent interferon induction. *PloS One*, *3*(4), e2032. https://doi.org/10.1371/journal.pone.0002032

Halpin, K., Bankamp, B., Harcourt, B. H., Bellini, W. J., & Rota, P. A. (2004). Nipah virus conforms to the rule of six in a minigenome replication assay. *The Journal of General Virology*, *85*(Pt 3), 701–707. https://doi.org/10.1099/vir.0.19685-0

Harcourt, B. H., Lowe, L., Tamin, A., Liu, X., Bankamp, B., Bowden, N., … Rota, P. A. (2005). Genetic characterization of Nipah virus, Bangladesh, 2004. *Emerging Infectious Diseases*, *11*(10), 1594–1597. https://doi.org/10.3201/eid1110.050513

Hata, N., Sato, M., Takaoka, A., Asagiri, M., Tanaka, N., & Taniguchi, T. (2001). Constitutive IFN-α/β Signal for Efficient IFN-α/β Gene Induction by Virus. *Biochemical and Biophysical Research Communications*, *285*(2), 518–525. https://doi.org/https://doi.org/10.1006/bbrc.2001.5159

Hausmann, S., Garcin, D., Delenda, C., & Kolakofsky, D. (1999). The Versatility of Paramyxovirus RNA Polymerase Stuttering. *Journal of Virology*, *73*(7), 5568 LP-5576.

Hidmark, A. S., McInerney, G. M., Nordstrom, E. K. L., Douagi, I., Werner, K. M., Liljestrom, P., & Karlsson Hedestam, G. B. (2005). Early alpha/beta interferon production by myeloid dendritic cells in response to UV-inactivated virus requires viral entry and interferon regulatory factor 3 but not MyD88. *Journal of Virology*, *79*(16), 10376–10385. https://doi.org/10.1128/JVI.79.16.10376-10385.2005

Homann, H. E., Hofschneider, P. H., & Neubert, W. J. (1990). Sendai virus gene expression in lytically and persistently infected cells. *Virology*, *177*(1), 131–140.

Hooper, P., Zaki, S., Daniels, P., & Middleton, D. (2001). Comparative pathology of the diseases caused by Hendra and Nipah viruses. *Microbes and Infection*, *3*(4), 315–322.

Horie, R., Yoneda, M., Uchida, S., Sato, H., & Kai, C. (2016). Region of Nipah virus C protein responsible for shuttling between the cytoplasm and nucleus. *Virology*, *497*, 294–304. https://doi.org/https://doi.org/10.1016/j.virol.2016.07.013

Hornung, V., Schlender, J., Guenthner-Biller, M., Rothenfusser, S., Endres, S., Conzelmann, K.-K., & Hartmann, G. (2004). Replication-Dependent Potent IFN-α Induction in Human Plasmacytoid Dendritic Cells by a Single-Stranded RNA Virus. *The Journal of Immunology*, *173*(10), 5935 LP-5943. https://doi.org/10.4049/jimmunol.173.10.5935

House, J. A., House, C., & Llewellyn, M. E. (1988). Characteristics of the porcine kidney cell line IB-RS-2 clone D10 (IB-RS-2 D10) which is free of hog cholera virus. *In Vitro Cellular & Developmental Biology : Journal of the Tissue Culture Association*, *24*(7), 677–682.

Hsu, V. P., Hossain, M. J., Parashar, U. D., Ali, M. M., Ksiazek, T. G., Kuzmin, I., … Breiman, R. F. (2004). Nipah virus encephalitis reemergence, Bangladesh. *Emerging Infectious Diseases*, *10*(12), 2082–2087. https://doi.org/10.3201/eid1012.040701

Hyatt, A. D., Zaki, S. R., Goldsmith, C. S., Wise, T. G., & Hengstberger, S. G. (2001). Ultrastructure of Hendra virus and Nipah virus within cultured cells and host animals. *Microbes and Infection*, *3*(4), 297–306.

Ikegame, S., Takeda, M., Ohno, S., Nakatsu, Y., Nakanishi, Y., & Yanagi, Y. (2010). Both RIG-I and MDA5 RNA Helicases Contribute to the Induction of Alpha/Beta Interferon in Measles Virus-Infected Human Cells. *Journal of Virology*, *84*(1), 372 LP-379. https://doi.org/10.1128/JVI.01690-09

Irie, T., Nagata, N., Yoshida, T., & Sakaguchi, T. (2008). Paramyxovirus Sendai virus C proteins are essential for maintenance of negative-sense RNA genome in virus particles. *Virology*, *374*(2), 495–505. https://doi.org/10.1016/j.virol.2008.01.004

Ivashkiv, L. B., & Donlin, L. T. (2014). Regulation of type I interferon responses. *Nature Reviews. Immunology*, *14*(1), 36–49. https://doi.org/10.1038/nri3581

Jamin, M., & Yabukarski, F. (2017). Nonsegmented Negative-Sense RNA Viruses-Structural Data Bring New Insights Into Nucleocapsid Assembly. *Advances in Virus Research*, *97*, 143–185. https://doi.org/10.1016/bs.aivir.2016.09.001

Jego, G., Palucka, A. K., Blanck, J.-P., Chalouni, C., Pascual, V., & Banchereau, J. (2003). Plasmacytoid dendritic cells induce plasma cell differentiation through type I interferon and interleukin 6. *Immunity*, *19*(2), 225–234.

Jensen, K. S., Adams, R., Bennett, R. S., Bernbaum, J., Jahrling, P. B., & Holbrook, M. R. (2018). Development of a novel real-time polymerase chain reaction assay for the quantitative detection of Nipah virus replicative viral RNA. *PloS One*, *13*(6), e0199534–e0199534. https://doi.org/10.1371/journal.pone.0199534

Kasloff, S. B., & Weingartl, H. M. (2016). Swine alveolar macrophage cell model allows optimal replication of influenza A viruses regardless of their origin. *Virology*, *490*, 91–98. https://doi.org/10.1016/j.virol.2016.01.006

Kato, H., Takeuchi, O., Sato, S., Yoneyama, M., Yamamoto, M., Matsui, K., … Akira, S. (2006). Differential roles of MDA5 and RIG-I helicases in the recognition of RNA viruses. *Nature*, *441*(7089), 101–105. https://doi.org/10.1038/nature04734

Kawai, T., & Akira, S. (2007). Antiviral signaling through pattern recognition receptors. *Journal of Biochemistry*, *141*(2), 137–145. https://doi.org/10.1093/jb/mvm032

Kawai, T., & Akira, S. (2008). Toll-like Receptor and RIG-1-like Receptor Signaling. *Annals of the New York Academy of Sciences*, *1143*(1), 1–20. https://doi.org/10.1196/annals.1443.020

Kawasaki, T., & Kawai, T. (2014). Toll-like receptor signaling pathways. *Frontiers in Immunology*, *5*, 461. https://doi.org/10.3389/fimmu.2014.00461

Kerr, M. C., Lindsay, M. R., Luetterforst, R., Hamilton, N., Simpson, F., Parton, R. G., … Teasdale, R. D. (2006). Visualisation of macropinosome maturation by the recruitment of sorting nexins. *Journal of Cell Science*, *119*(19), 3967 LP-3980. https://doi.org/10.1242/jcs.03167

Khakpour, S., Wilhelmsen, K., & Hellman, J. (2015). *Vascular endothelial cell Toll-like receptor pathways in sepsis*. *Innate Immunity* (Vol. 21). https://doi.org/10.1177/1753425915606525

Killip, M. J., Young, D. F., Precious, B. L., Goodbourn, S., & Randall, R. E. (2012). Activation of the beta interferon promoter by paramyxoviruses in the absence of virus protein synthesis. *The Journal of General Virology*, *93*(Pt 2), 299–307. https://doi.org/10.1099/vir.0.037531-0

Kulkarni, S., Volchkova, V., Basler, C. F., Palese, P., Volchkov, V. E., & Shaw, M. L. (2009). Nipah virus edits its P gene at high frequency to express the V and W proteins. *Journal of Virology*, *83*(8), 3982–3987. https://doi.org/10.1128/JVI.02599-08

Kumagai, Y., Takeuchi, O., Kato, H., Kumar, H., Matsui, K., Morii, E., … Akira, S. (2007). Alveolar macrophages are the primary interferon-alpha producer in pulmonary infection with RNA viruses. *Immunity*, *27*(2), 240–252. https://doi.org/10.1016/j.immuni.2007.07.013

Lamb, R. A., Mahy, B. W., & Choppin, P. W. (1976). The synthesis of sendai virus polypeptides in infected cells. *Virology*, *69*(1), 116–131.

Lamb, R. A., & Parks, G. D. (2013). Paramyxoviridae: the viruses and their replication. In B. N. Fields, D. M. Knipe, & P. M. Howley (Eds.), *Fields Virology* (6th ed., pp. 957–995). Philadelphia: Lippincott, Williams, and Wilkins.

Lamp, B., Dietzel, E., Kolesnikova, L., Sauerhering, L., Erbar, S., Weingartl, H., & Maisner, A. (2013). Nipah virus entry and egress from polarized epithelial cells. *Journal of Virology*, *87*(6), 3143–3154. https://doi.org/10.1128/JVI.02696-12

Lee, H. K., Lund, J. M., Ramanathan, B., Mizushima, N., & Iwasaki, A. (2007). Autophagy-dependent viral recognition by plasmacytoid dendritic cells. *Science (New York, N.Y.)*, *315*(5817), 1398–1401. https://doi.org/10.1126/science.1136880

Levy, D. E., Marie, I., Smith, E., & Prakash, A. (2002). Enhancement and diversification of IFN induction by IRF-7-mediated positive feedback. *Journal of Interferon & Cytokine Research : The Official Journal of the International Society for Interferon and Cytokine Research*, *22*(1), 87–93. https://doi.org/10.1089/107999002753452692

Li, M., Embury-Hyatt, C., & Weingartl, H. M. (2010). Experimental inoculation study indicates swine as a potential host for Hendra virus. *Veterinary Research*, *41*(3), 33. https://doi.org/10.1051/vetres/2010005

Liljeroos, L., Huiskonen, J. T., Ora, A., Susi, P., & Butcher, S. J. (2011). Electron cryotomography of measles virus reveals how matrix protein coats the ribonucleocapsid within intact virions. *Proceedings of the National Academy of Sciences of the United States of America*, *108*(44), 18085–18090. https://doi.org/10.1073/pnas.1105770108

Lim, J. P., & Gleeson, P. A. (2011). Macropinocytosis: an endocytic pathway for internalising large gulps. *Immunology & Cell Biology*, *89*(8), 836–843. https://doi.org/10.1038/icb.2011.20

Lin, R., Genin, P., Mamane, Y., & Hiscott, J. (2000). Selective DNA binding and association with the CREB binding protein coactivator contribute to differential activation of alpha/beta interferon genes by interferon regulatory factors 3 and 7. *Molecular and Cellular Biology*, *20*(17), 6342–6353.

Lin, W., Qiu, Z., Liu, Q., & Cui, S. (2013). Interferon induction and suppression in swine testicle cells by porcine parvovirus and its proteins. *Veterinary Microbiology*, *163*(1–2), 157–161. https://doi.org/10.1016/j.vetmic.2012.11.032

Liu, P., Jamaluddin, M., Li, K., Garofalo, R. P., Casola, A., & Brasier, A. R. (2007). Retinoic acid-inducible gene I mediates early antiviral response and Toll-like receptor 3 expression in respiratory syncytial virus-infected airway epithelial cells. *Journal of Virology*, *81*(3), 1401–1411. https://doi.org/10.1128/JVI.01740-06

Livak, K. J., & Schmittgen, T. D. (2001). Analysis of relative gene expression data using real-time quantitative PCR and the 2(-Delta Delta C(T)) Method. *Methods (San Diego, Calif.)*, *25*(4), 402–408. https://doi.org/10.1006/meth.2001.1262

Lo, M. K., Harcourt, B. H., Mungall, B. A., Tamin, A., Peeples, M. E., Bellini, W. J., & Rota, P. A. (2009). Determination of the henipavirus phosphoprotein gene mRNA editing frequencies and detection of the C, V and W proteins of Nipah virus in virus-infected cells. *The Journal of General Virology*, *90*(Pt 2), 398–404. https://doi.org/10.1099/vir.0.007294-0

Lo, M. K., Miller, D., Aljofan, M., Mungall, B. A., Rollin, P. E., Bellini, W. J., & Rota, P. A. (2010). Characterization of the antiviral and inflammatory responses against Nipah virus in endothelial cells and neurons. *Virology*, *404*(1), 78–88. https://doi.org/10.1016/j.virol.2010.05.005

Lo, M. K., Peeples, M. E., Bellini, W. J., Nichol, S. T., Rota, P. A., & Spiropoulou, C. F. (2012). Distinct and overlapping roles of Nipah virus P gene products in modulating the human endothelial cell antiviral response. *PloS One*, *7*(10), e47790–e47790. https://doi.org/10.1371/journal.pone.0047790

Lo, M. K., & Rota, P. A. (2008). The emergence of Nipah virus, a highly pathogenic paramyxovirus. *Journal of Clinical Virology*, *43*(4), 396–400. https://doi.org/https://doi.org/10.1016/j.jcv.2008.08.007

Loney, C., Mottet-Osman, G., Roux, L., & Bhella, D. (2009). Paramyxovirus ultrastructure and genome packaging: cryo-electron tomography of sendai virus. *Journal of Virology*, *83*(16), 8191–8197. https://doi.org/10.1128/JVI.00693-09

Longhi, S., Bloyet, L.-M., Gianni, S., & Gerlier, D. (2017). How order and disorder within paramyxoviral nucleoproteins and phosphoproteins orchestrate the molecular interplay of transcription and replication. *Cellular and Molecular Life Sciences : CMLS*, *74*(17), 3091–3118. https://doi.org/10.1007/s00018-017-2556-3

Loo, Y.-M., & Gale Jr, M. (2011). Immune signaling by RIG-I-like receptors. *Immunity*, *34*(5), 680–692. https://doi.org/10.1016/j.immuni.2011.05.003

López, C. B., Moltedo, B., Alexopoulou, L., Bonifaz, L., Flavell, R. A., & Moran, T. M. (2004). TLR-independent induction of dendritic cell maturation and adaptive immunity by negative-strand RNA viruses. *Journal of Immunology (Baltimore, Md. : 1950)*, *173*(11), 6882–6889.

Luby, S. P., Gurley, E. S., & Hossain, M. J. (2009). Transmission of human infection with Nipah virus. *Clinical Infectious Diseases : An Official Publication of the Infectious Diseases Society of America*, *49*(11), 1743–1748. https://doi.org/10.1086/647951

Maisner, A., Neufeld, james, & Weingartl, H. (2009). Organ- and endotheliotropism of Nipah virus infections in vivo and in vitro. *Thromb Haemost*, *102*(12), 1014–1023. https://doi.org/10.1160/TH09-05-0310

Manuse, M. J., & Parks, G. D. (2010). TLR3-dependent upregulation of RIG-I leads to enhanced cytokine production from cells infected with the parainfluenza virus SV5. *Virology*, *397*(1), 231–241. https://doi.org/10.1016/j.virol.2009.11.014

Manzoni, T. B., & Lopez, C. B. (2018). Defective (interfering) viral genomes re-explored: impact on antiviral immunity and virus persistence. *Future Virology*, *13*(7), 493–503. https://doi.org/10.2217/fvl-2018-0021

Marianneau, P., Guillaume, V., Wong, T., Badmanathan, M., Looi, R. Y., Murri, S., … Contamin, H. (2010). Experimental infection of squirrel monkeys with nipah virus. *Emerging Infectious Diseases*, *16*(3), 507–510. https://doi.org/10.3201/eid1603.091346

Markusic, M., Santak, M., Kosutic-Gulija, T., Jergovic, M., Jug, R., & Forcic, D. (2014). Induction of IFN-alpha subtypes and their antiviral activity in mumps virus infection. *Viral Immunology*, *27*(10), 497–505. https://doi.org/10.1089/vim.2014.0028

Mathieu, C., Guillaume, V., Sabine, A., Ong, K. C., Wong, K. T., Legras-Lachuer, C., & Horvat, B. (2012b). Lethal Nipah virus infection induces rapid overexpression of CXCL10. *PloS One*, *7*(2), e32157. https://doi.org/10.1371/journal.pone.0032157

Mathieu, C., Guillaume, V., Volchkova, V. A., Pohl, C., Jacquot, F., Looi, R. Y., … Horvat, B. (2012a). Nonstructural Nipah virus C protein regulates both the early host proinflammatory response and viral virulence. *Journal of Virology*, *86*(19), 10766–10775. https://doi.org/10.1128/JVI.01203-12

Mathieu, C., Pohl, C., Szecsi, J., Trajkovic-Bodennec, S., Devergnas, S., Raoul, H., … Horvat, B. (2011). Nipah virus uses leukocytes for efficient dissemination within a host. *Journal of Virology*, *85*(15), 7863–7871. https://doi.org/10.1128/JVI.00549-11

McNab, F., Mayer-Barber, K., Sher, A., Wack, A., & O'Garra, A. (2015). Type I interferons in infectious disease. *Nature Reviews. Immunology*, *15*(2), 87–103. https://doi.org/10.1038/nri3787

Meager, A. (2002). Biological assays for interferons. *Journal of Immunological Methods*, *261*(1–2), 21–36.

Melchjorsen, J., Jensen, S. B., Malmgaard, L., Rasmussen, S. B., Weber, F., Bowie, A. G., … Paludan, S. R. (2005). Activation of innate defense against a paramyxovirus is mediated by RIG-I and TLR7 and TLR8 in a cell-type-specific manner. *Journal of Virology*, *79*(20), 12944–12951. https://doi.org/10.1128/JVI.79.20.12944-12951.2005

Middleton, D. J., Morrissy, C. J., van der Heide, B. M., Russell, G. M., Braun, M. A., Westbury, H. A., … Daniels, P. W. (2007). Experimental Nipah Virus Infection in Pteropid Bats (Pteropus poliocephalus). *Journal of Comparative Pathology*, *136*(4), 266–272. https://doi.org/https://doi.org/10.1016/j.jcpa.2007.03.002

Middleton, D. J., & Weingartl, H. M. (2012). Henipaviruses in their natural animal hosts. *Current Topics in Microbiology and Immunology*, *359*, 105–121. https://doi.org/10.1007/82_2012_210

Middleton, D. J., Westbury, H. A., Morrissy, C. J., van der Heide, B. M., Russell, G. M., Braun, M. A., & Hyatt, A. D. (2002). Experimental Nipah virus infection in pigs and cats. *Journal of Comparative Pathology*, *126*(2–3), 124–136. https://doi.org/10.1053/jcpa.2001.0532

Mills, J. N., Alim, A. N. M., Bunning, M. L., Lee, O. B., Wagoner, K. D., Amman, B. R., … Ksiazek, T. G. (2009). Nipah virus infection in dogs, Malaysia, 1999. *Emerging Infectious Diseases*, *15*(6), 950–952. https://doi.org/10.3201/eid1506.080453

Mizushima, N., Ohsumi, Y., & Yoshimori, T. (2002). Autophagosome formation in mammalian cells. *Cell Structure and Function*, *27*(6), 421–429.

Mohd Nor, M. N., Gan, C. H., & Ong, B. L. (2000). Nipah virus infection of pigs in peninsular Malaysia. *Revue Scientifique et Technique (International Office of Epizootics)*, *19*(1), 160–165.

Mosca, J. D., & Pitha, P. M. (1986). Transcriptional and posttranscriptional regulation of exogenous human beta interferon gene in simian cells defective in interferon synthesis. *Molecular and Cellular Biology*, *6*(6), 2279–2283.

Nfon, C. K., Marszal, P., Zhang, S., & Weingartl, H. M. (2012). Innate immune response to Rift Valley fever virus in goats. *PLoS Neglected Tropical Diseases*, *6*(4), e1623. https://doi.org/10.1371/journal.pntd.0001623

Noton, S. L., & Fearns, R. (2015). Initiation and regulation of paramyxovirus transcription and replication. *Virology*, *479–480*, 545–554. https://doi.org/https://doi.org/10.1016/j.virol.2015.01.014

Okonski, K.M., & Samuel, C.E. (2013) Stress Granule Formation Induced by Measles Virus is Protein Kinase PKR Dependent and Impaired by RNA Adenosine Deaminase ADAR1. *Journal of Virology, 87*(2):756-766. https://doi.org/10.1128/JVI.02270-12.

Ong, S. T., Yusoff, K., Kho, C. L., Abdullah, J. O., & Tan, W. S. (2009). Mutagenesis of the nucleocapsid protein of Nipah virus involved in capsid assembly. *The Journal of General Virology*, *90*(Pt 2), 392–397. https://doi.org/10.1099/vir.0.005710-0

Parisien, J.-P., Bamming, D., Komuro, A., Ramachandran, A., Rodriguez, J. J., Barber, G., … Horvath, C. M. (2009). A shared interface mediates paramyxovirus interference with antiviral RNA helicases MDA5 and LGP2. *Journal of Virology*, *83*(14), 7252–7260. https://doi.org/10.1128/JVI.00153-09

Park, A., Yun, T., Vigant, F., Pernet, O., Won, S. T., Dawes, B. E., … Lee, B. (2016). Nipah Virus C Protein Recruits Tsg101 to Promote the Efficient Release of Virus in an ESCRT-Dependent Pathway. *PLoS Pathogens*, *12*(5), e1005659–e1005659. https://doi.org/10.1371/journal.ppat.1005659

Park, M.-S., Shaw, M. L., Muñoz-Jordan, J., Cros, J. F., Nakaya, T., Bouvier, N., … Basler, C. F. (2003). Newcastle disease virus (NDV)-based assay demonstrates interferon-antagonist activity for the NDV V protein and the Nipah virus V, W, and C proteins. *Journal of Virology*, *77*(2), 1501–1511. https://doi.org/10.1128/JVI.77.2.1501-1511.2003

Patch, J. R., Crameri, G., Wang, L.-F., Eaton, B. T., & Broder, C. C. (2007). Quantitative analysis of Nipah virus proteins released as virus-like particles reveals central role for the matrix protein. *Virology Journal*, *4*, 1. https://doi.org/10.1186/1743-422X-4-1

Paterson, R. G., Leser, G. P., Shaughnessy, M. A., & Lamb, R. A. (1995). The paramyxovirus SV5 V protein binds two atoms of zinc and is a structural component of virions. *Virology*, *208*(1), 121–131. https://doi.org/10.1006/viro.1995.1135

Pernet, O., Pohl, C., Ainouze, M., Kweder, H., & Buckland, R. (2009). Nipah virus entry can occur by macropinocytosis. *Virology*, *395*(2), 298–311. https://doi.org/10.1016/j.virol.2009.09.016

Pernet, O., Wang, Y. E., & Lee, B. (2012). Henipavirus receptor usage and tropism. *Current Topics in Microbiology and Immunology*, *359*, 59–78. https://doi.org/10.1007/82_2012_222

Petes, C., Odoardi, N., & Gee, K. (2017). The Toll for Trafficking: Toll-Like Receptor 7 Delivery to the Endosome. *Frontiers in Immunology*, *8*, 1075. https://doi.org/10.3389/fimmu.2017.01075

Pichlmair, A., Schulz, O., Tan, C.-P., Rehwinkel, J., Kato, H., Takeuchi, O., … Reis e Sousa, C. (2009). Activation of MDA5 requires higher-order RNA structures generated during virus infection. *Journal of Virology*, *83*(20), 10761–10769. https://doi.org/10.1128/JVI.00770-09

Pickering, B. S., Hardham, J. M., Smith, G., Weingartl, E. T., Dominowski, P. J., Foss, D. L., … Weingartl, H. M. (2016). Protection against henipaviruses in swine requires both, cell-mediated and humoral immune response. *Vaccine*, *34*(40), 4777–4786. https://doi.org/10.1016/j.vaccine.2016.08.028

Pitulescu, M. E., & Adams, R. H. (2010). Eph/ephrin molecules--a hub for signaling and endocytosis. *Genes & Development*, *24*(22), 2480–2492. https://doi.org/10.1101/gad.1973910

Plumet, S., Duprex, W. P., & Gerlier, D. (2005). Dynamics of Viral RNA Synthesis during Measles Virus Infection. *Journal of Virology*, *79*(11), 6900 LP-6908. https://doi.org/10.1128/JVI.79.11.6900-6908.2005

Plumet, S., Herschke, F., Bourhis, J.-M., Valentin, H., Longhi, S., & Gerlier, D. (2007). Cytosolic 5'-triphosphate ended viral leader transcript of measles virus as activator of the RIG I-mediated interferon response. *PloS One*, *2*(3), e279. https://doi.org/10.1371/journal.pone.0000279

Pomorska-Mól, M., Markowska-Daniel, I., & Kwit, K. (2012). Immune and acute phase response in pigs experimentally infected with H1N2 swine influenza virus. *FEMS Immunology & Medical Microbiology*, *66*(3), 334–342.

Prakash, A., Smith, E., Lee, C.-K., & Levy, D. E. (2005). Tissue-specific positive feedback requirements for production of type I interferon following virus infection. *The Journal of Biological Chemistry*, *280*(19), 18651–18657. https://doi.org/10.1074/jbc.M501289200

Razzuoli, E., Villa, R., Sossi, E., & Amadori, M. (2010). Characterization of the Interferon-α Response of Pigs to the Weaning Stress. *Journal of Interferon & Cytokine Research*, *31*(2), 237–247. https://doi.org/10.1089/jir.2010.0041

Reikine, S., Nguyen, J. B., & Modis, Y. (2014). Pattern Recognition and Signaling Mechanisms of RIG-I and MDA5. *Frontiers in Immunology*, *5*, 342. https://doi.org/10.3389/fimmu.2014.00342

Rima, B. K., & Duprex, W. P. (2009). The Measles Virus Replication Cycle BT - Measles: History and Basic Biology. In D. E. Griffin & M. B. A. Oldstone (Eds.) (pp. 77–102). Berlin, Heidelberg: Springer Berlin Heidelberg. https://doi.org/10.1007/978-3-540-70523-9_5

Rodriguez, J. J., Cruz, C. D., & Horvath, C. M. (2004). Identification of the nuclear export signal and STAT-binding domains of the Nipah virus V protein reveals mechanisms underlying interferon evasion. *Journal of Virology*, *78*(10), 5358–5367.

Rodriguez, J. J., Parisien, J.-P., & Horvath, C. M. (2002). Nipah virus V protein evades alpha and gamma interferons by preventing STAT1 and STAT2 activation and nuclear accumulation. *Journal of Virology*, *76*(22), 11476–11483.

Rodriguez, K. R., & Horvath, C. M. (2013). Amino acid requirements for MDA5 and LGP2 recognition by paramyxovirus V proteins: a single arginine distinguishes MDA5 from RIG-I. *Journal of Virology*, *87*(5), 2974–2978. https://doi.org/10.1128/JVI.02843-12

Rodriguez, K. R., & Horvath, C. M. (2014). Paramyxovirus V protein interaction with the antiviral sensor LGP2 disrupts MDA5 signaling enhancement but is not relevant to LGP2-mediated RLR signaling inhibition. *Journal of Virology*, *88*(14), 8180–8188. https://doi.org/10.1128/JVI.00737-14

Rota, P. A., & Lo, M. K. (2012). Molecular Virology of the Henipaviruses BT - Henipavirus: Ecology, Molecular Virology, and Pathogenesis. In B. Lee & P. A. Rota (Eds.) (pp. 41–58). Berlin, Heidelberg: Springer Berlin Heidelberg. https://doi.org/10.1007/82_2012_211

Runge, S., Sparrer, K. M. J., Lässig, C., Hembach, K., Baum, A., García-Sastre, A., … Hopfner, K.-P. (2014). In vivo ligands of MDA5 and RIG-I in measles virus-infected cells. *PLoS Pathogens*, *10*(4), e1004081–e1004081. https://doi.org/10.1371/journal.ppat.1004081

Sanchez-Aparicio, M. T., Feinman, L. J., Garcia-Sastre, A., & Shaw, M. L. (2018). Paramyxovirus V Proteins Interact with the RIG-I/TRIM25 Regulatory Complex and Inhibit RIG-I Signaling. *Journal of Virology*, *92*(6). https://doi.org/10.1128/JVI.01960-17

Sang, Y., Bergkamp, J., & Blecha, F. (2014). Molecular Evolution of the Porcine Type I Interferon Family: Subtype-Specific Expression and Antiviral Activity. *PLOS ONE*, *9*(11), e112378.

Sato, M., Hata, N., Asagiri, M., Nakaya, T., Taniguchi, T., & Tanaka, N. (1998). Positive feedback regulation of type I IFN genes by the IFN-inducible transcription factor IRF-7. *FEBS Letters*, *441*(1), 106–110.

Satterfield, B. A., Cross, R. W., Fenton, K. A., Agans, K. N., Basler, C. F., Geisbert, T. W., & Mire, C. E. (2015). The immunomodulating V and W proteins of Nipah virus determine disease course. *Nature Communications*, *6*, 7483. https://doi.org/10.1038/ncomms8483

Satterfield, B. A., Cross, R. W., Fenton, K. A., Borisevich, V., Agans, K. N., Deer, D. J., … Mire, C. E. (2016). Nipah Virus C and W Proteins Contribute to Respiratory Disease in Ferrets. *Journal of Virology*, *90*(14), 6326–6343. https://doi.org/10.1128/JVI.00215-16

Schmidt, A., Endres, S., & Rothenfusser, S. (2011). Pattern recognition of viral nucleic acids by RIG-I-like helicases. *Journal of Molecular Medicine*, *89*(1), 5–12. https://doi.org/10.1007/s00109-010-0672-8

Schroder, M., & Bowie, A. G. (2005). TLR3 in antiviral immunity: key player or bystander? *Trends in Immunology*, *26*(9), 462–468. https://doi.org/10.1016/j.it.2005.07.002

Shabman, R. S., Morrison, T. E., Moore, C., White, L., Suthar, M. S., Hueston, L., … Heise, M. T. (2007). Differential induction of type I interferon responses in myeloid dendritic cells by mosquito and mammalian-cell-derived alphaviruses. *Journal of Virology*, *81*(1), 237–247. https://doi.org/10.1128/JVI.01590-06

Shaw, M. L. (2009). Henipaviruses employ a multifaceted approach to evade the antiviral interferon response. *Viruses*, *1*(3), 1190–1203. https://doi.org/10.3390/v1031190

Shaw, M. L., Cardenas, W. B., Zamarin, D., Palese, P., & Basler, C. F. (2005). Nuclear localization of the Nipah virus W protein allows for inhibition of both virus- and toll-like receptor 3-triggered signaling pathways. *Journal of Virology*, *79*(10), 6078–6088. https://doi.org/10.1128/JVI.79.10.6078-6088.2005

Shaw, M. L., Garcia-Sastre, A., Palese, P., & Basler, C. F. (2004). Nipah virus V and W proteins have a common STAT1-binding domain yet inhibit STAT1 activation from the cytoplasmic and nuclear compartments, respectively. *Journal of Virology*, *78*(11), 5633–5641. https://doi.org/10.1128/JVI.78.11.5633-5641.2004

Shiell, B. J., Gardner, D. R., Crameri, G., Eaton, B. T., & Michalski, W. P. (2003). Sites of phosphorylation of P and V proteins from Hendra and Nipah viruses: newly emerged members of Paramyxoviridae. *Virus Research*, *92*(1), 55–65.

Silva, M. C., Guerrero-Plata, A., Gilfoy, F. D., Garofalo, R. P., & Mason, P. W. (2007). Differential activation of human monocyte-derived and plasmacytoid dendritic cells by West Nile virus generated in different host cells. *Journal of Virology*, *81*(24), 13640–13648. https://doi.org/10.1128/JVI.00857-07

Singh, P., & Ramamoorthy, S. (2016a). Lack of strong anti-viral immune gene stimulation in Torque Teno Sus Virus1 infected macrophage cells. *Virology*, *495*, 63–70. https://doi.org/10.1016/j.virol.2016.04.028

Singh, P., & Ramamoorthy, S. (2016b). Immune gene expression in swine macrophages expressing the Torque Teno Sus Virus1 (TTSuV1) ORF-1 and 2 proteins. *Virus Research*, *220*, 33–38. https://doi.org/10.1016/j.virusres.2016.04.004

Sleeman, K., Bankamp, B., Hummel, K. B., Lo, M. K., Bellini, W. J., & Rota, P. A. (2008). The C, V and W proteins of Nipah virus inhibit minigenome replication. *The Journal of General Virology*, *89*(Pt 5), 1300–1308. https://doi.org/10.1099/vir.0.83582-0

Stachowiak, B., & Weingartl, H. M. (2012). Nipah Virus Infects Specific Subsets of Porcine Peripheral Blood Mononuclear Cells. *PLOS ONE*, *7*(1), e30855.

Steinman, R. M., & Banchereau, J. (2007). Taking dendritic cells into medicine. *Nature*, *449*, 419.

Sugai, A., Sato, H., Yoneda, M., & Kai, C. (2013). Phosphorylation of Measles Virus Nucleoprotein Affects Viral Growth by Changing Gene Expression and Genomic RNA Stability. *Journal of Virology*, *87*(21), 11684 LP-11692. https://doi.org/10.1128/JVI.01201-13.

Swiecki, M., & Colonna, M. (2011) Type I interferons: diversity of sources, production pathways and effects on immune responses. *Curr Opin Virol*. 1(6):463-475.

Takeuchi, K., Tanabayashi, K., Hishiyama, M., Yamada, Y. K., Yamada, A., & Sugiura, A. (1990). Detection and characterization of mumps virus V protein. *Virology*, *178*(1), 247–253.

Tan, C. T., Goh, K. J., Wong, K. T., Sarji, S. A., Chua, K. B., Chew, N. K., … Jusoh, M. R. (2002). Relapsed and late-onset Nipah encephalitis. *Annals of Neurology*, *51*(6), 703–708. https://doi.org/10.1002/ana.10212

Tovey, M. G., Streuli, M., Gresser, I., Gugenheim, J., Blanchard, B., Guymarho, J., … Gigou, M. (1987). Interferon messenger RNA is produced constitutively in the organs of normal individuals. *Proceedings of the National Academy of Sciences of the United States of America*, *84*(14), 5038–5042.

Tsai, W.-C., & Lloyd, R.E. (2014) Cytoplasmic RNA Granules and Viral Infection. *Annual Review of Virology*, *1*(1):147-170. https://doi.org/10.1146/annurev-virology-031413-085505

Uchida, S., Horie, R., Sato, H., Kai, C., & Yoneda, M. (2018). Possible role of the Nipah virus V protein in the regulation of the interferon beta induction by interacting with UBX domain-containing protein1. *Scientific Reports*, *8*(1), 7682. https://doi.org/10.1038/s41598-018-25815-9

Vera-Velasco, N. M., García-Murria, M. J., Sánchez del Pino, M. M., Mingarro, I., & Martinez-Gil, L. (2018). Proteomic composition of Nipah virus-like particles. *Journal of Proteomics*, *172*, 190–200. https://doi.org/https://doi.org/10.1016/j.jprot.2017.10.012

Virtue, E. R., Marsh, G. A., & Wang, L.-F. (2011). Interferon signaling remains functional during henipavirus infection of human cell lines. *Journal of Virology*, *85*(8), 4031–4034. https://doi.org/10.1128/JVI.02412-10

Wang, P., Yang, L., Cheng, G., Yang, G., Xu, Z., You, F., … Sutton, R. E. (2013). UBXN1 interferes with Rig-I-like receptor-mediated antiviral immune response by targeting MAVS. *Cell Reports*, *3*(4), 1057–1070. https://doi.org/10.1016/j.celrep.2013.02.027

Weber, F., Wagner, V., Rasmussen, S. B., Hartmann, R., & Paludan, S. R. (2006). Double-stranded RNA is produced by positive-strand RNA viruses and DNA viruses but not in detectable amounts by negative-strand RNA viruses. *Journal of Virology*, *80*(10), 5059–5064. https://doi.org/10.1128/JVI.80.10.5059-5064.2006

Weingartl, H. M., Sabara, M., Pasick, J., van Moorlehem, E., & Babiuk, L. (2002). Continuous porcine cell lines developed from alveolar macrophages: partial characterization and virus susceptibility. *Journal of Virological Methods*, *104*(2), 203–216.

Weingartl, H. M., Zhang, S., Marszal, P., McGreevy, A., Burton, L., & Wilson, W. C. (2014). Rift Valley fever virus incorporates the 78 kDa glycoprotein into virions matured in mosquito C6/36 cells. *PloS One*, *9*(1), e87385. https://doi.org/10.1371/journal.pone.0087385

Weingartl, H., Czub, S., Copps, J., Berhane, Y., Middleton, D., Marszal, P., … Czub, M. (2005). Invasion of the central nervous system in a porcine host by nipah virus. *Journal of Virology*, *79*(12), 7528–7534. https://doi.org/10.1128/JVI.79.12.7528-7534.2005

White, J. M., & Whittaker, G. R. (2016). Fusion of Enveloped Viruses in Endosomes. *Traffic (Copenhagen, Denmark)*, *17*(6), 593–614. https://doi.org/10.1111/tra.12389

Wong, K. T., Grosjean, I., Brisson, C., Blanquier, B., Fevre-Montange, M., Bernard, A., … Deubel, V. (2003). A golden hamster model for human acute Nipah virus infection. *The American Journal of Pathology*, *163*(5), 2127–2137. https://doi.org/10.1016/S0002-9440(10)63569-9

Wright, P. J., Crameri, G., & Eaton, B. T. (2005). RNA synthesis during infection by Hendra virus: an examination by quantitative real-time PCR of RNA accumulation, the effect of ribavirin and the attenuation of transcription. *Archives of Virology*, *150*(3), 521–532. https://doi.org/10.1007/s00705-004-0417-5

Yabukarski, F., Lawrence, P., Tarbouriech, N., Bourhis, J.-M., Delaforge, E., Jensen, M. R., … Jamin, M. (2014). Structure of Nipah virus unassembled nucleoprotein in complex with its viral chaperone. *Nature Structural &Amp; Molecular Biology*, *21*, 754.

Yamaguchi, M., Kitagawa, Y., Zhou, M., Itoh, M., & Gotoh, B. (2014). An anti-interferon activity shared by paramyxovirus C proteins: Inhibition of Toll-like receptor 7/9-dependent alpha interferon induction. *FEBS Letters*, *588*(1), 28–34. https://doi.org/10.1016/j.febslet.2013.11.015

Yob, J. M., Field, H., Rashdi, A. M., Morrissy, C., van der Heide, B., Rota, P., … Ksiazek, T. (2001). Nipah virus infection in bats (order Chiroptera) in peninsular Malaysia. *Emerging Infectious Diseases*, *7*(3), 439–441. https://doi.org/10.3201/eid0703.010312

Yoneda, M., Guillaume, V., Ikeda, F., Sakuma, Y., Sato, H., Wild, T. F., & Kai, C. (2006). Establishment of a Nipah virus rescue system. *Proceedings of the National Academy of*

Sciences of the United States of America, *103*(44), 16508–16513. https://doi.org/10.1073/pnas.0606972103

Yoneda, M., Guillaume, V., Sato, H., Fujita, K., Georges-Courbot, M.-C., Ikeda, F., … Kai, C. (2010). The Nonstructural Proteins of Nipah Virus Play a Key Role in Pathogenicity in Experimentally Infected Animals. *PLOS ONE*, *5*(9), e12709.

Young, V. A., Dillon, P. J., & Parks, G. D. (2006). Variants of the Paramyxovirus Simian virus 5 with accelerated or delayed viral gene expression activate proinflammatory cytokine synthesis. *Virology*, *350*(1), 90–102. https://doi.org/https://doi.org/10.1016/j.virol.2006.01.006

Yount, J. S., Gitlin, L., Moran, T. M., & Lopez, C. B. (2008). MDA5 participates in the detection of paramyxovirus infection and is essential for the early activation of dendritic cells in response to Sendai Virus defective interfering particles. *Journal of Immunology (Baltimore, Md. : 1950)*, *180*(7), 4910–4918.

Appendices

A.1 Buffers/Formulations

A.1.1 CMC Overlay

Sample formulation

Preparation of	1	x CMC overlay
	100	ml required
	1.75	% final

1 Put magnetic stirring bar in a bottle
2 Add 74.57 ml **milli-Q water**
3 Heat to almost boiling point
4 Add slowly 1.75 g of **CMC** (Millipore-Sigma, Cat. No. C4888)
5 Stir on a magnetic stirrer until CMC is dissolved
6 Heat again if necessary. Do not boil
7 Autoclave at 121°C for 15 min
8 Cool to 37°C
9 Add (ml):

10.00	**10X DMEM** (Millipore-Sigma, Cat. No. D2429)
4.00	**7.5% BSA Fraction V** (Millipore-Sigma, Cat. No. A8412)
4.93	**7.5% $NaHCO_3$** (Wisent Bioproducts, Cat. No. 609-105-EL)
2.50	**1M HEPES** (Wisent Biproducts, Cat. No. 330-050-EL)
1.00	**0.4 g/L Folic Acid** (100x) (Wisent Bioproducts, Cat. No. 609-315-QL)
1.00	**200 mM L-Glu** (GlutaMAX™ Supplement, ThermoFisher Scientific, Cat. No. 35050-061)
1.00	**100mM (11.0 mg/ml) Sodium Pyruvate** (Millipore-Sigma, Cat. No. 58636)
1.00	**100x Pen/Strep** (Wisent Bioproducts, Cat. No. 450-201-EL)

10 Mix on magnetic stirrer until ready to use

A.1.2 SDS-PAGE Sample Loading Preparation

Reagent	**Volume added (µl)**
4X NuPAGE™ LDS Sample Buffer (Invitrogen, Cat. No. NP0007)	6.25
10X NuPAGE™ Sample Reducing Agent (Invitrogen, Cat. No. NP0009)	2.5
Sample in 2% SDS-HALT	16.25
Total	25

A.2 Primers and Probes

Primer	Sequence (5'→3')	Primer sequence source	Target	Product bp and location	Purpose
NiV-N forward (Ni-NP1209)	GCAAGAGAGTAATGTTCAGGCTAGAG	Guillaume *et al* 2004	Nipah virus N gene	106 nts 1321-1426	rRT-PCR
NiV-N reverse (Ni-NP1314)	CTGTTCTATAGGTTCTTCCCCTTCAT	Guillaume *et al* 2004	Nipah virus N gene	106 nts 1321-1426	rRT-PCR
Armoured Enterovirus Forward (EVarmRNA-F)	CCTGTCGTAACGCGCAAGT	Pickering *et al* 2016	Enterovirus 5' UTR	76 nts 506-581	rRT-PCR
Armoured Enterovirus Reverse (EVarmRNA-R)	CAGCCACAATAAAATAAAAGGAAACA	Pickering *et al* 2016	Enterovirus 5' UTR	76 nts 506-581	rRT-PCR
Whole P gene forward	ACCAGGTAATGCTCGCACAA	NCBI reference sequence NC_002728.1; design with Primer3 web 4.0.0	Nipah virus P gene	2467 nts 2201-4667	Whole gene cloning; sequencing
Whole P gene reverse	TCGTCTGAGGGCTGGAATGA	NCBI reference sequence NC_002728.1; design with Primer3 web 4.0.0	Nipah virus P gene	2467 nts 2201-4667	Whole gene cloning; sequencing

Primer	Sequence (5'→3')	Primer sequence source	Target	Product bp and location	Purpose
P gene sequencing forward 1	GACGAAGAGGCAGATCAGC	NCBI reference sequence NC_002728.1; design with Primer3 web 4.0.0	Nipah virus P gene nt 2694 start	N/A	Sequencing
P gene sequencing forward 2	GACTGGGCAGAAGGTTCAGA	NCBI reference sequence NC_002728.1; design with Primer3 web 4.0.0	Nipah virus P gene nt 3129 start	N/A	Sequencing
P gene sequencing forward 3	GCACAGACGCGAAATATCCA	NCBI reference sequence NC_002728.1; design with Primer3 web 4.0.0	Nipah virus P gene nt 3625 start	N/A	Sequencing
P gene sequencing reverse 1	CAATGGTTGAGAGTGCGGTG	NCBI reference sequence NC_002728.1; design with Primer3 web 4.0.0	Nipah virus P gene nt 4108 start	N/A	Sequencing
P gene sequencing reverse 2	CGCAGTGGAAGCATTCAGTT	NCBI reference sequence NC_002728.1; design with Primer3 web 4.0.0	Nipah virus P gene nt 3770 start	N/A	Sequencing
P gene sequencing reverse 3	TGCAGGATCAGACAGGTTTCT	NCBI reference sequence NC_002728.1; design with Primer3 web 4.0.0	Nipah virus P gene nt 3011 start	N/A	Sequencing

Primer	Sequence (5'→3')	Primer sequence source	Target	Product bp and location	Purpose
NiV-L forward	AGACGAAGCAAGCTGGACGA	NCBI reference sequence NC_002728.1; design with Primer3 web 4.0.0	Nipah virus L gene	133 nts 13045-13177	rRT-PCR
NiV-L reverse	TGCTCATCCTTAACCATCCCGT	NCBI reference sequence NC_002728.1; design with Primer3 web 4.0.0	Nipah virus L gene	133 nts 13045-13177	rRT-PCR
Cyclophilin forward	TAACCCCACCGTCTTCTT	Stachowiak and Weingartl 2012	Sus scrofa peptidylprolyl isomerase A (PPIA) mRNA [Stachowiak and Weingartl 2012] NCBI Reference Sequence NM_214353.1	368 nts 10-377	rRT-PCR
Cyclophilin reverse	TGCCATCCAACCACTCAG	Stachowiak and Weingartl 2012	Sus scrofa peptidylprolyl isomerase A (PPIA) mRNA [Stachowiak and Weingartl 2012] NCBI Reference Sequence NM_214353.1	368 nts 10-377	rRT-PCR
IFNα forward	TCAGCTGCAATGCCATCTG	Dawson *et al* 2005	Sus scrofa domestica PoIFN-alpha 1 gene [Dawson *et al* 2005] GenBank accession X57191.1	108 nts 522-629	rRT-PCR

Primer	Sequence (5'→3')	Primer sequence source	Target	Product bp and location	Purpose
IFNα reverse	AGGGAG AGATTC TCCTCA TTTGTG	Dawson *et al* 2005	Sus scrofa domestica PoIFN-alpha 1 gene [Dawson *et al* 2005] GenBank accession X57191.1	108 nts 522-629	rRT-PCR
IFNβ forward	CTGGCT GGAATG AAACCG TC	NCBI reference sequence NM_001003923 .1; design with Primer3 web 4.0.0	*Sus scrofa* interferon beta 1 mRNA	125 nts 293-417	rRT-PCR
IFNβ reverse	AATGGT CATGTC TCCCCT GG	NCBI reference sequence NM_001003923 .1; design with Primer3 web 4.0.0	*Sus scrofa* interferon beta 1 mRNA	125 nts 293-417	rRT-PCR
Probe	**Sequence (5' → 3')**	**Probe sequence source**	**Target**	**Target location**	**Purpose**
NiV-N probe	6-FAM-TGCAGG AGGTGT GCTCAT TGGAGG -TAMRA	Guillaume *et al* 2004	Nipah virus N gene	nts 1360-1383	rRT-PCR
Armoured Enterovirus probe	TET-CGTGGC GGAACC GACTAC TTTGG-MGB-NFQ	Pickering *et al* 2016	Armoured enterovirus RNA	nts 526-548	rRT-PCR; extraction control

A.3 Master Mixes

A.3.1 NiV-N rRT-PCR Master Mix

Kit: Rotor-Gene Multiplex RT-PCR Kit (Qiagen, Cat. No. 204974)

Reagent	**Volume per reaction tube (µl)**
RNase-Free Water	3.75
2X Rotor-Gene Multiplex RT-PCR Master Mix	12.5
Probe for Nipah (1pmol/µl)	1
Probe for Entero (6pmol/µl)	0.5
Rotor-Gene RT-Mix	0.25
Primer NiV-N Forward (10 pmol/µl)	0.5
Primer NiV-N Reverse (10 pmole/µl)	0.5
Primer Armoured Enterovirus Forward (20 pmol/µl)	0.5
Primer Armoured Enterovirus Reverse (20 pmol/µl)	0.5
Template	5
Final volume	25

A.3.2 NiV-N vs NiV-L SYBR Green rRT-PCR

Kit: QuantiNova SYBR Green RT-PCR Kit (Qiagen, Cat. No. 20154)

Reagent	**Volume per reaction tube (µl)**
2X QuantiNova Master Mix	10
100X QuantiNova RT mix	0.2
10 µM Forward primer (NiV-N, NiV-L)	0.4
10 µM Reverse primer (NiV-N, NiV-L)	0.4
Nuclease-free water	6
Template	3
Total	20

A.3.3 IFNα/IFNβ mRNA SYBR Green rRT-PCR

Kit: QuantiNova SYBR Green RT-PCR Kit (Qiagen, Cat. No. 20154)

Reagent	**Volume per reaction tube (µl)**
2X QuantiNova Master Mix	5
100X QuantiNova RT mix	0.1
10 µM Forward primer (IFNα, IFNβ, cyclophilin)	0.3
10 µM Reverse primer (IFNα, IFNβ, cyclophilin)	0.3
Nuclease-free water	0.3
Template	4
Total	10

A.3.4 Whole P Gene Amplification RT-PCR

Kit: SuperScript II One-Step RT-PCR for Long Templates Kit (Invitrogen, Cat. No. 11922010)

Reagent	**Volume per reaction tube (µl)**
2X reaction mix	25
10 µM Whole P Gene Forward primer	2
10 µM Whole P Gene Reverse primer	2
RT/Platinum Taq HiFi Mix	2
Nuclease free water	9
RNA template	10 (with $1x10^7$ copies)

A.3.5 Cycle Sequencing of P Gene

Kit: BigDye Terminator v3.1 Cycle Sequencing Kit (Applied Biosystems, Cat. No. 4337455)

Reagent	**Volume per reaction tube (µl)**
Nuclease-free water	13.5
5X sequencing buffer	3.5
BigDye Terminator v3.1 RR-100 mix	1
100 µM P gene sequencing primer	1
cDNA template	1

A.4 (rRT)-PCR Reaction Conditions

A.4.1 NiV-N probe-based rRT-PCR: NiV-N and Enterovirus, on Rotor-Gene Q

Step	Temperature	Time at Temperature	Acquiring?
Reverse Transcription: Hold	50°C	30 min	No
Initial Enzyme Activation: Hold	95°C	15 min	No
Amplification/Detection: Cycle (x45)			
Denaturation	95°C	15 sec	No
Annealing/Extension	60°C	60 sec	Green (510 nm), Yellow (557 nm)
Melt	N/A	N/A	N/A

A.4.2 NiV-N vs NiV-L SYBR Green rRT-PCR, on Rotor-Gene Q

Step	Temperature	Time at Temperature	Acquiring?
Reverse Transcription: Hold	50°C	20 min	No
Initial Enzyme Activation: Hold	95°C	2 min	No
Amplification/Detection: Cycle (x45)			
Denaturation	95°C	15 sec	No
Annealing	60°C	60 sec	No
Extension	77°C	15 sec	Green (510 nm)
Melt	55-95°C, 1°C/step	90 sec pre-melt 5 sec/step	Green (510 nm)

A.4.3 IFNα/IFNβ mRNA SYBR Green rRT-PCR, on Rotor-Gene Q

IFNα and cyclophilin

Step	Temperature	Time at Temperature	Acquiring?
Reverse Transcription: Hold	50°C	20 min	No
Initial Enzyme Activation: Hold	95°C	2 min	No
Amplification/Detection: Cycle (x45)			
Denaturation	94°C	15 sec	No
Annealing	56°C	30 sec	No
Extension	72°C	30 sec	Green (510 nm)
Melt	60-95°C, 1°C/step	90 sec pre-melt 5 sec/step	Green (510 nm)

IFNβ

Step	Temperature	Time at Temperature	Acquiring?
Reverse Transcription: Hold	50°C	20 min	No
Initial Enzyme Activation: Hold	95°C	2 min	No
Amplification/Detection: Cycle (x35)			
Denaturation	95°C	15 sec	No
Annealing/Extension	60°C	30 sec	Green (510 nm)
Melt	55-95°C, 1°C/step	90 sec pre-melt 5 sec/step	Green (510 nm)

A.4.4 Whole P Gene RT-PCR, on GeneAmp 9700

Step	Temperature	Time at Temperature
Reverse Transcription: Hold	50°C	20 min
RT inactivation, initial denaturation: Hold	94°C	3 min
Amplification: Cycle (x30)		
Denaturation	94°C	15 sec
Annealing	55°C	30 sec
Extension	68°C	3 min
Final Extension	72°C	5 min

A.4.5 Cycle Sequencing of P Gene, on GeneAmp 9700

Step	Temperature	Time at Temperature
Reverse Transcription: Hold	96°C	2 min
Amplification: Cycle (x25)		
Denaturation	96°C	30 sec
Annealing	50°C	15 sec
Extension	60°C	4 min

A.5 Sample Calculations

A.5.1 Virus Titer from Plaque Count

$$\text{Plaque titer (PFU/ml)} = \frac{\text{Average number of plaques per well at dilution } 10^{-x} \text{ (PFU)}}{10^{-x} \times \text{volume titered (ml)}}$$

E.g. An average count of 25 PFU in the wells inoculated with 0.1 ml of the 10^{-3} dilution of a sample:

$$\text{Plaque titer (PFU/ml)} = \frac{25 \text{ PFU}}{0.001 \times 0.1 \text{ ml}} = 2.5 \times 10^5 \text{ PFU/ml}$$

A.5.2 MOI Determination for Inocula

$$\text{Volume stock virus required} = \text{number of cells per well} \times \text{MOI} \div \text{stock titer} \times \text{number of wells}$$

E.g. Want to infect 12 wells at MOI 0.1 with virus of titer 1×10^6 PFU/ml and count of 2.5×10^5 cells per well.

$$\text{Volume of stock virus required} = \frac{2.5 \times 10^5 \text{ cells}}{1 \text{ well}} \times \frac{0.1 \text{ PFU}}{1 \text{ cell}} \times \frac{1 \text{ ml}}{1 \times 10^6 \text{ PFU}} \times 12 \text{ wells}$$

Volume of stock virus required = 0.3 ml

A.5.3 Amount of Protein Added per Well in SDS-PAGE

Example: PEG-precipitated virus

$$\frac{3.85 \text{ µg viral protein}}{1 \text{ µL viral protein prep}} \times \frac{16.25 \text{ µl viral protein prep}}{25 \text{ µl prep and loading buffer}} \times \frac{20 \text{ µl prep and loading buffer}}{1 \text{ well}}$$

= 50.05 µg viral protein / well

A.5.4 Ratio of N to L RNA (ΔC_T N – L; modified Livak and Schmittgen $2^{-\Delta\Delta Ct}$ Method [Livak and Schmittgen 2001])

Example data: NiV-ΔV in IPAM31 cell supernatants

	Technical replicate 1	Technical replicate 2	Average
N primers C_T	15.5	15.3	15.4
L primers C_T	14.2	14.5	14.35

Step 1: ΔC_T (the logarithm of the ratio of two values is equal to the difference between the logarithms of each of the two values)

ΔC_T = Average (of technical replicates) of C_T of N RNA - Average (of technical replicates) of C_T of L RNA

$\Delta C_T = 15.4 – 14.35$

$\Delta C_T = 1.05$

Conclusion: The log2 of the ratio of N to L RNA in this NiV-ΔV-infected IPAM31 cell supernatants ($\log_2$(N/L), or ΔC_T N – L) is 1.05.

Further analysis: linearizing this ratio ($2^{\Delta Ct}$) gives the fold difference in the amount of N and L RNA.

$2^{\Delta Ct} = 2^{(1.05)}$

$2^{\Delta Ct} = 2.07$

Since C_T of L RNA < C_T of N RNA, there is more L RNA than N RNA.

Conclusion: There is 2.07 times more L RNA than there is N RNA in this supernatant sample.

A.5.5 Fold Change in IFNα/β mRNA (Livak and Schmittgen $2^{-\Delta\Delta Ct}$ Method [Livak and Schmittgen 2001])

Example data: NiV-ΔV-infected IPAM31 cells compared to mock-infected IPAM31 cells at 24 hpi, looking at IFNβ mRNA expression.

	NiV-ΔV-infected IPAM31		**Mock-infected IPAM31**	
IFNβ C_T values	28.3	28.0	31.2	31.5
IFNβ C_T average of technical replicates	28.15		31.35	
Cyclophilin C_T values	16.4	16.7	16.0	16.1
Cyclophilin C_T average of technical replicates	16.55		16.05	

Step 1: ΔC_T (normalizing expression of target gene to total RNA/reference gene)

ΔC_T = Average (of technical replicates) of C_T of mRNA of interest (IFNβ) - Average (of technical replicates) of C_T of reference mRNA (cyclophilin) in each sample

NiV-ΔV-infected IPAM31	**Mock-infected IPAM31**
ΔC_T = 28.15 – 16.55	ΔC_T = 31.35 – 16.05
= 11.6	= 15.3

Step 2: $\Delta\Delta C_T$ (comparing expression change relative to control sample)

$\Delta\Delta C_T$ = ΔC_T of IFNβ mRNA in test sample (NiV-ΔV-infected IPAM31) - ΔC_T of cyclophilin mRNA in control sample (mock-infected IPAM31)

$\Delta\Delta C_T$ = 11.6 – 15.3

$\Delta\Delta C_T$ = -3.7

Step 3 Option 1: $2^{-\Delta\Delta CT}$ (to linearize data into "fold change" form)

$2^{-\Delta\Delta CT} = 2^{(3.7)}$

$2^{-\Delta\Delta CT} = 13.0$

Step 3 Option 2: $-\Delta\Delta C_T$ (to express in $\log_2$ format, with positive increases in values reflecting positive increases in $\log_2$ mRNA expression)

$-\Delta\Delta C_T = -1 * (\Delta\Delta C_T)$

$-\Delta\Delta C_T = -1 * (-3.7)$

$-\Delta\Delta C_T = 3.7$

Conclusion: IPAM31 cells infected with NiV-ΔV for 24 hpi produced 13.0 times more IFNβ (or 3.7 $\log_2$ more) than mock-infected IPAM31 cells after 24 hpi (in this replicate).

A.6 Antibodies

Antibody	Isotype	Source	Antigen	Application - Dilution
anti-Histone H3 (CST)	Rabbit polyclonal	CST 9715	Human histone H3, carboxy-terminal sequence	WB - 1:2000
anti-NiV P, V, W protein (F20NI58 aka P58)	Mouse monoclonal IgG1/k	NCFAD	BEI inactivated NiV	WB - 1:1000
anti-NiV W protein	Rabbit polyclonal	Li International	GAQTRNIHLLGR KTCLGRRVVQPG MFEDHPPTKKAR VSMRRMSN (W protein, aa 407-450)	WB - 1:1000 IEM - 1:100
anti-NiV V protein 1	Rabbit polyclonal	Li International	NPACSRITPLPRR QE (V protein, aa 432-446)	WB - NR IF - NR IEM - 1:50
anti-NiV V protein 2	Rabbit antiserum	M. Yoneda *et al* (2010)	CSRITPLPRRQE (V protein, aa 431-442)	WB - NR IEM - 1:50
Anti-NiV V protein 3	Rabbit polyclonal	Genscript	PLPRRQECQCGE CP (V protein, aa 436-449)	WB - NR

NR → not reactive